USING WAVE ATTENUATION TECHNIQUES FOR MONITORING OF STRESS LEVELS

by

PO-MING LIN

Thesis submitted to the faculty of the

Virginia Polytechnic Institute and State University

in partial fulfillment of the requirements for the degree of

Master of Science

in

Mining Engineering

APPROVED:

G. Faulkner, Chairman

C. Haycocks

M. Karmis

J.R. Lucas

September, 1987
Blacksburg, Virginia

USING WAVE ATTENUATION TECHNIQUES FOR MONITORING OF STRESS LEVELS

by

Po-Ming Lin

Gavin Faulkner, Chairman

Mining Engineering Department

(ABSTRACT)

Stress can have a significant effect on the stability of pillars. To get an accurate picture of pillar stability, information is needed not only on the initial stress magnitude and distribution but also on all subsequent stress changes.

Sonic methods have the potential to be among the fastest, most economical and least destructive means of stress measurement. Wave propagation velocity has long been applied to the investigation of the upper mantle and crust stress. Recently, it has also been applied to rock burst prediction and mine site investigations. Another parameter for investigating stress in rocks is the attenuation coefficient. Attenuation has been observed to be more sensitive to stress changes than wave velocity; however, the measurement of attenuation is more difficult than that of wave velocity.

In this study, the mechanism of sonic attenuation in rock is reviewed. Both the velocity and the attenuation of sound waves in five different rock types under various stress levels were examined in the laboratory. It was found that the relationship between the velocity ratio and stress and that between the attenuation ratio and stress, for a specific rock type, can be expressed by simplified second order polynomial equations.

ACKNOWLEDGMENTS

I would like to express my sincere gratitude and appreciation to Dr. Gavin Faulkner for his interest, help, and guidance during the course of my research. Special thanks to Drs. M. Karmis, C. Haycocks and J.R. Lucas for their help and suggestions.

Special thanks are also extended to in the Department of Geological Sciences and in the Electrical Engineering workshop for their kindness in loaning equipment.

Thanks to , , and for their help during sample testing. Thanks are extended to for his help and information.

A heartfelt thanks to my wife for her encouragement, patience and careful editing and formating of the manuscript. Finally a great deal of thanks is due to my mother for her support throughout my university career.

TABLE OF CONTENTS

LIST OF FIGURES

LIST OF TABLES

CHAPTER I

INTRODUCTION

Stress has a significant effect on the stability of underground structures. When designing tunnels, shafts and underground openings, the strength of the structure has to be great enough to withstand the applied stress, or failure may occur. Pillar failures and rock bursts are the result of excessive stress. On the other hand, if the strength of the structure is designed to be far in excess of the existing stress, failure may not occur, but economically this is often not viable. Therefore understanding the stress before excavation, and the re-distribution of stress after excavation, will be among the main tasks during the design of an excavation. However, in order to get an accurate picture of underground stability, one needs information not only on the virgin stress and the final re-distribution of stress but also on all the subsequent stress changes in the structure during the excavation.

There are several methods and devices available for measuring stress: the borehole deformation method (Merrill, 1967), the flatjack method (Panek and Stok, 1964), the hydraulic fracturing method (Haimson, 1973; 1978), and the wave velocity method (Obert, 1939; 1940). However, some of the methods require drilling borehole(s) and/or applying stress (strain) relief with overcoring. Some of the methods require cutting a slot. These processes are expensive and time consuming. Therefore, a nondestructive, fast, and economic method is needed.

The possibility of using wave velocities to study the stress in the earth's crust has long been investigated by seismologists. This idea grows from the observed relationship between stress and wave velocity. An observation was

first made in the U.S.S.R. that, prior to an earthquake, the ratio of longitudinal (V_p) to shear (V_s) velocity, V_p / V_s, decreased to an anomalously low value. When the ratio returned to its normal value, an earthquake occurred. This phenomenon was also found in California and New York State (Aggarwal *et al.*, 1973; Whitcomb *et al.*, 1973). This velocity change before an earthquake is due to the stress change preceding the earthquake. A similar premonitory effect was also reported before rock failure in mines (Brady, 1974; 1977), and in the laboratory (Soboley *et al.*, 1978). These reports indicate that the wave velocity is sensitive to stress changes.

In most sonic and ultrasonic testing, wave velocity has been used to study and measure rock properties, because wave velocity can be easily measured and identified. Several laboratory investigations show that many of the properties and processes that affect velocity also affect attenuation, and the effects on attenuation are greater than those on the velocity; in other words, attenuation is more senstive to stress change than velocity is. This suggest that attenuation may be a better parameter for using in stress measurement. However, the correlation between attenuation and stress change is not yet well known. The primary objectives of this study are: (1) to find the correlation between attenuation and stress change, (2) to compare the correlations between attenuation and stress change, and velocity and stress changes, (3) to clarify the feasibility of using attenuation to measure stress.

CHAPTER II

LITERATURE REVIEW

2. 1 STRESS AND STRESS MEASUREMENT

2. 1. 1 Source of Stresses and Their Estimation

In situ stresses are commonly derived from four sources. They are gravitational, tectonic, structural and residual forces. Theoretically, gravitational force is the most important stress which results from the gravity loading of the overburden. The tectonic stress comes from geological tectonic activities. Local structural inhomogeneities give rise to the structural stress, and the residual stress is the stress existing in the intergrain boundaries during mineral crystallization (Peng, 1978).

If one only considers the gravity loading of the overburden, then the vertical gravitational stress can be approximated by:

$$S_v = r \times h \qquad \text{(Phillips, 1948)}$$

where S_v is vertical stress, r is unit weight of rock, and h is vertical depth. Phillips also indicated that the horizontal stress, due to the constraint of lateral expansion by the neighboring rock mass, can be derived by the equation:

$$S_h = S_v \times \nu \ / (1 - \nu)$$

where S_h is horizontal stress, and ν is the Poisson's ratio. The Poisson's ratio for most rocks is between 0.2 and 0.33. Hence, according to Phillips' equation, the ratio of the horizontal and vertical stress will be between 0.25 and 0.5. However, in a tectonically active area, the ratio of horizontal to vertical stress is 1.5 or even as high as 2 (Hooker and Duvall, 1966). Moreover, the surface

topography is commonly not uniform, and the vertical stress can not be simply obtained by multiplying rock density by the depth of overburden. Furthermore, the tectonic activities and lithological inhomogeneities are difficult to estimate. Therefore, in situ stresses can not always be obtained directly from the above equations.

2. 1. 2 Stress Measurement

Many techniques for measuring stresses have already been developed. The main methods for measuring stresses are the borehole deformation method (Leeman, 1964a; 1964b; 1964c), the flatjack method (Panek and Stok, 1964), the hydraulic fracturing method (Haimson, 1973, 1978), and the wave velocity method (Obert, 1939; 1940; Proskuryakov, 1975). All these techniques can be divided into two groups, these being absolute stress measurement and relative stress measurement.

The relative stress measurement involves measuring the change of stress or strain as, for example, excavation takes place. The measurement can be made either by taking the difference between absolute measurements made at a specified period, or by permanently installing a gauge, making an initial reading, and then measuring the changes with respect to this reference value (Smith, 1973).

The advantage of the absolute measurements is that they are not subject to time dependent errors such as instrument drift and creep in the rock. However, absolute stress measurement usually requires stress or strain relief with overcoring.

The borehole deformation gauge developed by U.S.B.M. is one of the most popular devices for absolute in situ stress measurement, but, as with

other methods, it is necessary to apply stress or strain relief and overcoring. Moreover, the effective length of the test borehole can only be about 50 meters (Haimson, 1978).

Hydraulic fracturing was originally applied in the petroleum industry to enhance well production. This technique has been developed to measure in situ stress in rock (Haimson, 1973). A number of measurements, at depths between very near to the surface and 5000 meters, have been conducted very successfully in the United States and elsewhere. However, as with other measurements, a borehole is required. This is expensive and time consuming. Also, in some situations a fracture zone is not allowed.

Measuring the in situ stresses in rock by sonic propagation velocity depends on the passage of stress waves through rocks. The velocities of waves traveling through a material are related to the elastic modulus of that material. Therefore, wave velocity will change during propagation through a material as a result of an elastic modulus change which can be related to the stress level in the material being changed. Adams and Williamson in 1923 first reported that the elastic modulus of rock increases when the hydrostatic pressure on the exterior of the sample is increased, this increasing of the modulus is produced by the closing of the cracks. If the relationship between the velocity of waves and stress in the rock can be established, it will be possible to measure the in situ stress quickly and nondestructively.

Sonic methods involving ultrasonic and seismic waves are becoming more important in mining operations, site investigation, and characterization of rock mass in mineral exploration (Azarov and Kiselev, 1983; Gladwin, 1982). Techniques and equipment for ultrasonic velocity measurement in rocks have been developed and tested (Thill *et al.*, 1968;

Lewis and Tandanand, 1974). These techniques use waves with frequencies above 20 kilohertz to examine intact rocks and/or rock mass. Gladwin and Stacey (1974a) found that the ultrasonic pulse velocity is sensitive to the stress change in the rock, even when the change is only about 0.1 psi. Compared to conventional seismic velocity measurement, ultrasonic measurement is much faster and more efficient. The studies of seismic velocities under different stresses clearly demonstrated that the variation in velocity could predict earthquakes, rock failure and rock burst in mines.

2.2 PROPERTIES OF ULTRASONICS

Ultrasonics, a branch of acoustics, consists of vibratory waves at frequencies above approximately 20 kHz, which is above the hearing range of human beings. Sonic and ultrasonic waves are stress waves. They differ from light and other forms of electromagnetic radiation which can travel freely through a vacuum. Sonic and ultrasonic waves only exist within mass media and are transmitted from one mass to another mass by direct and intimate contact of the masses. However, they have the same distinct types of wave motion and follow the same general rules of propagation. For example, they are reflected from the surface of a medium and refracted when going from one medium into a different medium. Sonic and ultrasonic waves are also termed elastic waves, because only elastic media can sustain the vibrations which are required for their propagation (Ensminger, 1973).

2.3 HISTORY OF ULTRASONICS

The history of ultrasonics is part of the history of acoustics. A historical summary is given by Frederick (1965). He referred to Rudolph Koenig as the

first person to try to produce ultrasonic vibrations in the 1870's. This was followed by Galton, whose ultrasonic whistle was an improvement over Koenig's instruments and was developed in the late 1800's. During World War I, in order to combat the menace from enemy submarines, ultrasonic methods were developed to detect and locate submarines by Langevin in France. From then on, the technology of ultrasonics developed rapidly and has been applied to our daily living in many ways.

2. 4 APPLICATIONS OF ULTRASONICS

The use of ultrasonics is not limited to human beings. Some creatures such as bats, moths, and porpoises use ultrasonics for locating and identifying food, for navigational purposes and for detecting danger. The applications of ultrasonics by human beings can be separated into two groups, these being low intensity applications and high intensity applications. There are numerous low intensity applications such as process control, nondestructive testing, measurement of elastic properties, medical diagnosis and treatment and appliance control etc.. The main high intensity applications are cleaning, plastic bonding, machining and soldering. Ultrasonics have been widely applied in rock mechanics and geotechnics to determine elastic properties of rocks, to detect the quality of concrete, to measure the jointing of the rock mass, to calibrate the resonance frequency, and to measure the sound velocity (Frederick, 1965).

2. 5 TYPES OF WAVES

Seismic waves can be divided into two basic types of elastic waves these being body waves and surface waves. Body waves travel through the interior

of rocks as compressional waves and shear waves. Surface waves only travel along the surface or interfaces of materials and can be subdivided into four modes as Rayleigh waves, Love waves, Hydrodynamic waves, and Coupled waves. The first two modes of surface waves can be easily detected and identified, the latter two have somewhat dubious characteristics (Farmer, 1968).

Compressional waves are also called longitudinal or primary (P) waves. The direction of particle motion is parallel to the direction of the wave front. These waves travel in all directions in materials which resist compression. The velocity of compressional waves is the highest among all the waves, therefore, they are the first waves detected at a receiver and can be identified very easily. For this reason they have been selected as a popular tool in sonic research.

The relationships between compressional wave velocity (V_p) and the other elastic constants G, ν, K, E, and ρ are given as:

$$V_p = ((\lambda + 2G) / \rho) \quad (2.1)$$

$$= ((K + 4G/3) / \rho) \quad (2.2)$$

$$= (E(1 - \nu)/(\rho(1 + \nu)(1 - 2\nu))) \quad (2.3)$$

where: λ is Lame's constant = (3K - 2G) / 3,

G is rigidity modulus = E / (2(1 + ν)),

ρ is density,

K is bulk modulus = E / (3(1 - 2ν)),

E is Young's modulus,

ν is Poisson's ratio.

Shear waves are also called transverse or secondary (S) waves. Shear waves are only able to travel in solids, as they depend on the ability of the

transmitting material to resist changes in the shape. Due to the passage of shear waves, particles move in a direction perpendicular to that of wave propagation. The velocity of shear waves can be shown as:

$$V_s = (G / \rho) \qquad (2.4)$$

$$= (E / (2\rho (1 + \nu)) \qquad (2.5)$$

where: V_s is shear velocity,

G is rigidity modulus = E / (2(1 + ν)),

ν is Poisson's ratio,

E is Young's modulus,

ρ is density.

The ratio of compressional to shear velocity is

$$V_p / V_s = ((1 - \nu)/(1/2 - \nu)) \qquad (2.6)$$

As the Poisson's ratio for most rocks is between 0.2 and 0.33, the ratio of V_p / V_s which is calculated from equation 2.6 is between 1.5 and 2.

Rayleigh waves (R) travel along the free surface of a solid material. The particle motion is elliptical and retrograde with respect to the direction of propagation, and only exists in the vertical-radial plane. The velocity is slower than any of the body waves and is about nine tenths of the shear wave velocity. The dispersion of Rayleigh waves can provide useful information about layering in the earth's crust and upper mantle.

The particle motion of Love waves (Q) is of shear wave type and only exists in the horizontal transverse direction. The wave is observed only when there is a low-speed layer overlying a high-speed substratum. The velocity of Love waves is approximately equal to that of shear waves in the upper layer and they have a very short wave length.

2. 6 FACTORS AFFECTING VELOCITY

The major factors controlling wave velocity through a rock medium are density, degree of anisotropy, occurrence of fissures, porosity, water content, temperature, and stress. In this section, these factors will be reviewed.

2. 6. 1 Density

It is well understood that the more dense and compacted the rock is, the higher the propagation velocity will be. In the acoustic sense, the wave velocity is defined as:

$$V = (E / \rho) \qquad (2.7)$$

where: E is elasticity,

ρ is density.

The modulus of elasticity increases with increasing density. The absolute magnitude of the elastic modulus is much greater than that of density, thus it can be seen that the effect of elasticity on velocity is much greater than that of density (Anstey, 1977). Birch (1960, 1961) suggested that the velocities of elastic waves are a linear function of density for materials having a common atomic weight. Youash (1970) suggested a quasi-linear relationship between rock density and elastic wave velocity in the ultrasonic range, however, Gardner *et al.*, (1974) suggested a simple exponential relationship:

$$\rho = 0.23 \times V \qquad (2.8)$$

where: ρ is density,

V is velocity of seismic waves.

for all sedimentary rocks except salt and anhydrite (Figure 2.1). These studies indicate that it is possible to estimate the velocity in rocks from the bulk

density and vice versa.

2. 6. 2 Anisotropy

The inhomogeneity of rocks causes differences in the velocities of waves propagating in different directions. In layered rocks, the wave velocities in the direction parallel to the layer are always faster than those in the direction perpendicular to the layer. The ratio of the velocity traveling along the layer ($V_{//}$) to the velocity traveling perpendicular to the layer ($V_{\perp}$), $V_{//}/V_{\perp}$, is defined as the coefficient of anisotropy or anisotropy factor. Generally, the coefficient of anisotropy varies between 1.07 and 1.4 (Table 2.1). The anisotropy is due to layering, foliation, bedding, schistocity, metamorphism, structural fabrics, microcracks, and mineral orientation etc. (Birch, 1961; Youash, 1970; Attewell, 1970).

Anisotropy varies with stress such that when the stress increases the anisotropy decreases. The velocity in the direction parallel to the stress increases much faster than that in the direction perpendicular to the stress. Tocher (1957) suggested that this difference can be used to predict rock bursts in mines.

2. 6. 3 Porosity and Fissuring

Several studies have shown that any defects such as cracks, pores, and joints in rocks strongly influence their mechanical properties (Willard and McWillians, 1969). The velocities of waves propagating in the rocks are also affected. In general, the more defects that exist, the slower the velocity will be. The wave energy is reduced when waves pass through the defects, since the velocity of waves traveling in the defect fillings is slower than that of waves

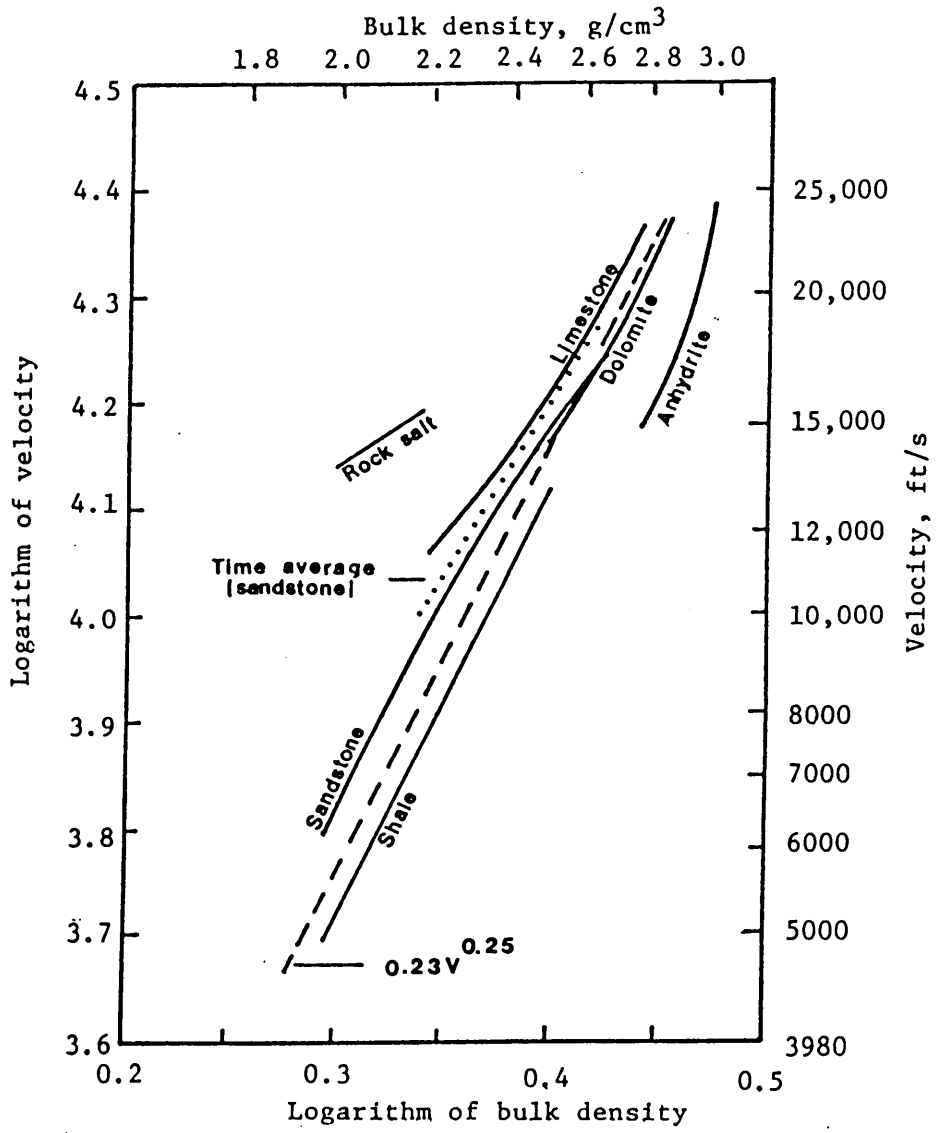

Figure 2.1 Velocity-versus-density relationships for different types of rocks.
(Gardner et al., 1974)

TABLE 2.1

Anisotropy Coefficient for Various Rocks
(Lama and Vutukuri, 1978)

Rock	Anisotropy Coefficient	Reference
Austin Chalk	1.17	Tocher (1957)
Homogeneous anhydrite	1.16	Dunoyer de Segonzac and Laherrere (1959)
Anhydrite with intercalated	1.12 to 1.14	Dunoyer de Segonzac and Laherrere (1959)
Limestone	1.08 to 1.10	Dunoyer de Segonzac and Laherrere (1959)
Arbuke limestone	1.30	Uhrig and Von Melle (1955)
Salt	no anisotropy	Dunoyer de Segonzac and Laherrere (1959)
Sandstone	no anisotropy	Dunoyer de Segonzac and Laherrere (1959)
Eagle Ford Shale	1.33	Uhrig and Von Melle (1955)
Pierre shale (Limon, Colo.)	1.18	Uhrig and Von Melle (1955)
Pierre shale (Last Chance, Colo.)	1.14	Uhrig and Von Melle (1955)
Cambridge slate	1.17	Tocher (1957)
Lorraine shale	1.40	Tocher (1957)
Gneiss (Hell Gate, N.Y.)	1.20	Birch (1960)
Mica schist (Woodsville, VT)	1.36	Birch (1960)
Granodiorite gneiss (Bethlehem, N.H.)	1.33	Birch (1960)
Gneiss (Pelham, Mass)	1.27	Birch (1960)

traveling in a rock framework. Wyllie *et al.* (1956) demonstrated the time average relationship between velocity and porosity as:

$$1/V = x / V_f + (1 - x)/ V_m \qquad (2.9)$$

where: V is velocity in saturated rock,

x is the porosity,

V_f is velocity in the fluid filling the pores,

V_m is the velocity in the mineral skeleton of the rocks.

Rzhevsky and Novik (1971) suggested that the relationship between compressional wave velocity and porosity is:

$$V = 5430 - 107n \qquad (2.10)$$

where: V is compressional velocity in m/s,

n is the percentage of porosity.

Stacey (1976) conducted a detailed investigation of velocity and jointing which resulted in a nonlinear relationship (Figure 2.2). However, Schilizzi (1982) suggested a linear relationship between velocity and frequency of cracks (Figure 2.3).

The velocity ratio is expressed as V_f / V_l where V_f is the P wave velocity of the rock mass in situ, and the V_l is the P wave velocity of an intact specimen. Both the velocity ratio and the velocity index, defined as $(V_f / V_l)^2$, have been chosen as a tool to examine the quality of rocks (Coon and Merrite, 1970; Thill and Jessup, 1982). However, several tests have shown that a relatively small stress is sufficient to close joints acoustically. Stacey (1976) reported that, even when the number of joints is eight, a confining stress of 2 MN/m^2 (300 psi) is sufficient to close them acoustically. New and West (1980) showed that, for chalk a stress of 60 psi, for weak sandstone a stress of 120 psi, and for hard rock a stress of 15 psi was sufficient to close the joints and

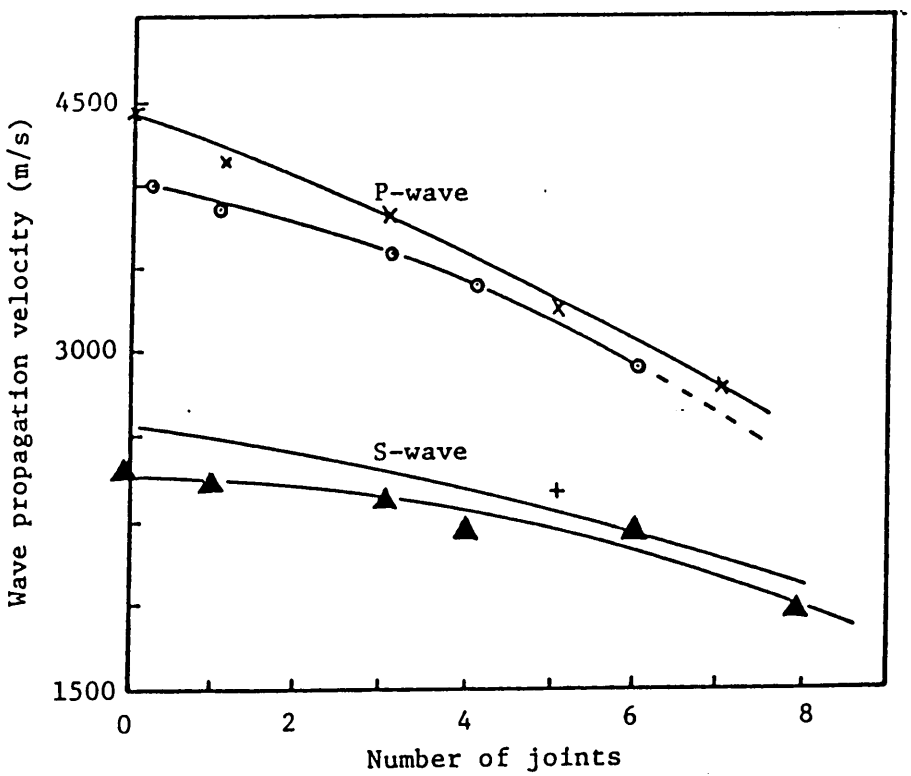

Figure 2.2 Effect of jointing on wave propagation velocity, with zero confining stress.
(Stacy, 1976)

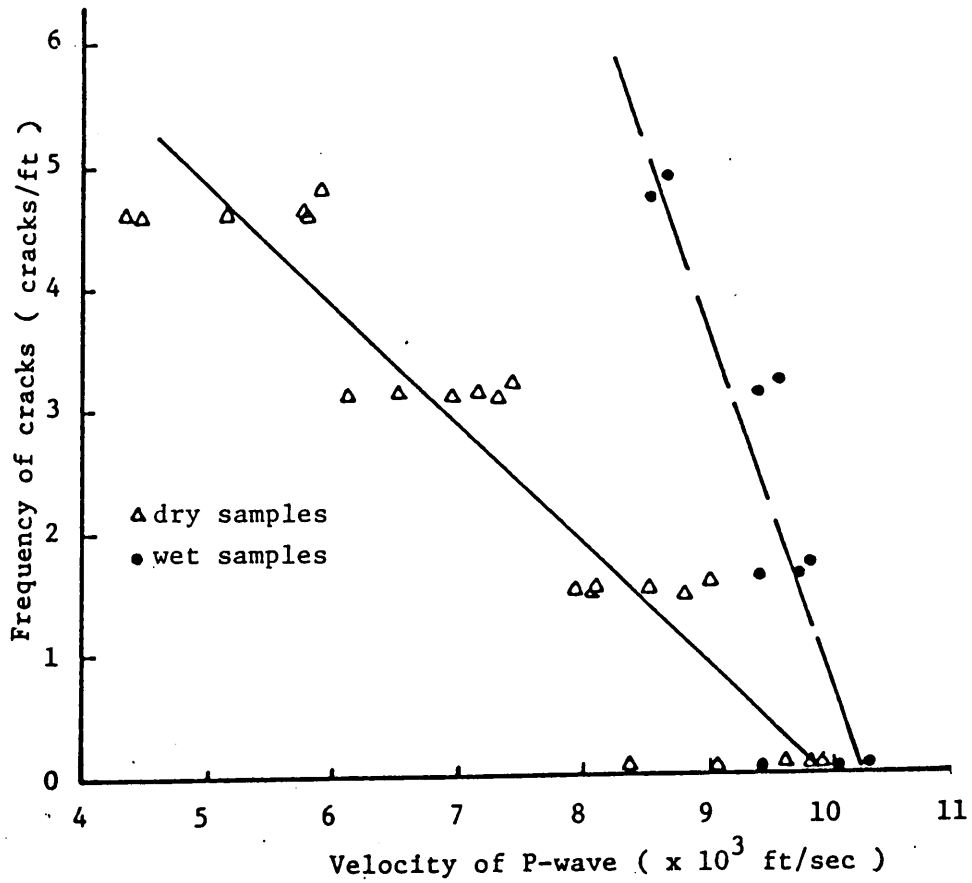

Figure 2.3 Comparison of sonic tests between dry and wet samples. (Schilizzi, 1982)

achieved a constant velocity for the P wave. This indicates that the P wave velocity is relatively insensitive to the joint frequency of the rock mass. One should be cautious when using wave velocity for rock classification.

2. 6. 4 Water Content

Water content can exist both with and without external pressure. Born and Owen suggested that the presence of water in a bonded material such as sandstone will soften or dissolve the bonding material to form a colloid, and thus decrease the velocity of a wave. If the material was not softened, the apparent velocity of a wave in it can be calculated by (Lama and Vutukuri, 1978):

$$V = V_f \times V_m/(n\ V_m + (1 - n)V_f) \qquad (2.11)$$

where: V is apparent velocity of wave,

V_f is wave velocity in the substance filling the pores,

V_m is wave velocity in the mineral skeleton of the rock,

n is porosity.

The compressional wave velocity in more porous rock which is completely saturated with water is lower than that in slightly porous rock, because V_f is less than V_m (Table 2.2). The shear wave velocity will remain almost constant because those waves only pass through the mineral skeleton.

Wyllie *et al.* (1956) observed that the velocity of compressional waves in rock increases with water content. When the saturation is below 10%, the velocity is erratic. The velocity is nearly constant between 10% and 70% saturation and increases with further saturation (Figure 2.4). However, under high external pressure, the compressional wave velocity increases only when the specimen is partially saturated. In completely water-saturated rock the

TABLE 2. 2

Velocity of Longitudinal Waves in Medium
(Data from Rzhevsky and Novik, 1971)

Medium	Apparent density (kg/m^3)	Velocity of P Wave (m/s)
Water	1000	1.485
Air	1.29	331.0
Ice	918	320.0
Limestone	2300 - 3000	3200 - 5500
Marble	2800	4950
Sandstone	2100 - 2900	2000 - 3600
Shale	2500 - 2720	2250

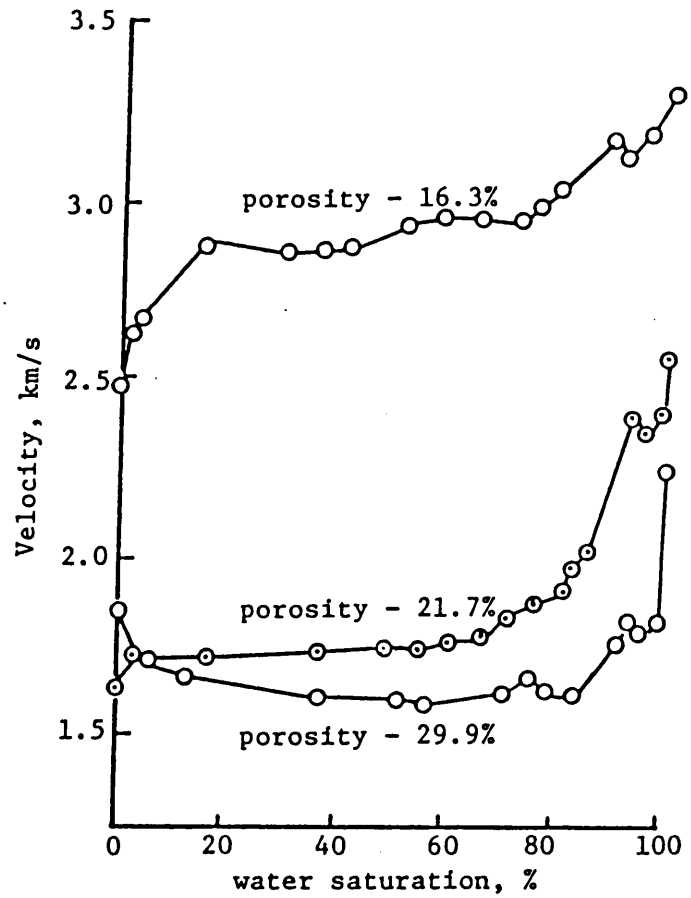

Figure 2.4 Longitudinal wave velocity (km/s) as a function of water saturation at atmospheric pressure. (Wyllie, Gregory and Gardner, 1956)

velocity is less than that in partially saturated rock, because cracks in completely saturated rock may not close as well as those in partially saturated rock (Figure 2.5). Undoubtedly the presence of cracks and the water content affect the velocity. Under zero stress conditions the velocity increases with increasing water content, because the cracks are not closed and the velocity through water filled pores is higher than that through air filled pores (See Table 2.2).

2. 6. 5 Temperature Dependence

Usually, the velocity of compressional waves falls with rising temperature. This is due to the unequal expansion of the crystals leading to internal cracking, or the crystals may be more loosely joined when the temperature rises. However, the influence of temperature on the wave velocity is less at high pressure than that at low pressure (Figure. 2.6) (Hughes and Maurette, 1956), because the effects of loose joints and unequal expansion are lessened by the action of pressure. King and Paulsson (1981) observed that the compressional wave velocity increases in granite (in central Sweden) as the temperature increases from 14°C to 78°C, both with and without pressure increasing from 0 to 24 MPa (3500 psi) (Figure 2.7). However, when the temperature is between 78°C and 98°C at zero pressure the velocity decreases. When the temperature is further increased to above 98°C, the velocity increases with increasing pressure. This can be explained that, below 78°C, both temperature and pressure tend to close original microcracks, so the velocity increases. Between 78°C and 98°C the temperature induces thermal microcracking so that velocity decreases. Above 98°C and under high pressure the thermal microcracks are closed again.

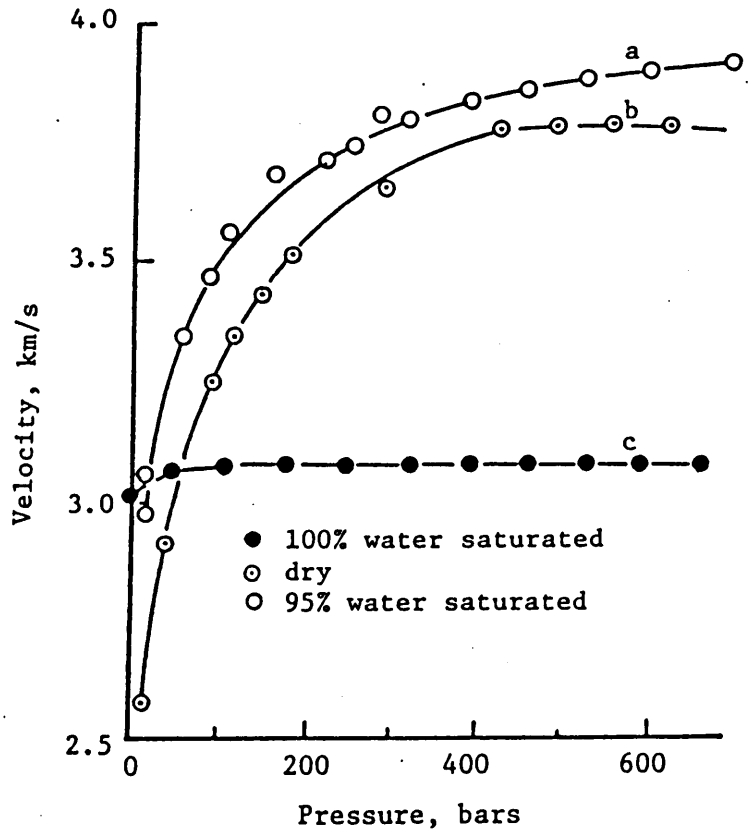

Figure 2.5 Longitudinal wave velocity (km/s) versus pressure for different water contents.
(Wyllie, Gregory and Gardner, 1956)

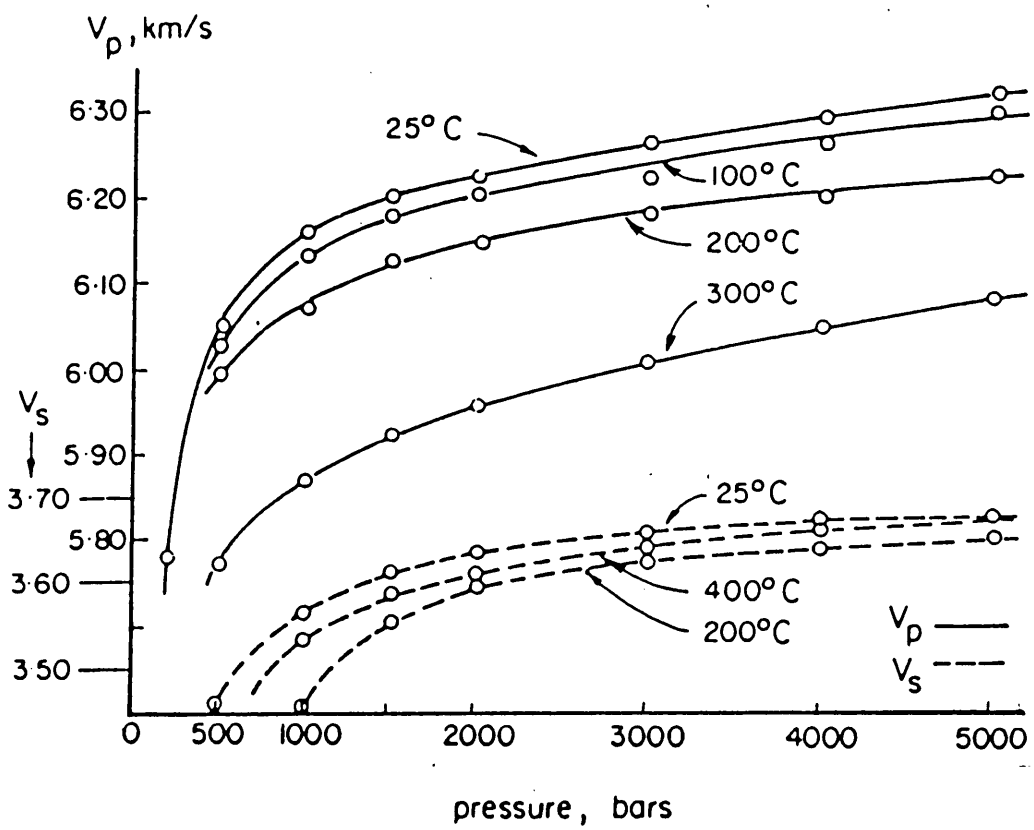

Figure 2.6 Compressional (V_p) and shear (V_s) velocities as a function of hydrostatic pressure at various temperatures. (Hughes and Maurette, 1957)

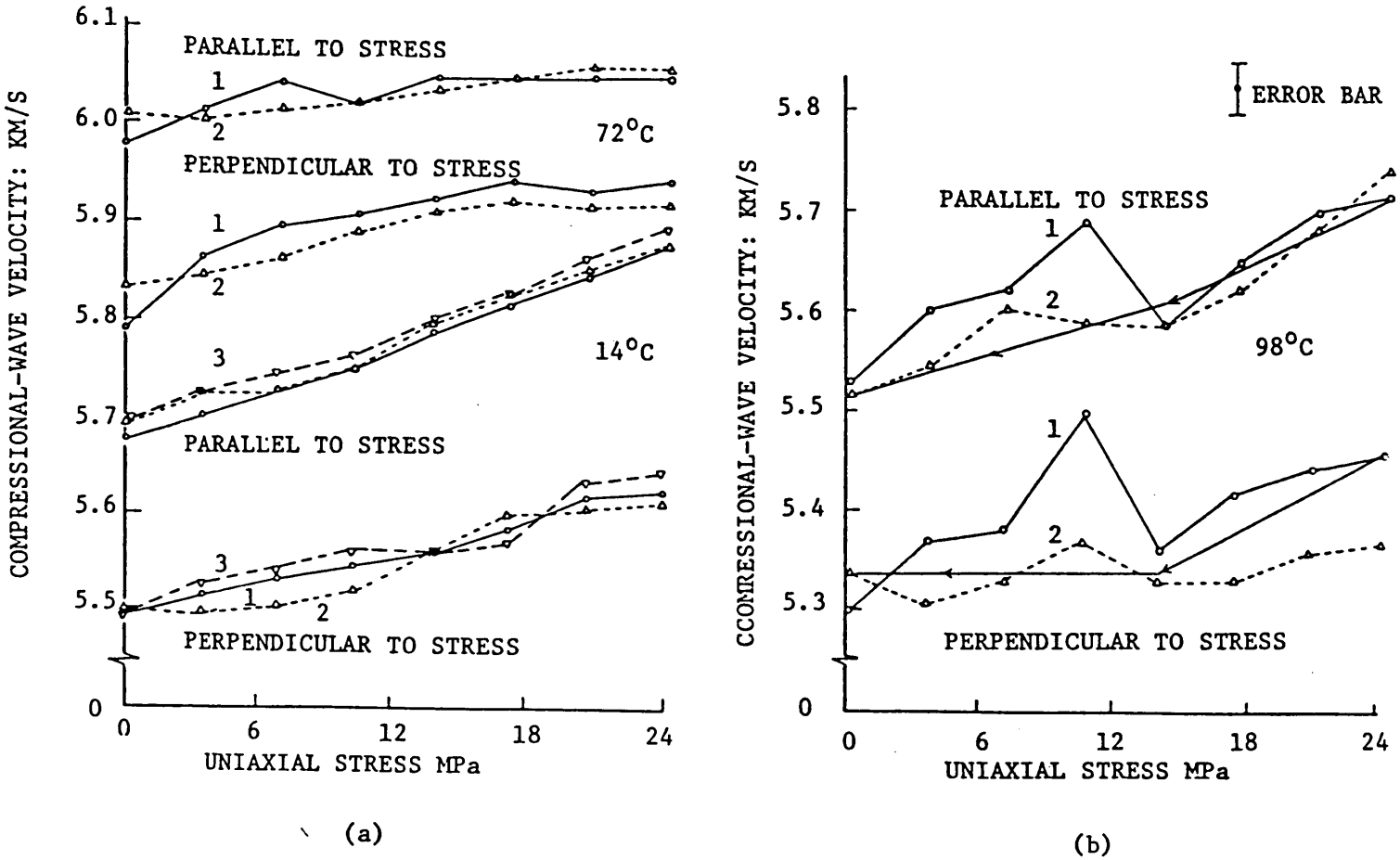

Figure 2.7. Compressional-wave velocity as a function of uniaxial stress (a) at 14 and 72°C and (b) at 98°C.
(King and Paulsson, 1981)

2. 6. 6 Velocity and Stress

All the factors as previously reviewed will affect wave velocities. However all these factors are also stress dependent. Generally, the velocities of waves increase with increasing stress. They increase significantly under low stress. Under high stress the velocities increase only slightly or even decrease when the stress exceeds a certain value. This is due to the fact that, at low stress, the porosity or number of defects decreases and the mechanical contact between the grains increases. At high stress the intrinsic properties of rock have been changed.

Tocher (1957) and Wyllie *et al.* (1958) indicated that the wave velocities in rocks under hydrostatic pressure or triaxial pressure are not significantly different. But the wave velocities under uniaxial pressure and measured in the direction parallel to the stress are changed significantly. They also pointed out that the anisotropic behavior of the rocks under uniaxial pressure can be a possible method to determine the state of stress in rocks in situ. Rzhevsky and Novik (1971) observed that in sandy marls with an initial porosity of 25%, at pressures up to 1000 kgf/cm^2 (14,000 psi), the compressional wave velocity increases by 50% to 60%; in less porous rocks the velocity increases only 5% to 20%. Under the same conditions the shear wave velocity increases much more slowly.

The velocity variation is found to be more sensitive to brittle fracturing than ductile behavior. In brittle rock the velocity reduction often occurs well in advance of structural collapse or rupture, commonly at 50% to 90% of ultimate strength (Thill, 1972; Soboley *et al.*, 1978). When the velocity begins to decrease, it is a precursor of rock failure (Figures 2.8, 2.9 and 2.10). This phenomenon was also observed in the laboratory (Tomashevskaya and

Khamidullin, 1972; Soboley *et al.*, 1978) and in the field (Brady, 1978).

2. 7 ATTENUATION

Attenuation refers to the diminishing of the intensity of a wave front as it propagates through a medium. This diminishing results from geometric spreading, scattering, and absorption (Ensmingor, 1973). In most rock, attenuation is significant when the propagation distance exceeds the wavelength by more than a few orders of magnitude. When a spherical wave spreads out from its source, the energy must be distributed over the area of the sphere. The area of the sphere increases as the square of the sphere's radius. Thus the energy per unit area varies inversely as the square of the distance from the source, $(\text{radius})^2$. The amplitude is proportional to the square root of the energy. Thus the amplitude is also inversely proportional to the distance traveled. This loss of amplitude is due to spreading. Additionally, there is a certain loss, due to absorption or internal friction, which is exponential with distance. Therefore, the amplitude of a wave which propagates in a homogeneous material falls off with distance (X) from the source. This can be shown as (Dobrin, 1976):

$$I_x = I \times \exp(-\alpha X) / X \qquad (2.12)$$

where: I_x is amplitude at distance X from source,

I is initial amplitude,

α is the attenuation coefficient which is the exponential decay constant of wave amplitude as its propagates.

The attenuation coefficient α can be expressed in terms of δ, the logarithmic decrement and Q, the quality factor (Bradley and Fort, 1966) as:

$$\alpha = \delta \times f / V = \pi \times f / Q \times V \qquad (2.13)$$

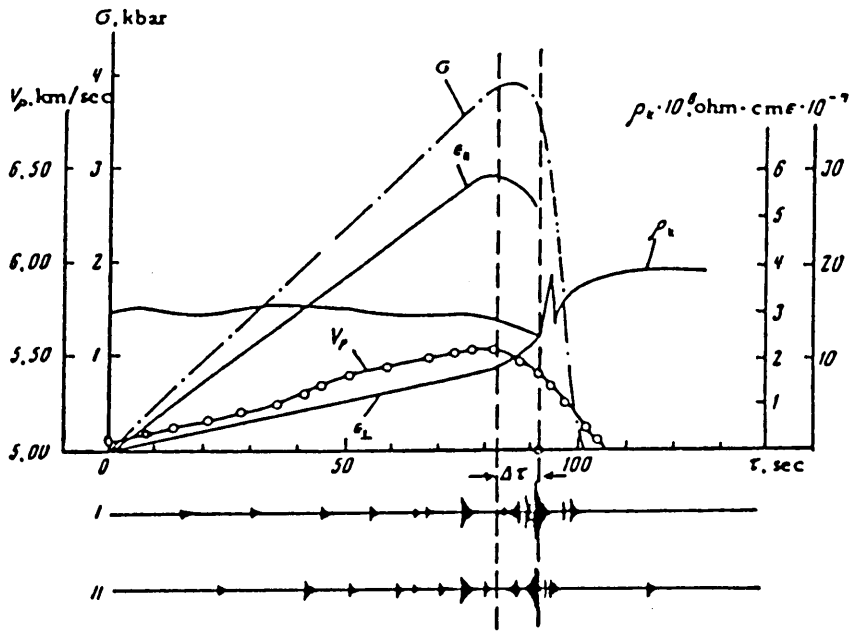

Figure 2.8 Examples of alteration in the physical characteristics of a rock specimen recorded simultaneously during a single experiment.
(Tomashevskaya and Khamidullin, 1972)

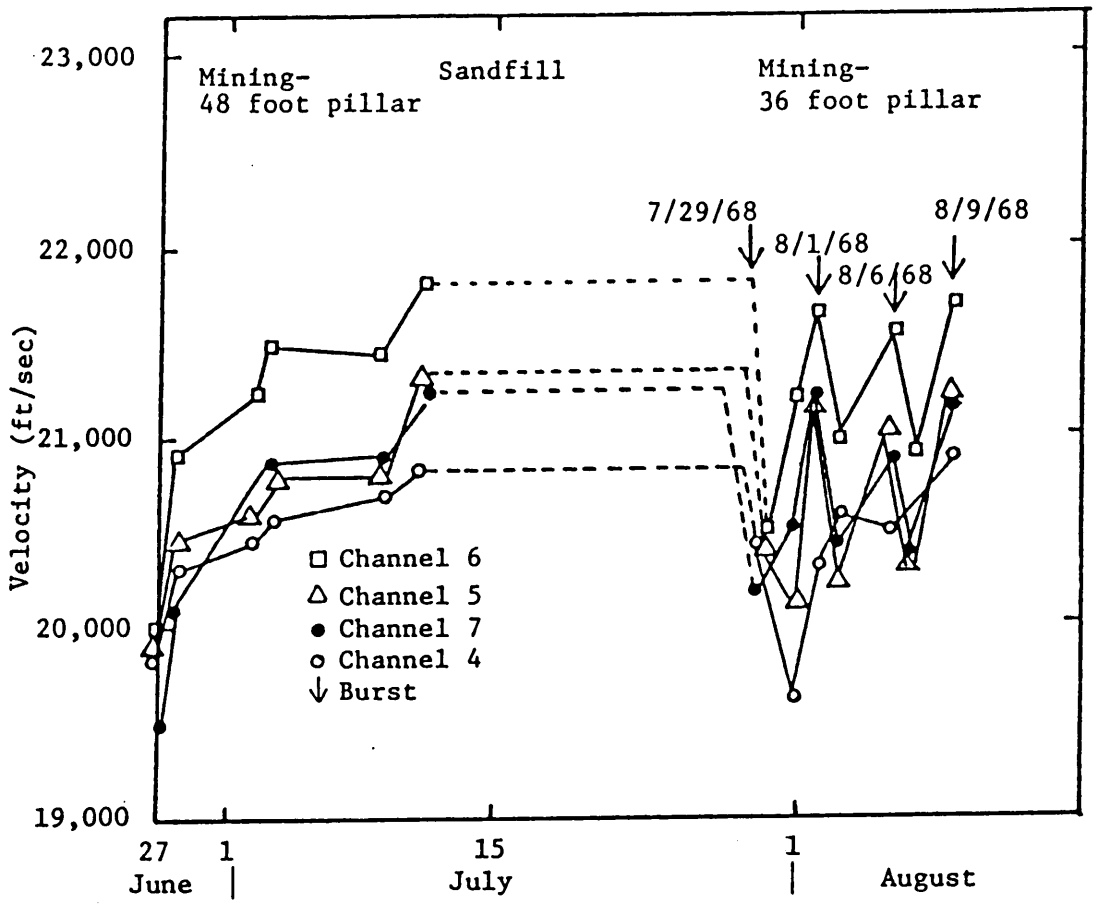

Figure 2.9 P-wave variation with time and pillar geometry (76R). (Brady, 1974)

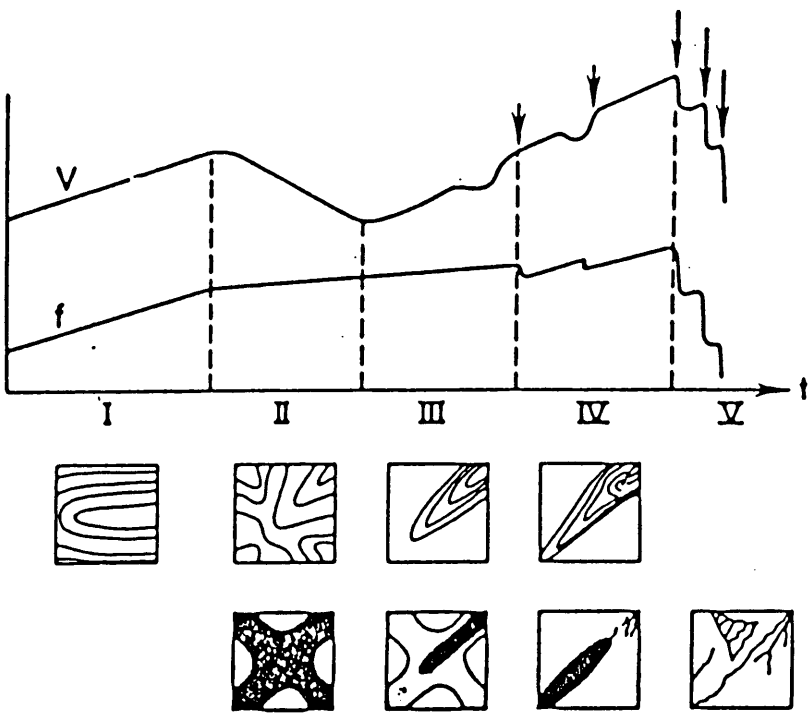

Figure 2.10 Schematic presentation of prisms leading to failure.
(Soboley et al., 1978)

where: f is frequency,

V is wave velocity,

δ is the natural logarithm of the ratio of the amplitudes of two successive cycles,

Q is a fraction of strain energy lost per stress cycle.

Auberger and Rinehart (1960) computed the attenuation coefficient, α, from

$$\alpha = (20 \times \log10 (I_x / I)) / (L - L_x) \qquad (2.14)$$

where: I_x is the amplitude of the first arrival wave at distance Lx,

I is the amplitude of the first arrival wave at distance L.

Gladwin and Stacey (1974) suggested a simple empirical relationship between the pulse rise time and the propagation time of a pulse (Figure 2.11) as:

$$\tau = \tau_0 + C \int dt/Q \qquad (2.15)$$

where: τ is pulse rise time,

τ_0 is the initial rise time (at t = 0),

Q is the quality factor,

C is a constant,

t is the travel time.

One can use equation 2.13 and 2.15 to compute the attenuation coefficient (McKenzie *et al.*, 1982).

Molina and Wack (1982) computed the attenuation coefficient from:

$$\alpha = 10 / L \times \log(E_1 / E_2) \qquad (2.16)$$

where: L is the path length of the ultrasonic wave in the sample,

E_1 and E_2 are the energies before and after a wave passes through the sample.

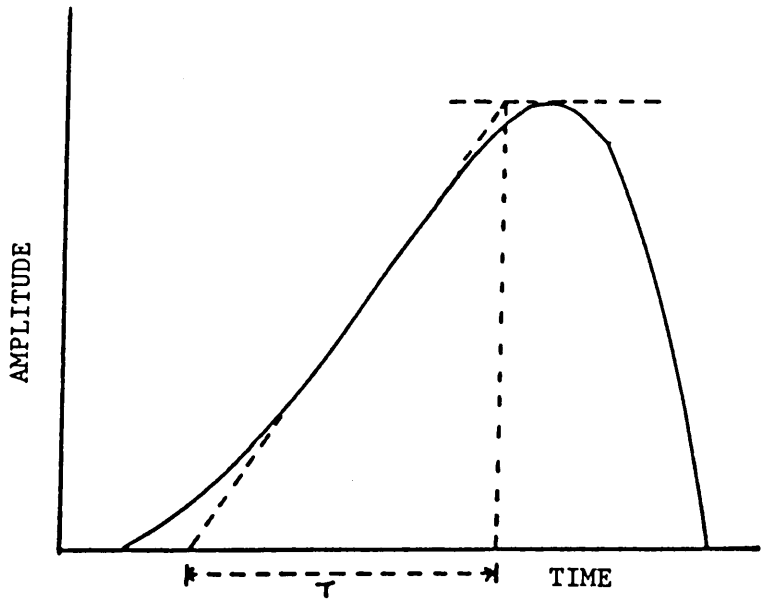

Figure 2.11 Rise time τ of a pulse is here defined in terms of the tangent of the point of maximum slope, extrapolated to zero and to the peak pulse amplitude.
(McKenzie, 1982)

The attenuation of compressional and shear waves in rocks, as with the velocities of waves in rocks, strongly depends on the physical state of the rocks. However, attenuation is much more sensitive than wave velocity to a change of physical state of a material. Generally, the experimental determination of attenuation is more difficult than the measurement of velocity. Attenuation measurements have been carried out in the laboratory using different techniques at variable frequencies (Attewell and Ramana, 1966; Bradley and Fort, 1966; Toksoz *et al.*, 1979). Their measurements showed that attenuation generally depends on frequency, fluid saturation, and pressure.

2. 7. 1 Attenuation as a Function of Frequency

Generally speaking, attenuation is proportional to frequency. Therefore the attenuation value obtained by an ultrasonic method is higher than that obtained by a lower frequency method (Johnston, 1981). Krishnamurthi and Balakrishna (1957) also showed that the attenuation increases with increasing frequency. Toksoz *et al.* (1979) detected a linear relationship between attenuation coefficient and frequency in the 0.1 to 1.0 MHz range for both compressional and shear waves in both dry and saturated rock (Figure 2.12).

2. 7. 2 Attenuation as a Function of Fluid Saturation

The type of saturant and the degree of saturation play important roles in attenuation (Gardner *et al.*, 1964). In general, attenuation increases with degree of saturation and increases rapidly at low degrees of saturation (Figure 2.13). Fluids with higher viscosities have a smaller effect on attenuation

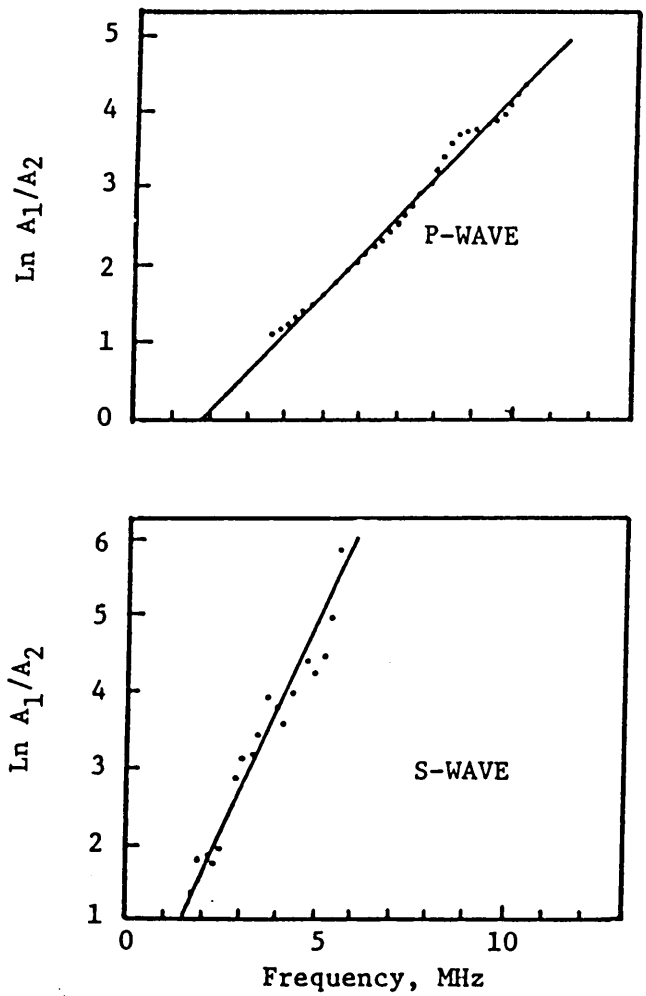

Figure 2.12 Attenuation characteristics of the Navajo sandstone.
(Tokson et al., 1979)

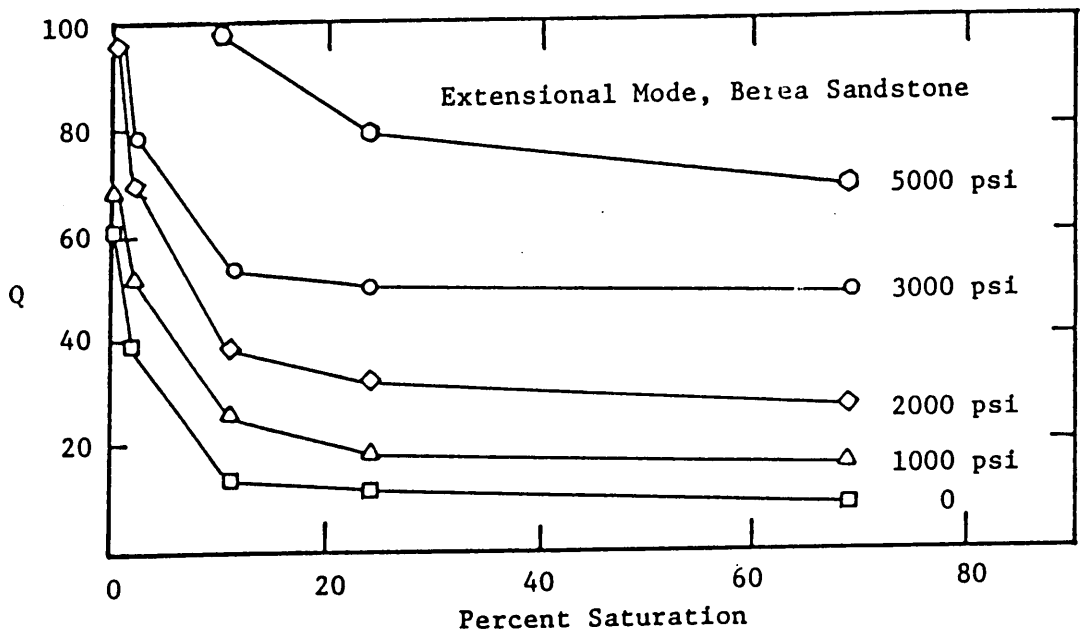

Figure 2.13 Q as a function of saturation and differential pressure in Berea sandstone, extensional mode. (Johnston et al., 1979)

because the high viscosity decreases the effective permeability (Wyllie *et al.*, 1962).

Spencer (1979) suggested that the shear wave attenuation was larger than that of a compressional wave in fully saturated sandstone, but less than that of a compressional wave in a partially saturated sample. Frisillo and Stewart (1980) reported that the maximum attenuation of compressional waves in Berea sandstone is at 70% water saturation at ultrasonic frequencies. Winkler and Nur (1982) pointed out that, in Massilion sandstone, shear wave attenuation increases with the degree of saturation and reaches a maximum at total saturation. However, with P waves, the maximum attenuation occurs between 60% to 90% water saturation and thereafter attenuation of P waves decreases. They also found that attenuation is much more sensitive to changes in rock properties than velocity is.

There are several different mechanisms responsible for attenuation phenomena (Figure 2.14). Johnston *et al.* (1979) proposed that attenuation results from the friction on the grain boundaries and thin cracks. Introduction of fluid into a dry rock will wet crack surfaces and grain boundaries. By this crack lubrication, frictional sliding is facilitated and the attenuation increases. Biot (1956a, b) claimed macroscopic fluid flow theory such that the rock frame is accelerated by the acoustic wave, and generates shear stress within the pore fluid. This stress decay exponentially away from the pore wall with a viscous skin depth that decreases with increasing frequency. The stress induces fluid flow between pores which causes attenuation. O'Connell and Budiansky (1977) suggested that inter-crack or squirt flow will occur as fully saturated cracks are compressed by stress waves and attenuation will depend upon the shape and orientation of the cracks.

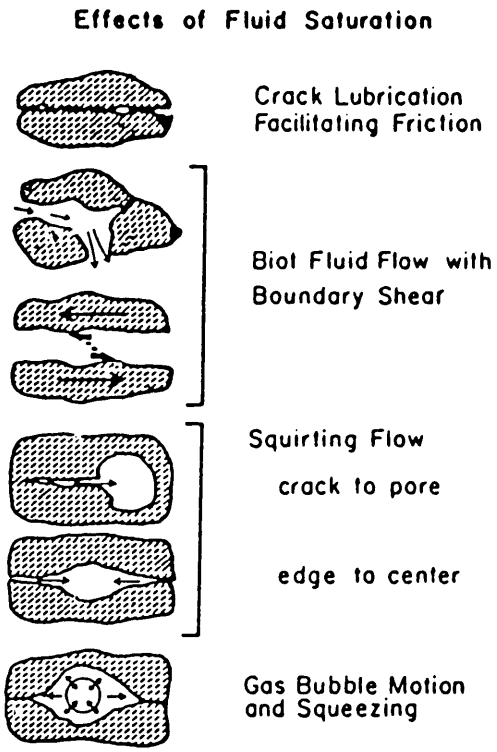

Figure 2.14 Schematic illustration of several proposed attenuation mechanisms for saturated and partially saturated rocks. (Johnston et al., 1979)

This mechanism may result in significant attenuation at seismic to ultrasonic frequencies. Mavko and Nur (1979) considered squirt flow in partially saturated cracks, where compression causes a liquid to flow into regions occupied by gas, resulting in significant attenuation at seismic frequencies.

2. 7. 3 Attenuation as a Function of Stress

As previously mentioned, the wave velocity changes significantly with pressure. This is also true for attenuation. When a rock is subjected to external pressure changes, as occur when stress is redistributed due to mining, the cracks in the rock will be closed. The crack closing induces an increase in elastic modulus. In all cases, attenuation decreases with increasing pressure at hydrostatic pressures (Johnston and Toksoz, 1980). The rate of attenuation decrease is higher at low pressures, and levels off at high pressures (Figure 2. 15). However, Lockner *et al.* (1977) pointed out that attenuation does not change the same way as velocity, which changes rapidly at low stress levels. Attenuation begins to decrease only when the stresses are sufficient to close the cracks, for Westerley Granite the stresses are about 500 bars (7350 psi). They also observed, when failure of Westerley Granite occurred, that the velocities had decreased by 12% - 30%, and the amplitude of waves had decreased by about 30%. Molina and Wack (1982) pointed out that the attenuation coefficient increases regularly with the compressive stress increase.

Thill (1972) suggested that the amplitude of the first received pulse increases as the confining pressure increases, and increases more rapidly in the low stress region. In the higher stress region the amplitude is nearly

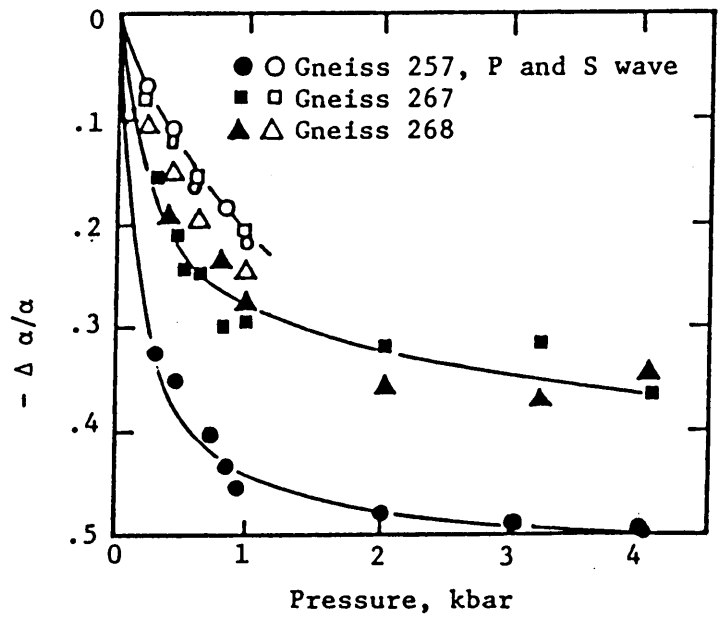

Figure 2.15 Change in the attenuation coefficients of P- and S-waves as functions of pressure for several gneisses. (Johnston et al., 1979)

constant, if the stress is increased further the amplitude will still remain constant or undergo little change. The amplitude increase is due to better coupling and crack closing. In contrast, the amplitude decrease is due to failure of the samples. Figure 2.16 shows how amplitudes are affected by the degree of jointing at varying confining pressures. Stacey (1976) suggested that the amplitudes of compressional waves and shear waves have great potential in assessing rock quality. Several observations have shown that in the same rock types under the same conditions the changes of attenuation are greater than changes of velocity (Johnston *et al.*, 1980; Winkler and Nur, 1982).

2. 8 TECHNIQUES OF SONIC TESTING

Three common methods may be applied to the sonic testing of rocks. They are the pulse echo method, the resonance method, and the pulse transmission method. Each method has applications and limitations which will be discussed in this section.

2. 8. 1 The Pulse Echo Method

The pulse echo method is mainly used for flaw detection (Figure 2.17) and works on a similar principle to that of navigational radar. Any physical flaws in a medium are likely to be acoustical discontinuities which will reflect ultrasonic waves. The travel time of an ultrasonic pulse transmitted from a transducer to a discontinuity and back again will give a measure of distance if the wave velocity in the medium is known. The location of the discontinuity can be determined and the magnitude of the echo will give some indications about the size of the discontinuity (Gooberman, 1968).

The advantages of this method are that only one surface of a specimen

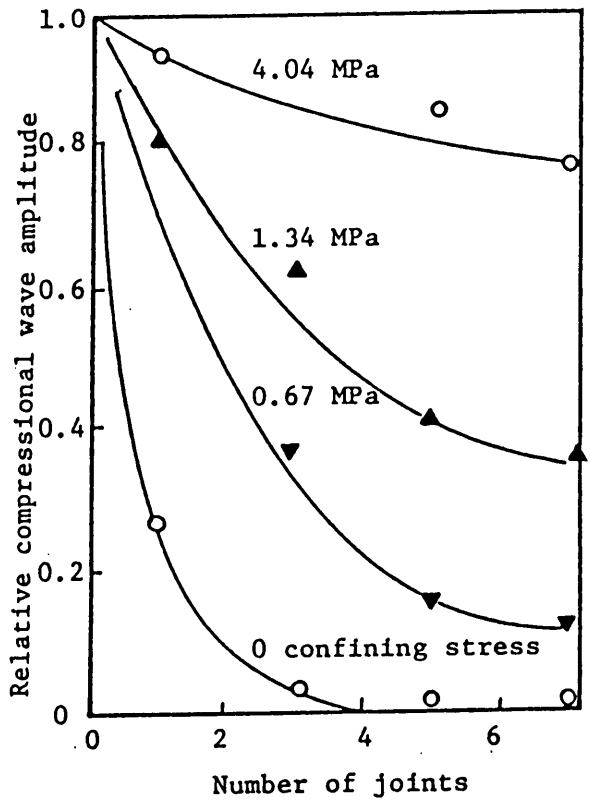

Figure 2.16 Relationship between compressional wave amplitude and number of joints (Stacy, 1976)

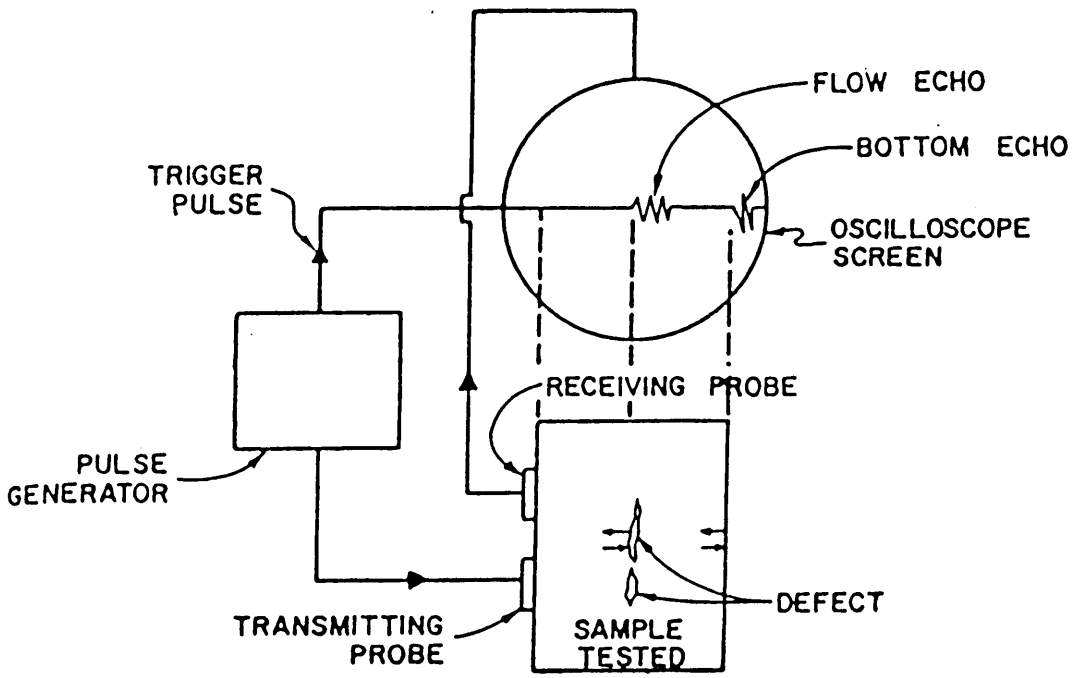

Figure 2. 17 The pulse echo technique.
(Tillman, 1978)

is required, and even a very small flaw in a large specimen can also be detected (Frederick, 1965).

2. 8. 2 The Resonance Method

The resonance method requires that a specific shape and size of rock specimen is supported or clamped at its center and induced to vibrate at its resonant frequency. The exciter and detector are appropriately located to excite and detect either longitudinal or torsional mechanical vibration. As the vibrational frequency approaches one of its resonant frequencies, a peak amplitude will be reached. A block diagram of resonant velocity measurement is shown in Figure 2.18. The torsional bar velocity (V_t) is equivalent to the shear velocity. The longitudinal bar velocity (V_o) can be calculated by the following equations (Lewis and Tandanand, 1974).

$$V_o = (f_n \times x) / (n \times k) \qquad (2.17)$$

$$= (2l \times f_n)/(n \times k) \qquad (2.18)$$

where: f_n is the resonant frequency of the nth longitudinal mode of vibration,

n is 1, 2, 3,...(order of vibration),

x is wavelength (m),

l is specimen length (m),

k is the correction factor.

The modulus of elasticity, E, can be computed by $E = \rho \times V_o^2$, and the modulus of rigidity, G, can be computed by $G = \rho \times V_t^2$, where ρ is weight density (kg/m^3).

In order to get an accurate resonant frequency, a cylindrical rod with a diameter to length ratio less than 0.2 is highly recommended. The resonance

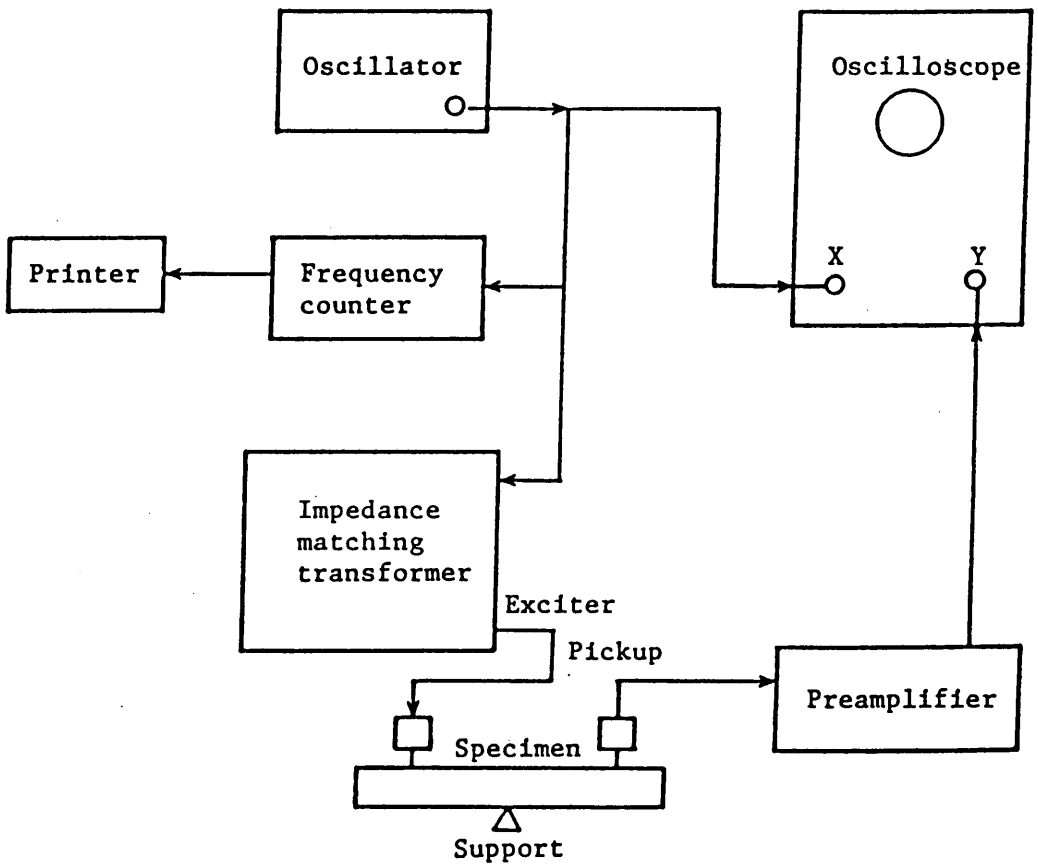

Figure 2.18 Resonance velocity measurement system. (Lewis and Tandanand, 1974)

method is the most convenient and accurate way to determine the bar velocity.

2. 8. 3 The Pulse Transmission Method

The pulse transmission method is best suited for determining the compressional and shear velocity in rocks. A rock sample is placed between transducers. One transducer acts as a transmitter, the other one acts as a receiver. Electrical pulses are supplied by a pulse generator. These electrical pulses are converted to mechanical waves by the transmitter and transmitted into the rock sample. After traveling through the sample, the mechanical waves are picked up by the receiver and reconverted to electrical pulses. Only the first arrival time is measured. This method can also be used in the field. A block diagram of the measurement system is shown in Figure 2.19.

The velocities of waves can be derived from (Lewis and Tandanand, 1974):

$$V_p \text{ or } V_s = S / T \qquad (2.19)$$

where: V_p and V_s are longitudinal and shear wave velocities, respectively,

S is travel distance or distance between transducers,

T is first arrival time.

From V_p and V_s, one can calculate Young's modulus by (Lewis and Tandanand, 1974):

$$E = \rho V_p^2 (1 + \nu) (1 - 2\nu)/(1 - \nu) \qquad (2.20)$$

$$E = \rho V_s^2 (3V_p^2 - 4V_s^2)/(V_p^2 - V_s^2) \qquad (2.21)$$

Poisson's ratio (ν) can be computed by (Lewis and Tandanand, 1974):

$$\nu = (V_p^2 - 2V_s^2)/(2(V_p^2 - V_s^2)) \qquad (2.22)$$

and bulk modulus (K) can be derived by:

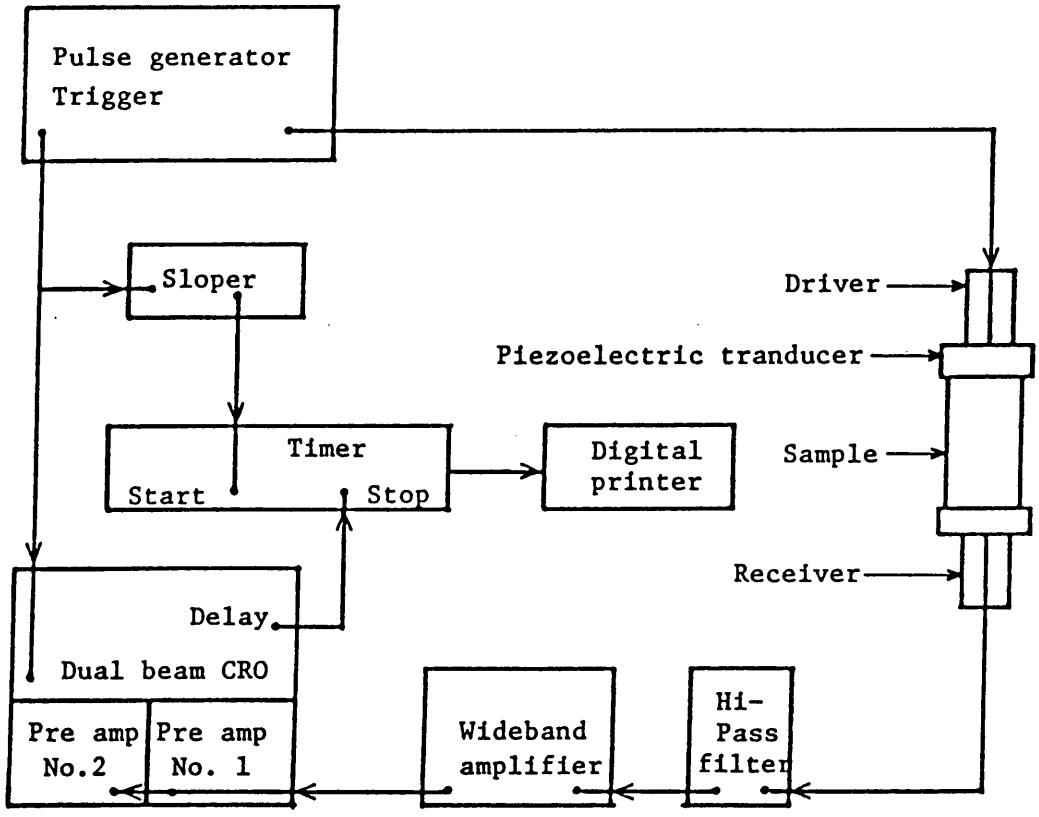

Figure 2.19 Ultrasonic pulse measurement system.
(Lewis and Tandanand, 1974)

$$K = \rho (3V_p^2 - 4V_s^2) / 3 \qquad (2.23)$$

2. 8. 4 Pulse Transmission Method for Determining Wave Velocity

The most common methods for determining wave velocity are the pulse transmission and the resonance methods. With the resonance method, the frequency is commonly in the range of 1 to 30 kHz, and with the pulse transmission method is in the range of 50 to 10,000 kHz. Therefore, the most notable difference between these two methods is the frequency under which the velocity is determined.

As mentioned in section 2.7.3, the pulse transmission method is best suited to measure wave velocity, therefore, it was selected for the velocity measurements in this study.

CHAPTER III

EXPERIMENTAL PROCEDURES

3.1 INTRODUCTION

In order to investigate the relationship between wave velocity, attenuation and strain of the rocks under different stress conditions, an experimental plan was designed making use of the MTS rock testing machine to conduct static and dynamic testing on a sample simultaneously. Unfortunately, the transducers detected a great deal of vibration signals coming from the vibration of the hydraulic system of the testing machine. These vibration signals masked the waveform to be detected, thus measurement was impossible. Therefore the strength tests, and the wave velocity and attenuation-under-stress tests were done separately and on different machines. The testing program will be described in detail in the following sections.

3.2 UNIAXIAL COMPRESSIVE STRENGTH TEST

One of the most important elastic constants is Young's modulus, which can be obtained from uniaxial compressive strength tests together with the strength of the tested sample. The modulus and strength are affected by both internal and external factors. The internal factors are mineralogy, grain size, porosity and jointing. The external factors are friction between platen and sample end surfaces, sample geometry, loading rate and testing environment.

3. 2. 1 Sample Preparation

Both cylindrical, NX (2.125 inch diameter) and cubic specimens were used in the testing program. The NX specimens were first cored from the collected samples. The 2276 core machine manufactured by Structural-Behavior Engineering Inc. was used. It is equipped with a water swivel, diamond core bit and 1.5 HP output power. The rotation speed can be varied from 150 rpm to 2000 rpm depending on rock type and core bit diameter.

The specimens were cut to have a length/diameter ratio between 2 - 2.5. The 24SS cutting machine (Highland Park Manufacturing Inc.) with an automatic feeding diamond disc saw was used to trim samples.

The end lapping of the specimens was flat to 0.025 mm and perpendicular to the axis to within 0.25°. A surface grinder manufactured by Swisher Co. with output power 1.5 HP and equipped with a fluid cooled, diamond cup-wheel was used. The preparation followed the specifications of ASTM (D2938) and the International Society for Rock Mechanics (Brown, 1981).

The cubic specimens were cut only by the slab saw without grinding. There were two sets of specimens for each of granite, sandstone and shale. The foliation of the mica in granite was cut to be both parallel and perpendicular to the long axis of separate sample sets. For sandstone samples, one set was dried naturally under room conditions for seven days. The other set was soaked in water for 7 days, and the bedding plane of shale was cut parallel and perpendicular to the long axis of each of two sets of samples.

3. 2. 2 Testing Equipment and Procedure

A one million pound capacity stiff testing machine manufactured by

M.T.S. was used to do the uniaxial strength test. The stiffness of the machine is achieved by using thick supports and loading parts as well as a feedback servo-control system. The system can remove load and machine strain energy very quickly as the specimen fails. A block diagram is shown in Figure 3.1.

The NX specimens were placed on the platen of the load frame. A constant loading rate, 100 psi/sec, was applied parallel to the long axis of specimen. A stress-deformation curve was plotted until sample failure. The Young's modulus and uniaxial compressive strength of a specimen can be determined from the load-displacement curve.

3. 3 WAVE VELOCITY AND AMPLITUDE MEASUREMENT

A pulse generator equipped with an oscilloscope, and a Sonicviewer were both used in measuring wave velocity and amplitude. Since the transducers were not designed to stand high pressure, the wave velocity and amplitude measurements could be made only in the direction perpendicular to the applied stress.

3. 3. 1 Measurement Equipment

The 350 high voltage pulse generator manufactured by the Velonex division of Varian was used. The characteristics of this pulse generator are a fast rise time (30 nanoseconds maximum) and adjustable pulse amplitude, duration, and repetition rate. The pulse amplitude can be varied from 0 to 400 volts, the peak voltage is 21 kV. The repetition rate is 3 to 100,000 pulses per second which can be varied in 9 steps. The pulse width can also be varied from 0.1 microseconds to 300 microseconds in 7 steps. The repetition

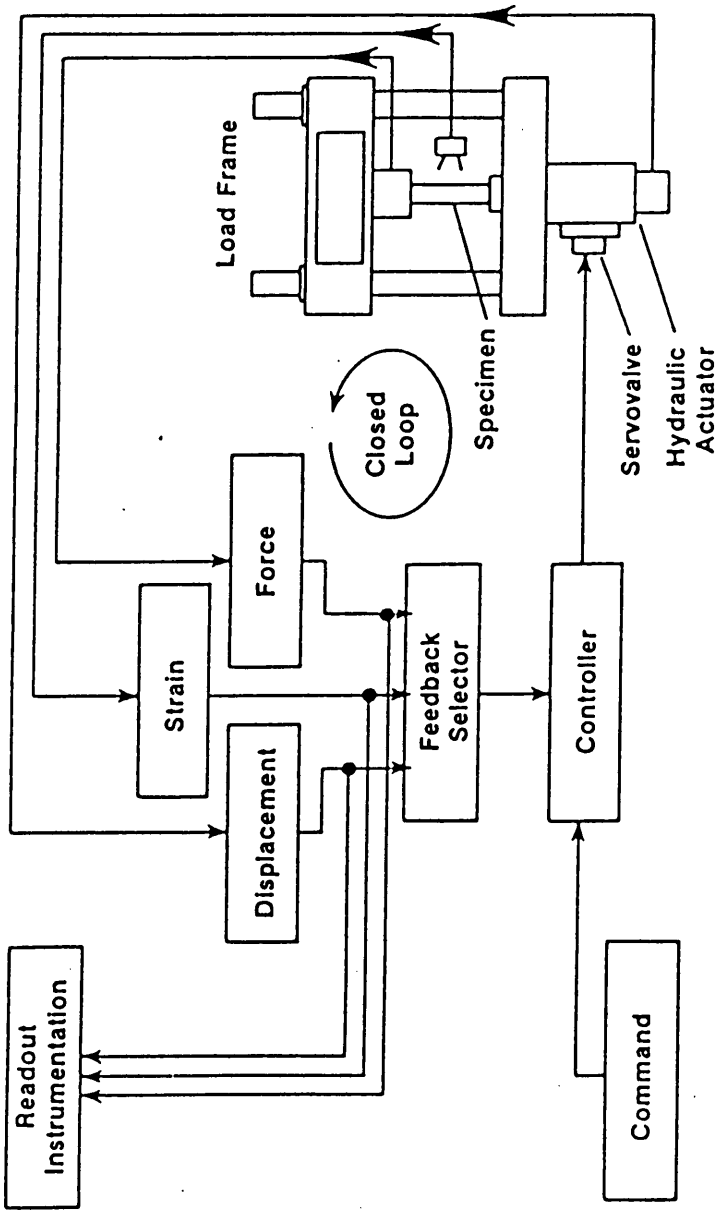

Figure 3.1 A block diagram of M.T.S. machine.
(M.T.S. Publication 160.03-01)

frequency and pulse width is controlled by a timing circuit. The processes are shown by a block diagram (Figure 3.2).

The 561A oscilloscope manufactured by Tektronix Inc., is essentially an indicator unit with provision for two plug-in units, 3B4 and 3A6. The 3B4 plug-in unit is a time base which controls the horizontal (X) deflection, and the 3A6 unit is a dual trace amplifier which controls the vertical (Y) deflection. The plug-in units can be changed in order to get the desired oscilloscope performance. The indicator unit consists of a cathode ray tube (CRT) and a calibrator. The calibrator is used to set an amplitude using a calibrated square wave. The rise time of the oscilloscope is 4 microseconds. The output voltage is ranged from 0.2 millivolts to 100 volts, peak to peak, in 18 steps. The horizontal sweep range is from 0.1 microsecond to 1 sec per division. The vertical band has a range from 0.01 volt to 10 volts per division.

A model 5217 New Sonicviewer manufactured by OYO Co. was used in measuring wave velocity. This unit is small, lightweight, and self-contained (Figure 3.3). It consists of a pulse generator, preamplifier, analog to digital converter, memory unit, cathode ray tube (CRT) and printer. It can be used to take velocity measurements of both rock samples in the laboratory, and rock mass in the field, with ultrasonic or sonic frequencies. The ultrasonic frequency is produced by a piezoelectric transducer, and the sonic frequency is induced by a hammer blow. The received waveforms can be shown on the cathode ray tube, the waveform image can also be printed from the built-in recorder. The first arrival time can be read directly from a cathode ray tube and also measured from the printed copy. The memory unit can store two waveforms which can be used for comparison purposes. The signal

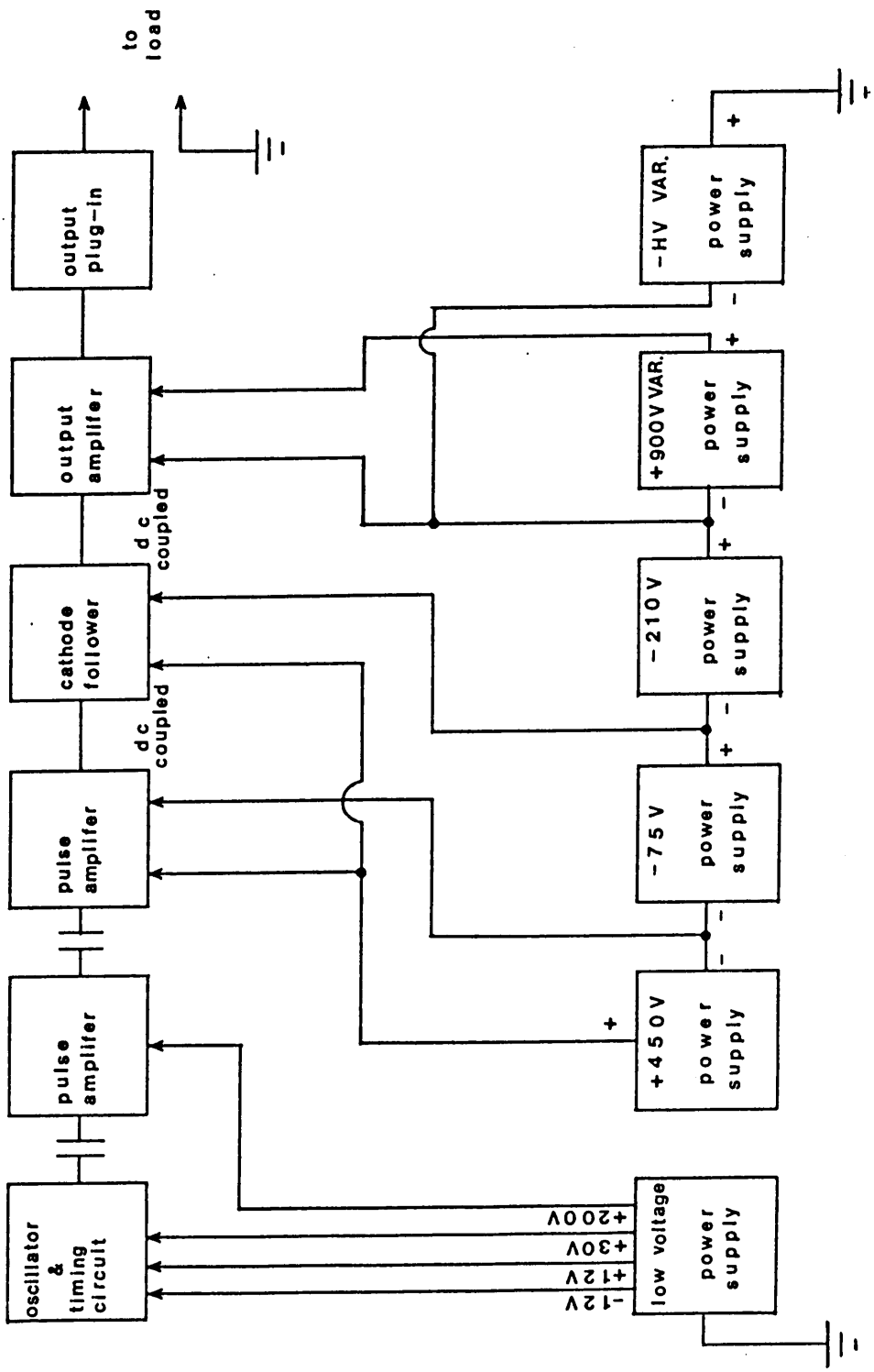

Figure 3.2 A block diagram of 350 pulse generator.
(Velonex instruction manual)

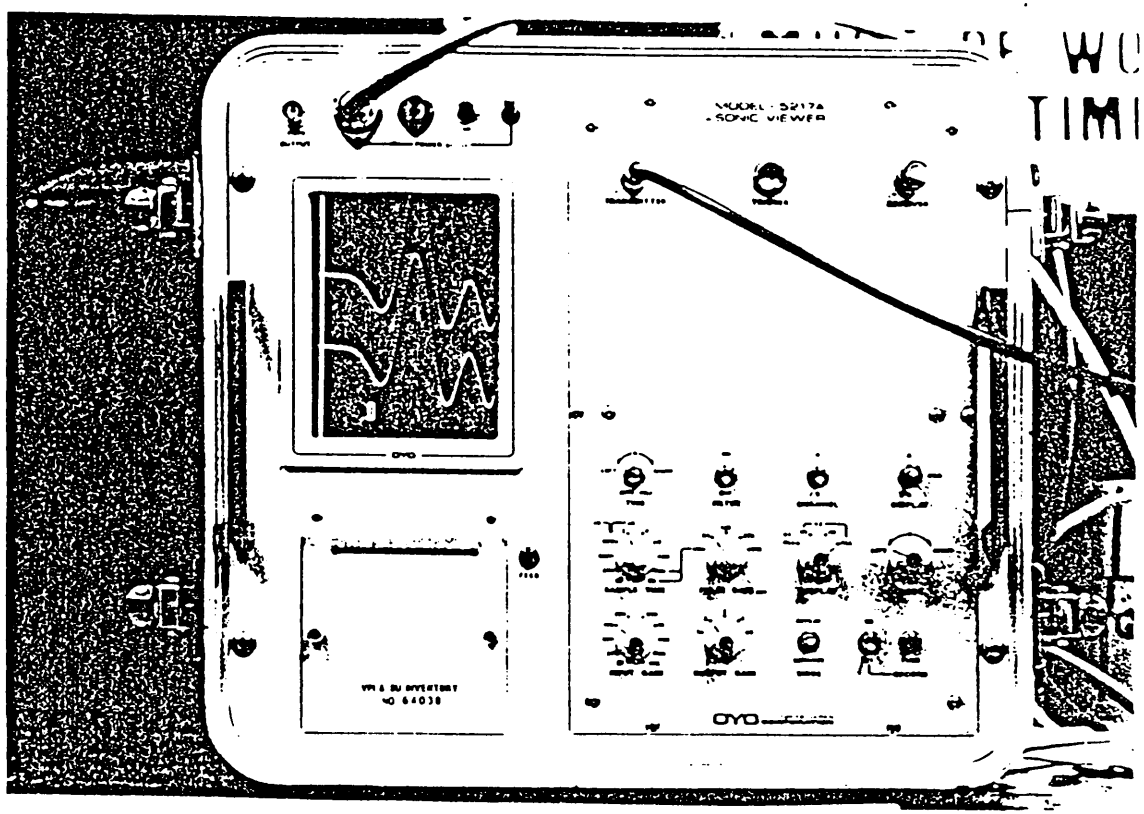

Figure 3.3: 5217 New Sonicviewer

enhancement feature allows the operator to build up a clear waveform even from a faint signal or weak input. A 12 volt battery is needed to supply power.

Transducers are used to convert electrical energy to mechanical energy and vice versa. A transducer converting electrical energy to mechanical energy and sending it into the sample under test is called a transmitter or emitter. The other one which receives mechanical energy from the tested sample and converts it to electrical energy is called a receiver. Two piezoelectric crystal P wave transducers were used for measuring P wave velocity and amplitude. The resonant frequency of the transducers was 2MHz.

In order to assure a good and constant contact between the transducer and rock sample during testing, the author designed a transducer holder which was made in the Mining Engineering Department workshop (Figure 3.4). The transducer holder consists of a frame part and a barrel part (Figure 3.5). The small barrels are used to hold the transducers, transducer supports and springs. The barrels are mounted on the frame and can be adjusted to contact different sizes of sample. A constant pressure is provided by the spring to make an even and repeatable coupling between the transducers and the tested sample. According to Hook's law $F = k \times X$, where F is force, k is the spring constant, and X is the compression or extension distance. Therefore, by fixing X, one can get a constant force or pressure from the spring.

3. 3. 2 Testing Procedures

A specimen was placed in a loading frame. The compressive load was provided by a 30 ton hydraulic jack which did not make any vibration during

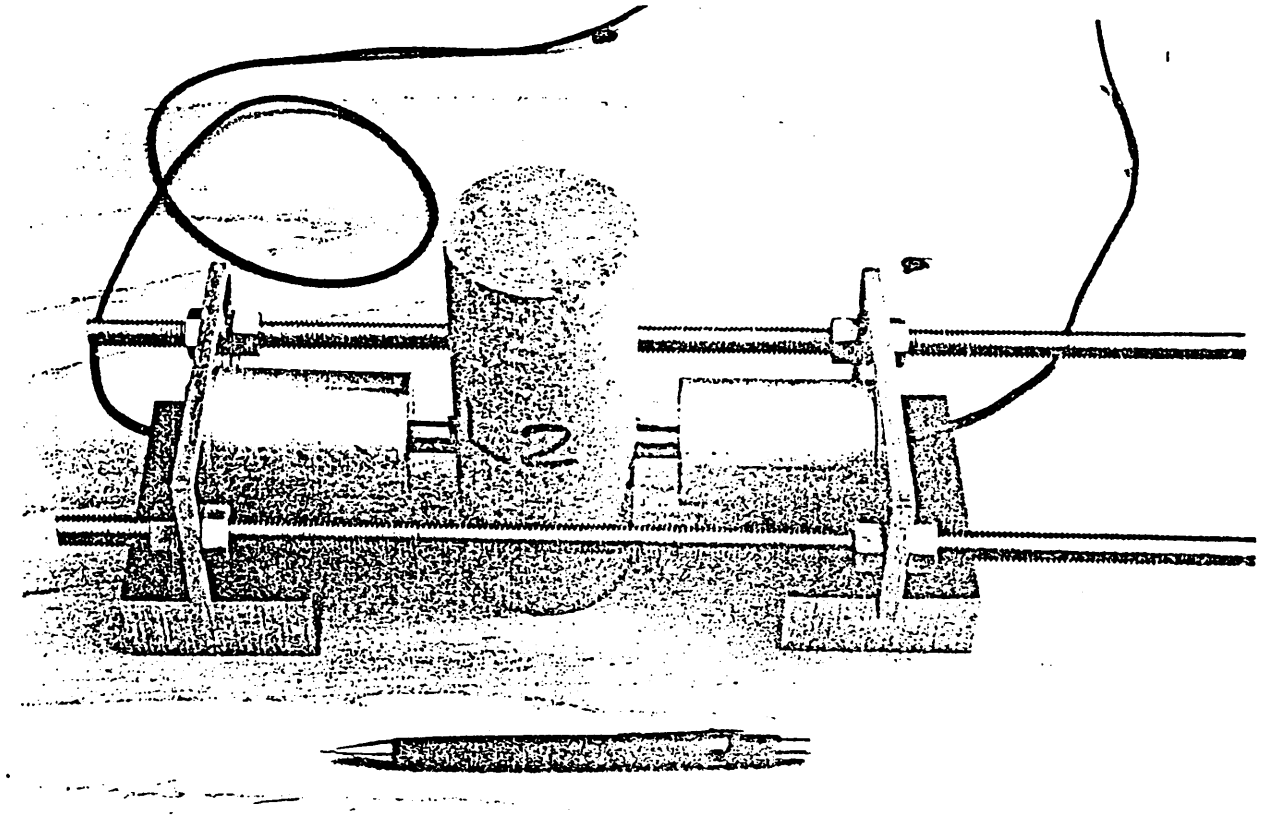

Figure 3.4: A general view of the transducer holder

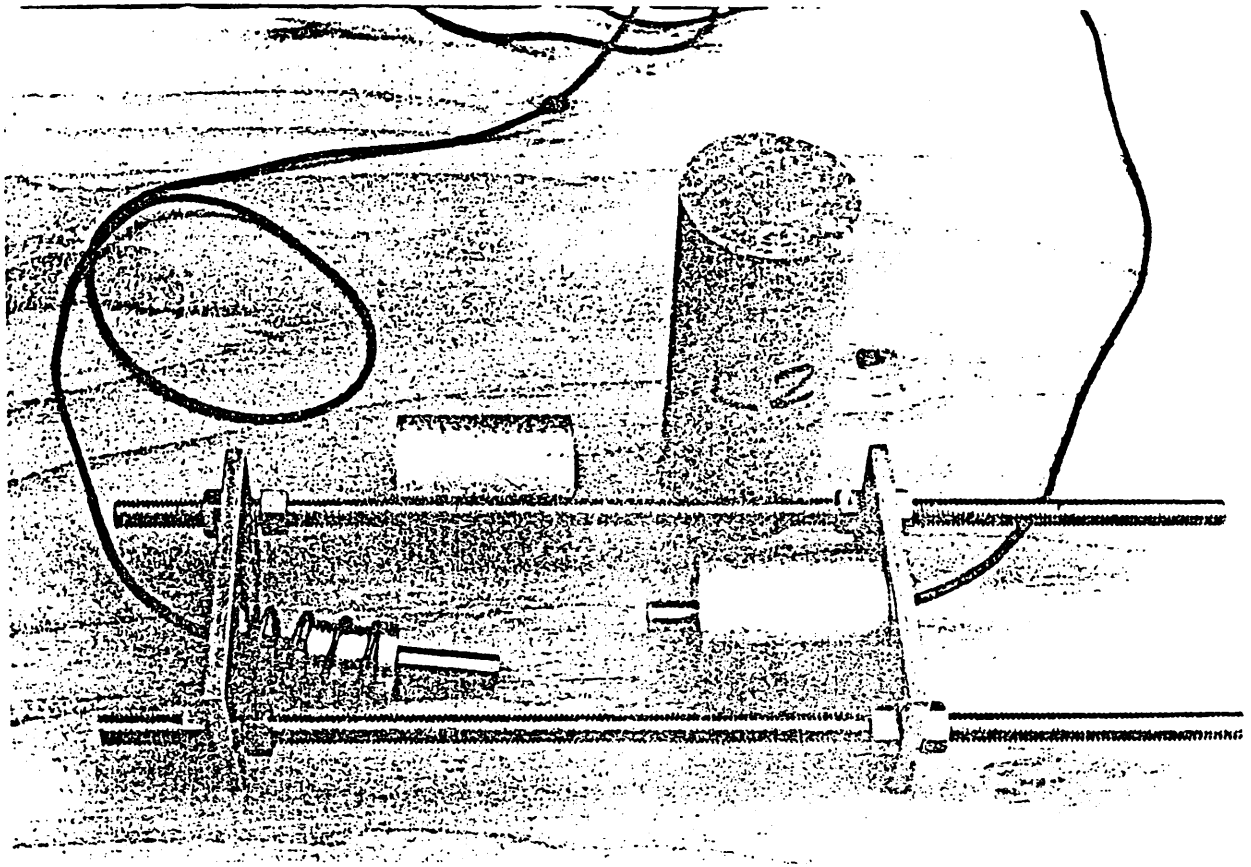

Figure 3.5: Exploded view of the transducer holder

and after pumping. Transducers were held in contact with the sample sides by the transducer holder with a constant pressure (about 10 psi) during the testing. Silicone grease was put between the P wave transducers and the sample in order to get a good coupling. Electric pulses were sent from the pulse generator. The first arrival time and the amplitude of the first peak under different stress levels were measured from the 561A oscilloscope. The stress was increased by one ton increments until rock failure occurred. The Sonicviewer was initially used to measure wave velocity and amplitude. However the waveform shown on its CRT has been digitized and cannot represent the real wave peak accurately. However it can be used in wave velocity measurement.

The absolute measurement of attenuation is more difficult than that of wave velocity. In addition to the mineral composition, grain size, texture, and porosity will also affect attenuation. Some other factors such as wave frequency, wave source intensity, and coupling between transducers and rock sample will also affect attenuation. In order to avoid this problem the incident pulse amplitude, the pulse frequency, the confining pressure on transducers and the location of emitter and receiver were fixed throughout the experiment. The only variable was axial stress. The testing equipment arrangement is shown in Figure 3.6.

3.4 DISCUSSION

A vernier caliper was used in measuring the dimensions of samples. The accuracy of the caliper is 0.001 inches. For the cylindrical samples, the diameter ranged from 1.950 to 2.125 inches, therefore the error in measuring the diameter was about 0.5%. For the cubic or prismatic samples, the

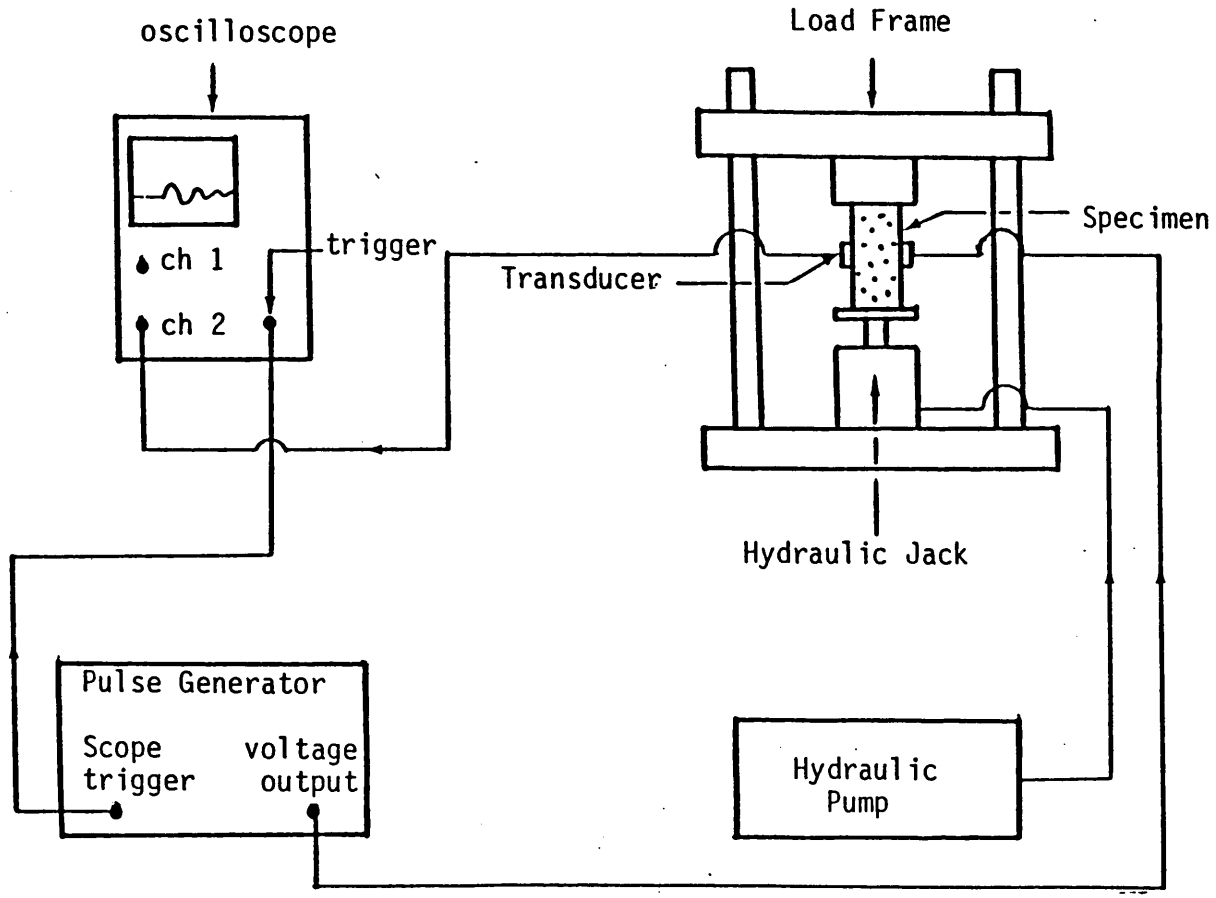

Figure 3.6. A block diagram of apparatus for sonic tests.

percentage of error in dimension measurement is less than that of the cylindrical samples.

The dimension error would affect the wave velocity as would the first arrival time. In some cases, the arrival time was not easy to identify. Before the first arrival, the trace on the CRT is supposed to be a straight line. However, this is not always the case. This problem occurred with some samples with the Sonicviewer, and the pulse generator when the pulse frequency was above 30 kHz and the stress was above 4000 psi. This was probably due to the microcracks and wavelength, as a short wavelength is easily affected by microcracks. The amplitude of the received wave is also affected by the coupling. For a better contact between the sample and the transducers, Schilizzi (1982) suggested putting PVC tape between the sample and the transducers, and one can also obtain good results by applying a thin layer of petroleum jelly on the contacting surface. However, it was found that better amplitude measurements can be obtained by applying a thin layer of silicon grease on the contact surface rather than PVC tape.

In order to improve the contact between the transducers and the curved sides of cylindrical samples, the sample surfaces on the opposite sides were ground off by about 0.06 inches. Therefore, by changing the line contact to face contact, more accurate measurement of amplitude could be obtained. The cross-sectional area of the sample only decreased by 1 - 2%, which had minimal effect on the stress-strain relationship. Additionally, in order to get more information from the test, multiple channels and receivers in the oscilloscope are needed, but multiple triggering should be prevented. The results of this testing are discussed in Chapter V. All the testing results are tabulated in Appendices A and B.

CHAPTER IV

GEOLOGICAL INFORMATION OF ROCK SAMPLES

4.1 SAMPLE DESCRIPTION

Samples of five different kinds of rock were used in this research. Marble and granite represent metamorphic and igneous rocks respectively, and both rocks can be quarried from surface or underground to be either a dimension or crushed stone and are very important construction materials. Sandstone, shale and limestone represent sedimentary rocks and are coal measure rocks.

4.1.1 Marble

Marble samples were collected from the Imperial Quarry, operated by the Vermont Marble Company, in Danby, Vermont. The Danby deposit belongs of the marble belt of the Vermont Valley which lies in the lowland between the Taconic Range on the West and the Green Mountains of the East (Figure 4.1). The Danby marble is located in the Columbian marble member of the Shelburne formation of Ordovician age. The formation consists of white calcitic marble with minor beds of light grey marble. The strike of the formation is N5°W, and dip is 80 - 90°E. The structure represents a syncline plunging to the south at approximately 6° with evidence of small drag flow folding to the west and south (Hewitt, 1961). The color of the marble is white with narrow dark grey bands. The calcite crystals are about 0.02 inch long and have been recrystallized. The density ranges from 0.097 to 0.098 lb/in^3.

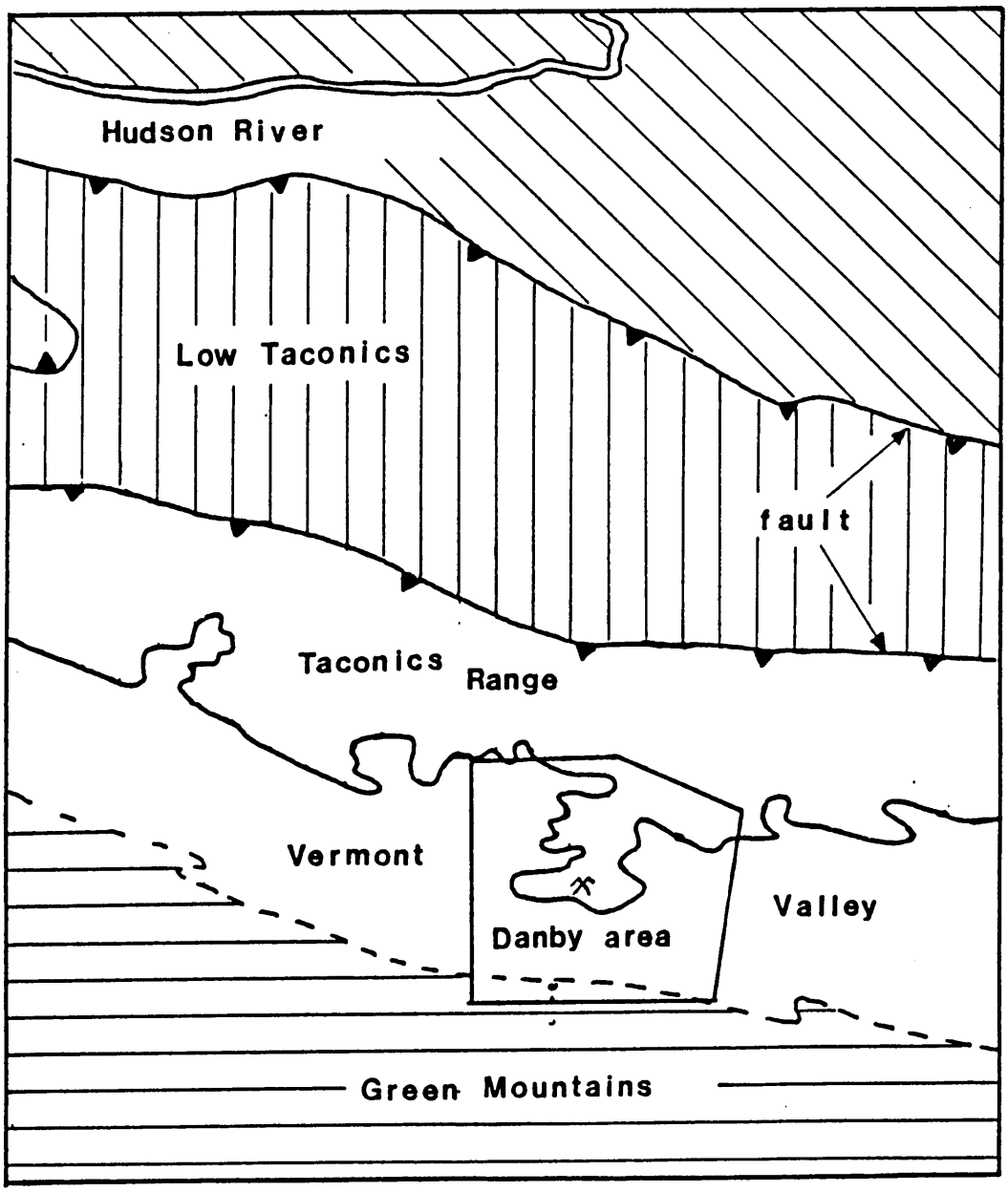

Figure 4.1 Geological map of Danby area.
(after Hewitt, 1961)

4. 1. 2 Granite

Granite samples were collected from the Mount Airy Granite Quarry, Surry County, North Carolina. Surry County is located in the Western Piedmont division of the Piedmont Plateau. The division is mostly underlain by pre-Cambrian gneisses and schists, penetrated in some places by granitic rocks which tend to form narrow northeast trending belts. Outcrops of granite in the Western Piedmont generally are limited to scattered boulders and flat-surface outcrop. The quarry is located over an area covering more than a hundred acres at a top and on the gentle slope of a large dome-like flat-surface outcrop. The deposit is a massive, uniform outcrop and is free from natural bedding planes and vertical cracks.

It is a surface dimension stone quarry. The granite is a biotite granite with a very light grey medium grain. The main components are quartz, feldspar, and biotite. The biotite has some tendency to segregate in streaks. However, all the minerals are evenly distributed. The rock has a uniform texture (Bates, 1969). The density varies from 0.092 to 0.097 lb/in^3.

4. 1. 3 Shale

Shales were collected from Beatrice Mine of the Island Creek Coal Company, Buchanan County, Virginia. They were from the top of the Pocahontas No. 3 coal seam within the Pocahontas Formation which is of Pennsylvanian age. The shale is dark grey, fine grained, with fine coal veins occasionally. The density ranges from 0.095 to 0.131 lb/in^3. Samples of the seat earth below this coal seam could not be prepared into suitable specimens for the testing program. The coal seam in the area where the shale samples were collected was mined by the room and pillar method.

4. 1. 4 Sandstone

Sandstone cores were obtained from the Carbon Fuel Company in the Cabin Creek District of Kanawha County, West Virginia. The hole was located just north of Dotson Fork off Slaughter Creek (Lessley, 1984). The hole was drilled vertically downward from the bottom of the Allegheny formation through the upper 900 ft of the Kanawha formation of the Pottsville group. Both of the formations are of Pennsylvanian age. The sandstone is grey, and fine to medium grained. The main components are quartz, mica and clay with grey shale streaks. The density varies from 0.085 to 0.097 lb/in^3. It is conglomeritic occasionally.

4. 1. 5 Limestone

Limestone samples from two different areas were tested in the laboratory. The limestone core samples were obtained from the U.S. Gypsum Co. and were cored from several vertical exploration holes drilled from the surface in Saltville, Virginia. However, the location of each drill hole cannot be identified. In the Saltville area, the limestone is found in the Little Valley Limestone formation which is of Mississippian age (Figure 4.2). The Little Valley Limestone formation consists predominantly of black, fine-grained argillaceous limestone. The density is in the range of 0.096 to 0.099 lb/in^3.

Several limestone blocks were collected from the Kimballton Mine, Virginia Lime Co., in Giles County, Virginia. The Kimballton Mine is mining limestone from the upper 65 feet of the Five Oaks limestone member which belongs to the Cliffield formation of Ordovician age. The thickness of the Five Oaks limestone member varies from 40 to 100 feet. It has its maximum thickness at locality 16 where it is close to the Kimballton Mine.

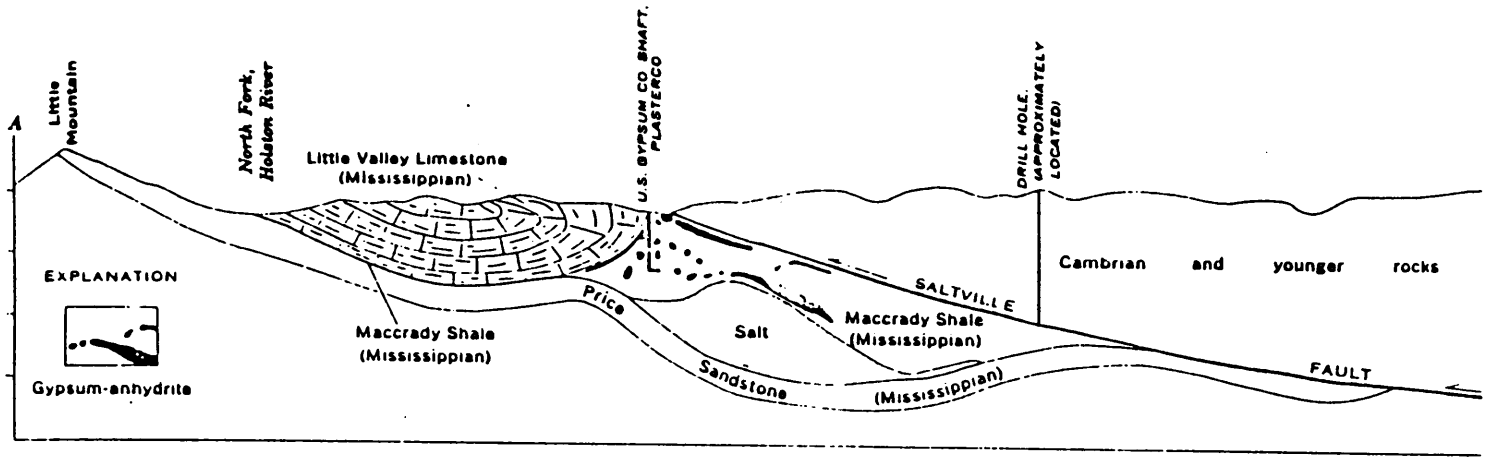

Figure 4.2 Crosssection geological information of Saltville. (after Nelson, 1958)

Figure 4.3 shows the distribution of limestone in the region of the Kimballton Mine. The Five Oaks limestone has a strike of N40°E and dips to the SE at 35° in this area and it gradually flattens to the northeast. The limestone of this member is very uniform, fine grained, dark gray, and contains high calcium.

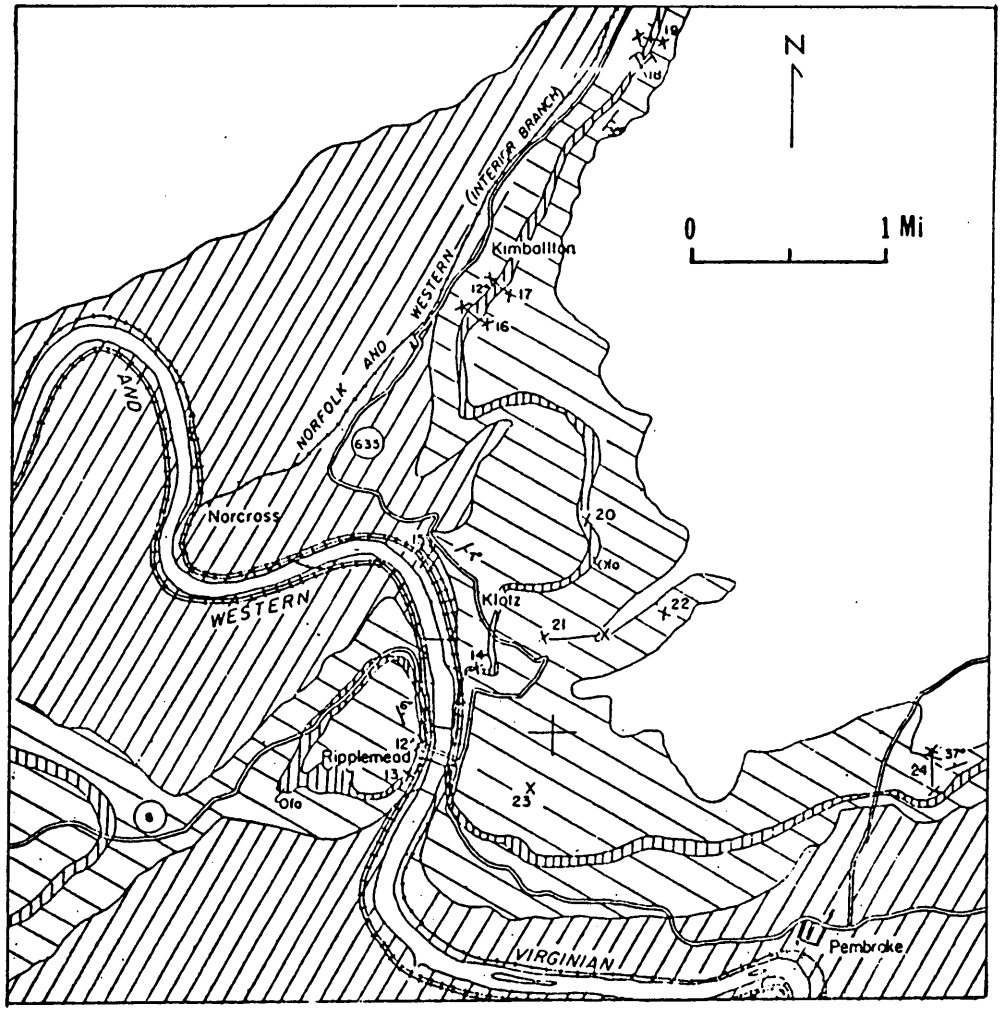

LEGEND

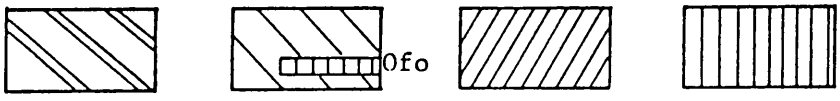

Limestone Mississippian

Limestone Ordovician

Dolomite Cambrian and Ordovician

Shale Cambrian

Ofo Ordovician Five Oaks member

Figure 4.3 Limestone distribution around Kimballton area. (Cooper, 1944)

CHAPTER V

TESTING RESULTS AND DISCUSSION

The results of the laboratory testing were analyzed statistically. A SAS program, developed by North Carolina University, and available on the mainframe computer at VPI has been applied to determine the mean, standard deviation, and correlation coefficient of strength and modulus of rocks. In addition, a regression model and SAS graph were made to visually inspect the relationships which exist between velocity ratio and stress, and between attenuation coefficient ratio and stress.

5.1 UNIAXIAL COMPRESSIVE STRENGTH

The uniaxial compressive strength and Young's moduli of rocks were calculated from the load-displacement curve. For air-dried sandstone samples the strength ranged from 10,630 to 15,920 psi and the Young's modulus ranged from 2.3×10^6 to 1.4×10^6 psi. For water saturated sandstone samples, the strength ranged from 9,650 to 12,570 psi, and the Young's modulus ranged from 1.0×10^6 to 1.7×10^7 psi. The differences in the strength and elastic modulus of samples from the same locality result from the inhomogeneity of the rocks. The variation of the axial stress and strain curves for cylindrical specimens of the dry sandstones are shown in Figure 5.1. Representative curves of the axial stress-strain results for cylindrical specimens of different rocks are shown in Figure 5.2. A summary of the mean strength and Young's modulus of different rock types is given in Tables 5.1 and 5.2, respectively.

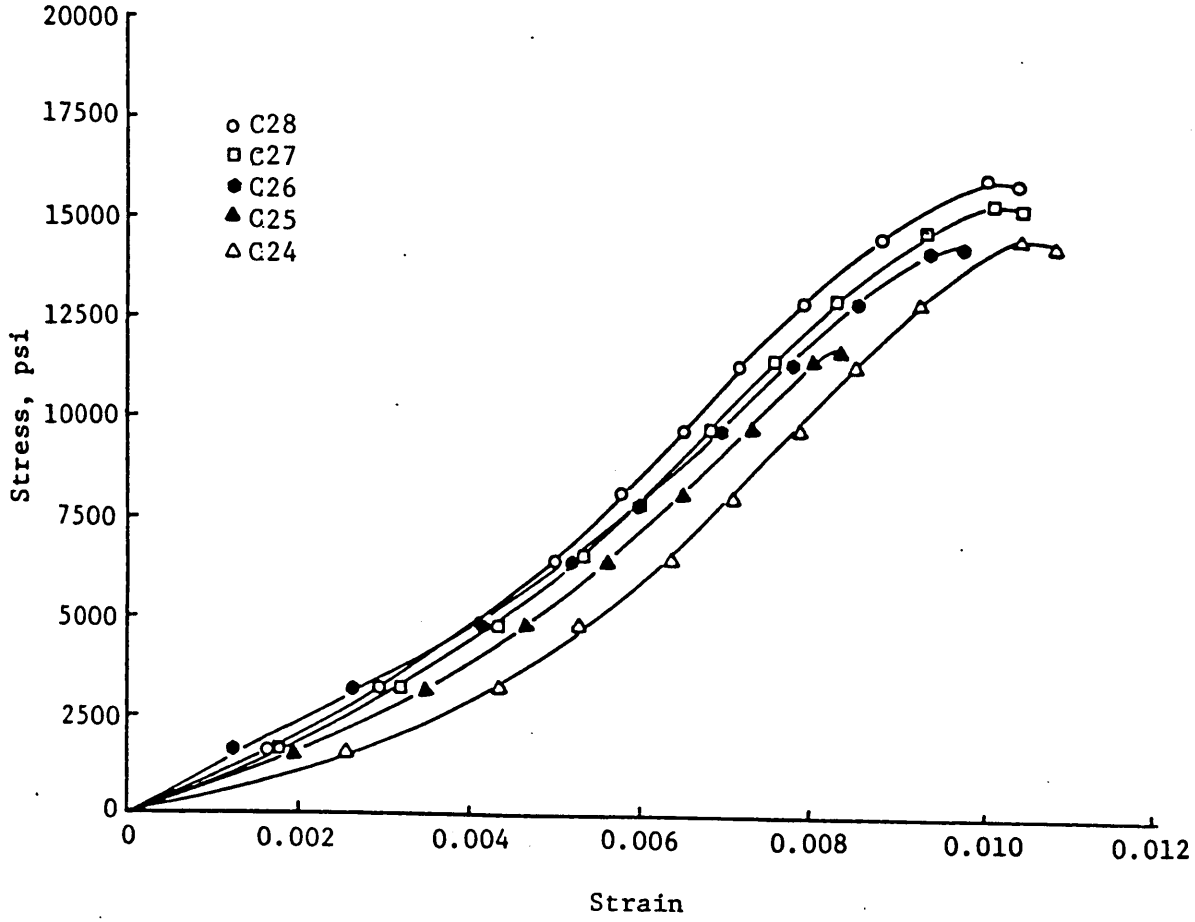

Figure 5.1 Stress-strain curves for dry sandstone under uniaxial compression.

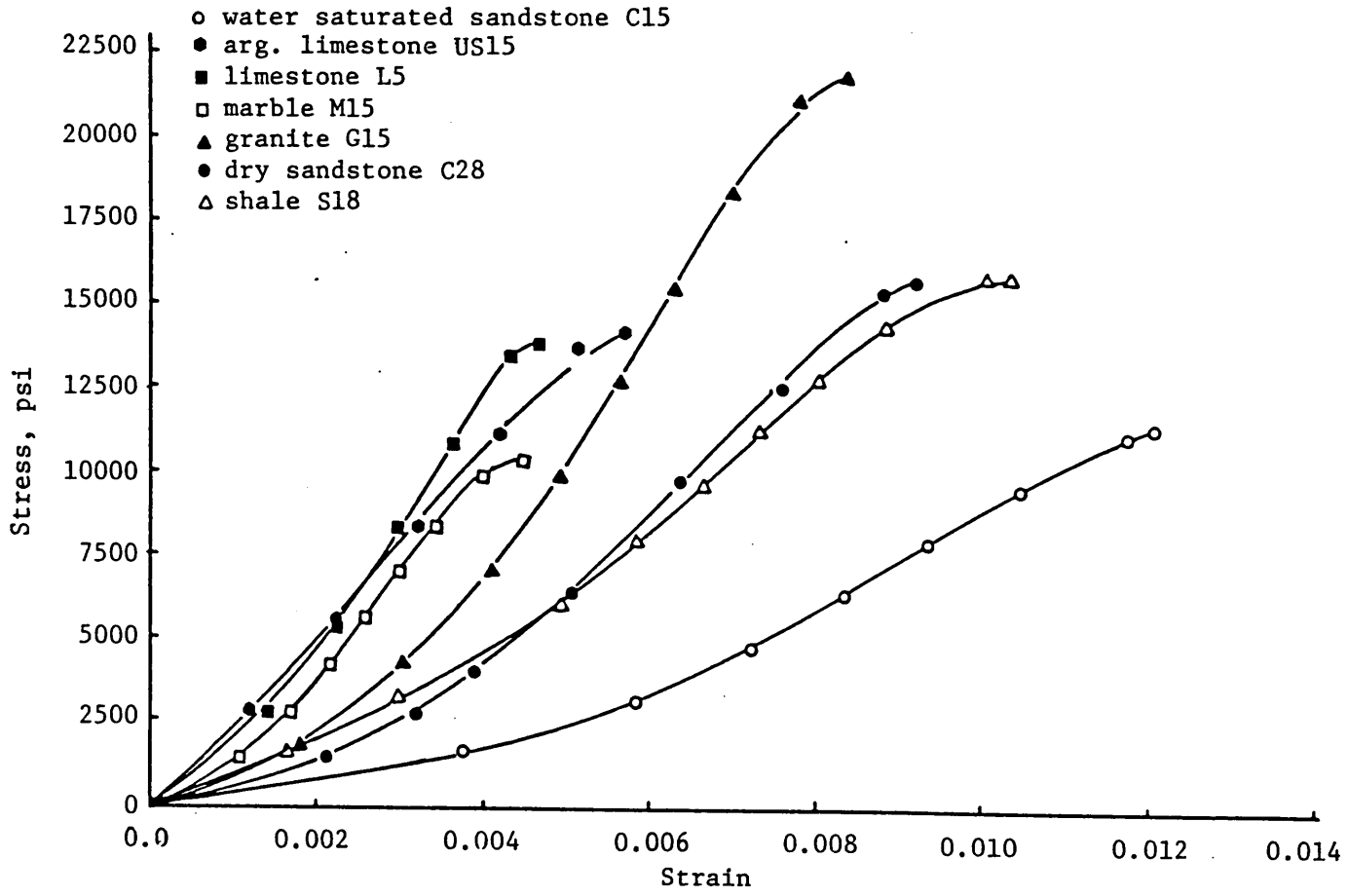

Figure 5.2 Stress-strain curves for rocks under uniaxial compression.

TABLE 5.1

Summary of the Compressive Strength Values of Samples

Rock Type	No. of Sample	Mean Strength (psi)	Standard Deviation	Minimum Strength(psi)	Maximum Strength(psi)
Marble	6	10648	331	10208	11038
Sandstone (dry)	5	14113	2075	10631	15915
Sandstone (wet)	6	10142	1254	8769	11414
Limestone (Arg.)	6	11890	1496	9758	13914
Limestone (Five Oaks)	4	16474	2990	12136	18981
Shale	5	12696	4304	8201	18216
Granite	6	17426	4627	11279	22590

TABLE 5.2

Summary of Young's Modulus of Samples

Rock Type	No. of Sample	Mean Value (psi)	Standard Deviation	Minimum Value(psi)	Maximum Value(psi)
Marble	6	4009519	1167388	2734393	6184490
Sandstone (dry)	5	1974395	355531	1401946	2319444
Sandstone (wet)	6	1377908	230322	1020013	1689601
Limestone (Arg.)	6	2251488	643178	1009674	2898527
Limestone (Five Oaks)	4	3608052	1113235	2454009	4979419
Shale	5	2628904	239982	2304130	2955708
Granite	6	2987903	846547	1724747	3999834

5.2 VELOCITY AND AMPLITUDE MEASUREMENT

The specific parameters measured in the sonic measurements were P wave velocity, P wave amplitude and the attenuation coefficient. The attenuation coefficient was computed using equation 2.14. The attenuation coefficient ratio (A/A_0) is the ratio of the attenuation coefficient at a specific stress (A) to the attenuation coefficient at zero stress (A_0). The velocity ratio (V/V_0) is the ratio of the velocity at a specific stress (V) to the velocity at zero stress (V_0). For marble at zero stress the wave velocity is 17,543 ft/sec, the attenuation coefficient is 7.7 dB/in. At 5000 psi, its wave velocity is 17,777 ft/sec and the attenuation coefficient is 9.25 dB/in. Therefore, at 5000 psi the velocity ratio is 1.01 and the attenuation coefficient ratio is 1.21. For argillaceous limestone, the wave velocity ranges from 15,895 ft/sec to 15,697 ft/sec under stress levels ranging from 0 to 9200 psi. Their attenuation coefficients vary from 6.73 dB/in to 13.08 dB/in. The value of their velocity ratios varies from 0.98 to 1.0 and that of their attenuation coefficient ratios varies from 1.0 to 1.94. Thus, it can be seen that the attenuation coefficient is more sensitive to stress change for these rocks.

Tables 5.3 and 5.4 show the correlation coefficients between velocity ratio and stress, and between attenuation coefficient ratio and stress for second, third and fourth order polynomials respectively. Under the same significance level (0.0001), the second order polynomial equation may be the most simplified and adequate way to describe the relationship that exists. Most of the correlation coefficients are above 0.90 for the stress and velocity ratio, and, for stress and attenuation, the coefficient is about 0.99. The constants for all the second order polynomial equations are listed in tables 5.5 and 5.6.

TABLE 5.3
Correlation Coefficient between Velocity Ratio and Stress for Different Order Polynomials

Rock Type	2nd Order	3rd Order	4th Order
Sandstone (dry)	0.998	0.998	0.999
Sandstone (wet)	0.957	0.993	0.995
Limestone (Arg.)	0.957	0.991	0.994
Limestone (Five Oaks)	0.816	0.850	0.866
Shale (perpendicular)	0.923	0.968	0.991
Shale (parallel)	0.895	0.933	0.957
Granite (parallel)	0.993	0.993	0.997
Granite (perpendicular)	0.993	0.996	0.997
Marble	0.969	0.983	0.988

TABLE 5.4

Correlation Coefficient between AttenuationRatio and Stress for Different Order Polynomials

Rock Type	2nd Order	3rd Order	4th Order
Sandstone (dry)	0.999	0.999	0.999
Sandstone (wet)	0.972	0.989	0.996
Limestone (Arg.)	0.997	0.999	0.999
Limestone (Five Oaks)	0.999	0.999	0.999
Shale (perpendicular)	0.993	0.996	0.996
Shale (parallel)	0.993	0.994	0.994
Granite (parallel)	0.999	0.999	0.999
Granite (perpendicular)	0.997	0.998	0.999
Marble	0.978	0.998	0.999

TABLE 5.5

Constants for Velocity Ratio Equation of Different Rocks

Rock Type	c (10^{-9})	b (10^{-5})	a
Sandstone (dry)	-1.213	1.847	1.000
Sandstone (wet)	-1.896	1.780	1.000
Limestone (Arg.)	-0.016	-0.143	1.000
Limestone (Five Oaks)	-0.087	0.081	1.000
Shale (perpendicular)	-0.004	0.007	1.000
Shale (parallel)	-0.197	0.235	1.000
Granite (parallel)	-1.923	3.210	1.000
Granite (perpendicular)	-2.883	4.088	1.000
Marble	-3.414	1.847	1.000

TABLE 5.6

Constants for Attenuation Ratio Equation of Different Rocks

Rock Type	c (10^{-9})	b (10^{-5})	a
Sandstone (dry)	-1.923	8.584	1.000
Sandstone (wet)	0.210	1.779	1.000
Limestone (Arg.)	7.904	2.823	1.000
Limestone (Five Oaks)	0.277	1.647	1.000
Shale (perpendicular)	1.618	-2.769	1.000
Shale (parallel)	2.161	0.388	1.000
Granite (parallel)	-0.011	1.766	1.000
Granite (perpendicular)	0.668	-1.551	1.000
Marble	3.101	3.069	1.000

5. 2. 1 Velocity Measurement

The effect of the axial stress on the compressional wave velocity observed in this study is consistent with that observed in previous investigations (Lockner, 1977; Gladwin, 1982; Su, 1982). The P wave velocities increase significantly under low stress (at 0 - 2000 psi level) as compared to the wave velocity at zero stress. At higher stress (from 2000 to 6000 psi and above), the velocities increase only slightly or even flatten off. When the stress exceeds a certain critical value the velocity decreases. These characteristics can be explained by Bieniawski's fracture process concept (Bieniawski, 1967) or Price's rock deformation curve (Price, 1979). The relationship between velocity and stress is schematically shown in Figure 5.3. During stage AB, the rock is being initially stressed and the prexisting pore spaces, or microcracks, orientated at suitable angles to the stress, will be closed. These will increase the wave velocity significantly. Between B and C, the rock is undergoing recoverable (linear) elastic deformation. The elastic modulus is constant and the dilation is not significant. The density (ρ) may or may not change. The velocity, $v = (E/\rho)$, will increase slightly or even remain constant. From C to D, fracture is initiated and the rock is under partially recoverable deformation which causes the wave velocity to decrease. During stage DE, the rock undergoes irrecoverable deformation, fracture propagates unstably, and thus wave velocity decreases until rock failure occurs. The curve of the wave velocity ratio versus axial stress is similar to that of velocity versus stress.

Figures 5.4 and 5.5 show the velocity ratios of air-dried sandstone plotted against the applied axial stress. At zero stress, the mean velocity of dry sandstone is 12,498 ft/sec and that of water saturated sandstone is 13,950 ft/sec.

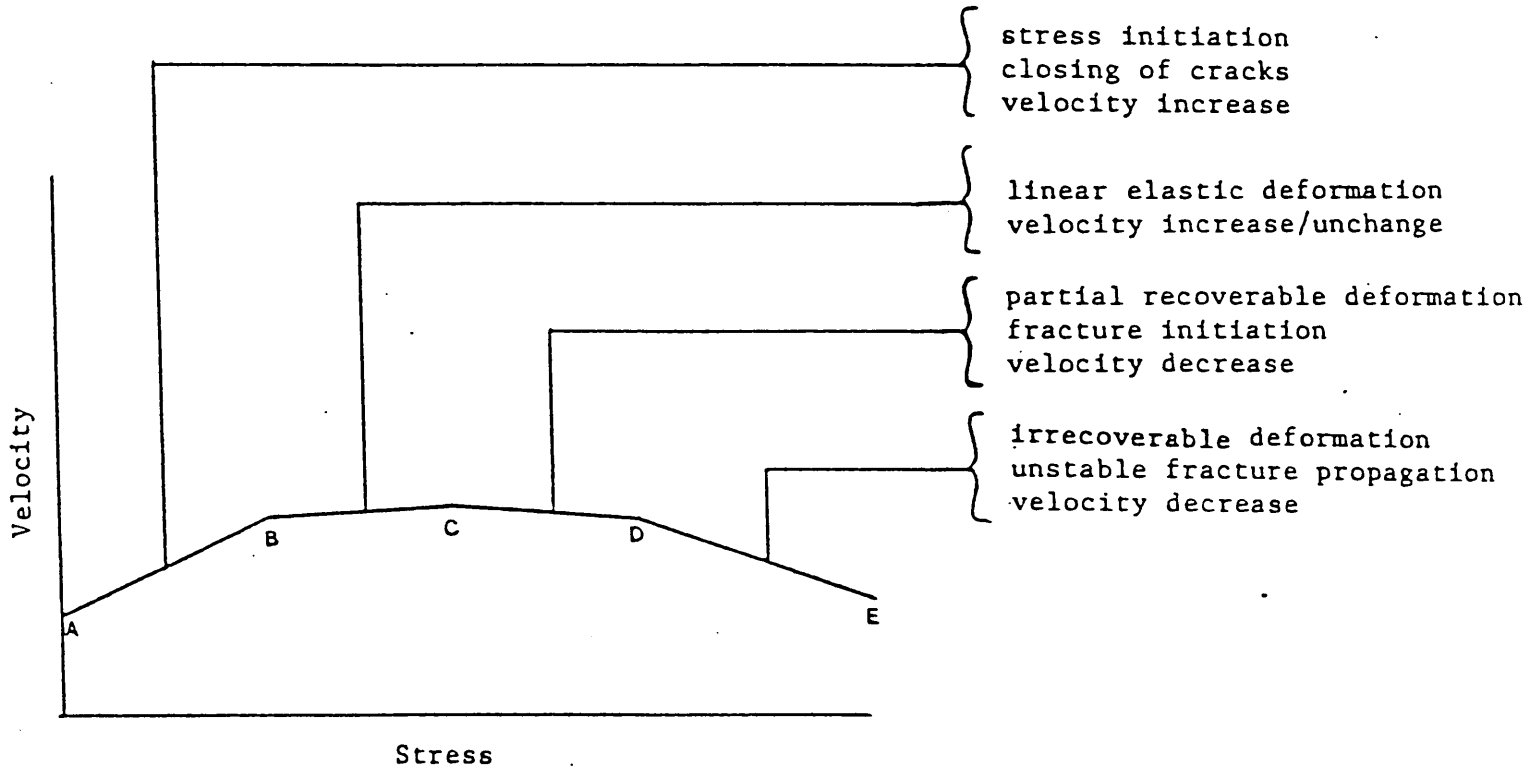

Figure 5.3 Schematic showing the relation of the wave velocity to stress.

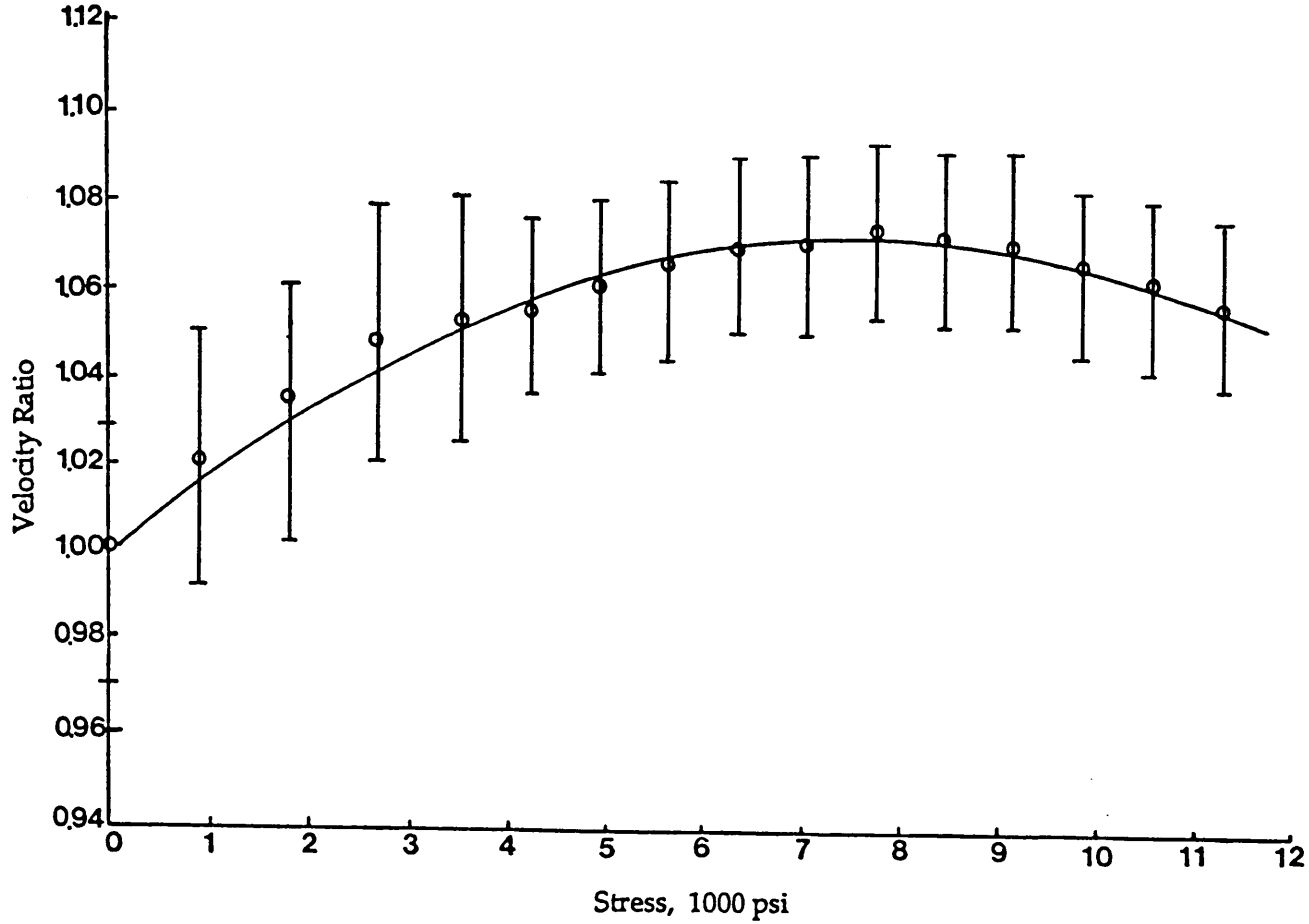

Figure 5.4 Velocity ratio versus uniaxial compressive stress for dry sandstone samples.

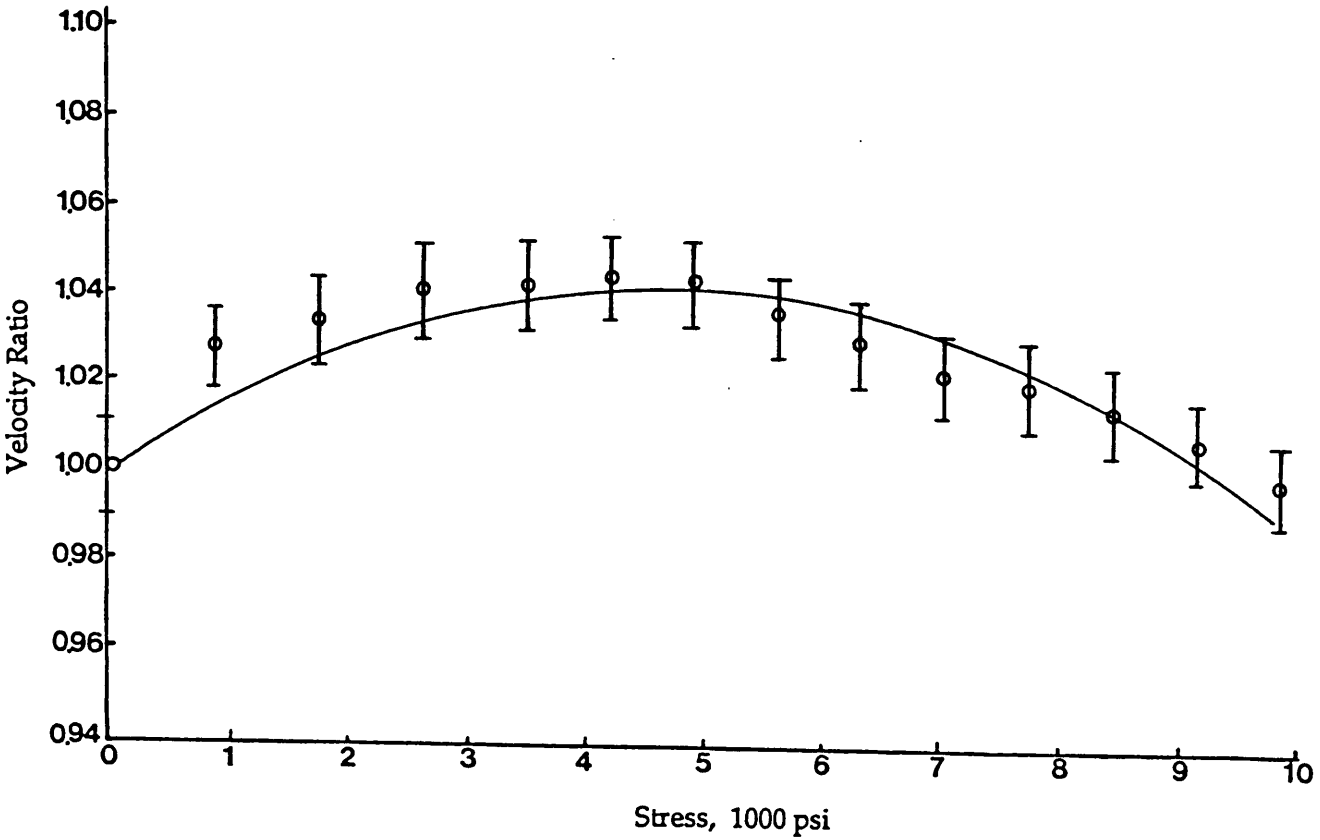

Figure 5.5 Velocity ratio versus uniaxial compressive stress for water saturated sandstone samples.

There is about a 12 % velocity increase from dry sandstone to water saturated sandstone at zero stress. At 5000 psi, the velocity in water saturated sandstone increases about 10% as compared to the dry samples under same stress. At 10,000 psi, this velocity increase is only about 6%. These result from the fact that waves travel faster in water than in air (See Table 2.2). At zero stress, in water saturated samples, all the pores and cracks are filled with water which gives rise to the large increase in velocity as compared to air-dried samples with same porosity. At higher stress levels, the pores and cracks are partially closed, and the water content decreases, which results in a smaller increase in velocity as compared to the air-dried samples under the same stress. A second order relationship between the stress (σ) and wave velocity in the direction perpendicular to the applied stress was obtained using the SAS program.

The calibration curve for dry sandstone is:

$$V/V_o = 1.00 + 1.847 \times 10^{-5}\,\sigma - 1.213 \times 10^{-9}\,\sigma^2. \qquad (5.1)$$

The calibration curve for water saturated sandstone is:

$$V/V_o = 1.00 + 1.780 \times 10^{-5}\,\sigma - 1.896 \times 10^{-9}\,\sigma^2. \qquad (5.2)$$

The calibration curves for the two sets of granite are shown in Figures 5.6 and 5.7 respectively. The result indicates that, when the applied stress is parallel to the mica foliation, the measured velocity is slower than that of the samples with the applied stress perpendicular to the mica foliation. The relationship between the velocity ratio and stress for the granites can be expressed as:

$$V/V_o = 1.00 + 3.210 \times 10^{-5}\,\sigma - 1.923 \times 10^{-9}\,\sigma^2 \qquad (5.3)$$

(applied stress parallel to the foliation),

$$V/V_o = 1.00 + 4.088 \times 10^{-5}\,\sigma - 2.883 \times 10^{-9}\,\sigma \qquad (5.4)$$

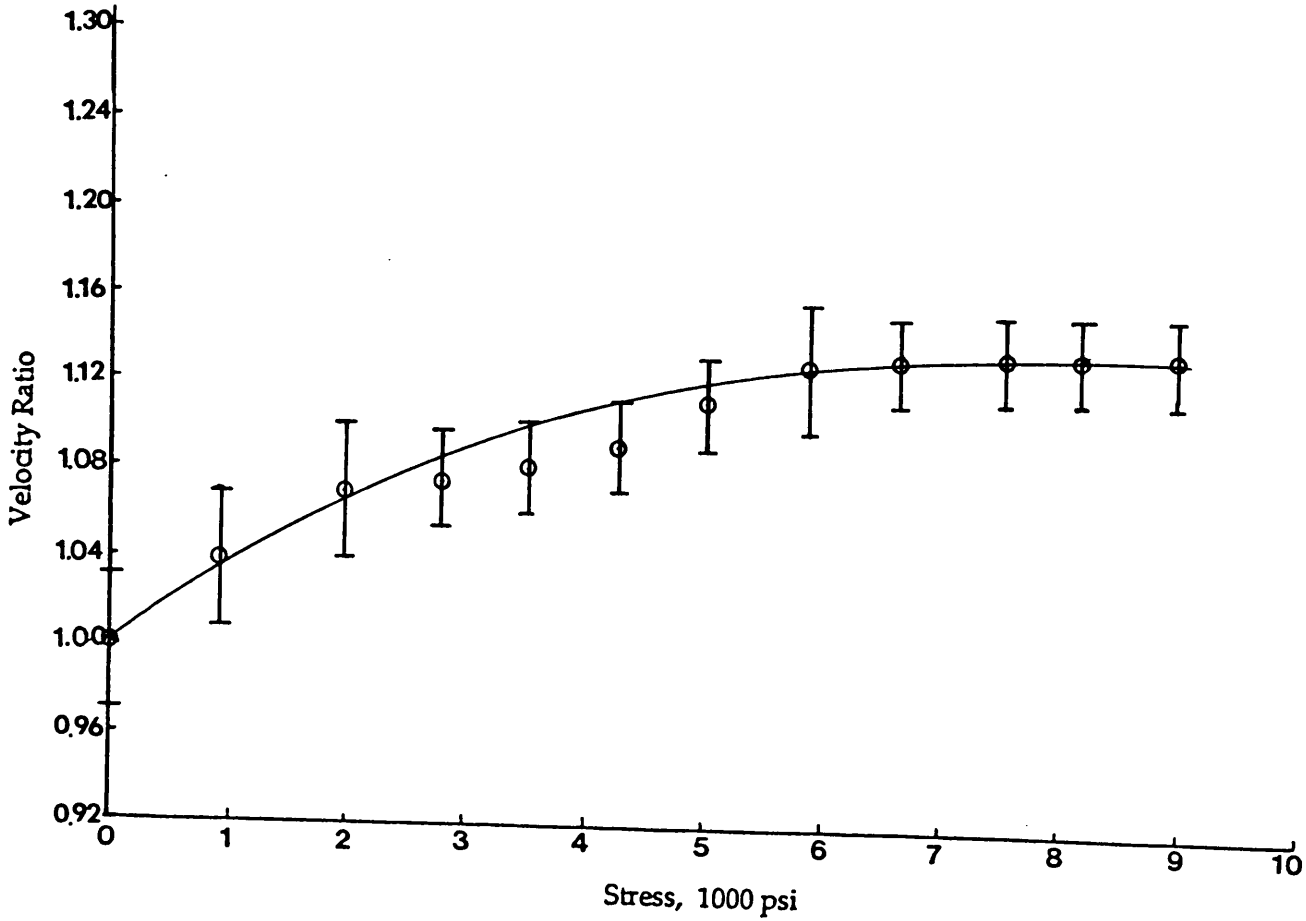

Figure 5.6 Velocity ratio versus uniaxial compressive stress for granite samples. (The applied stress is parallel to the mica foliation.)

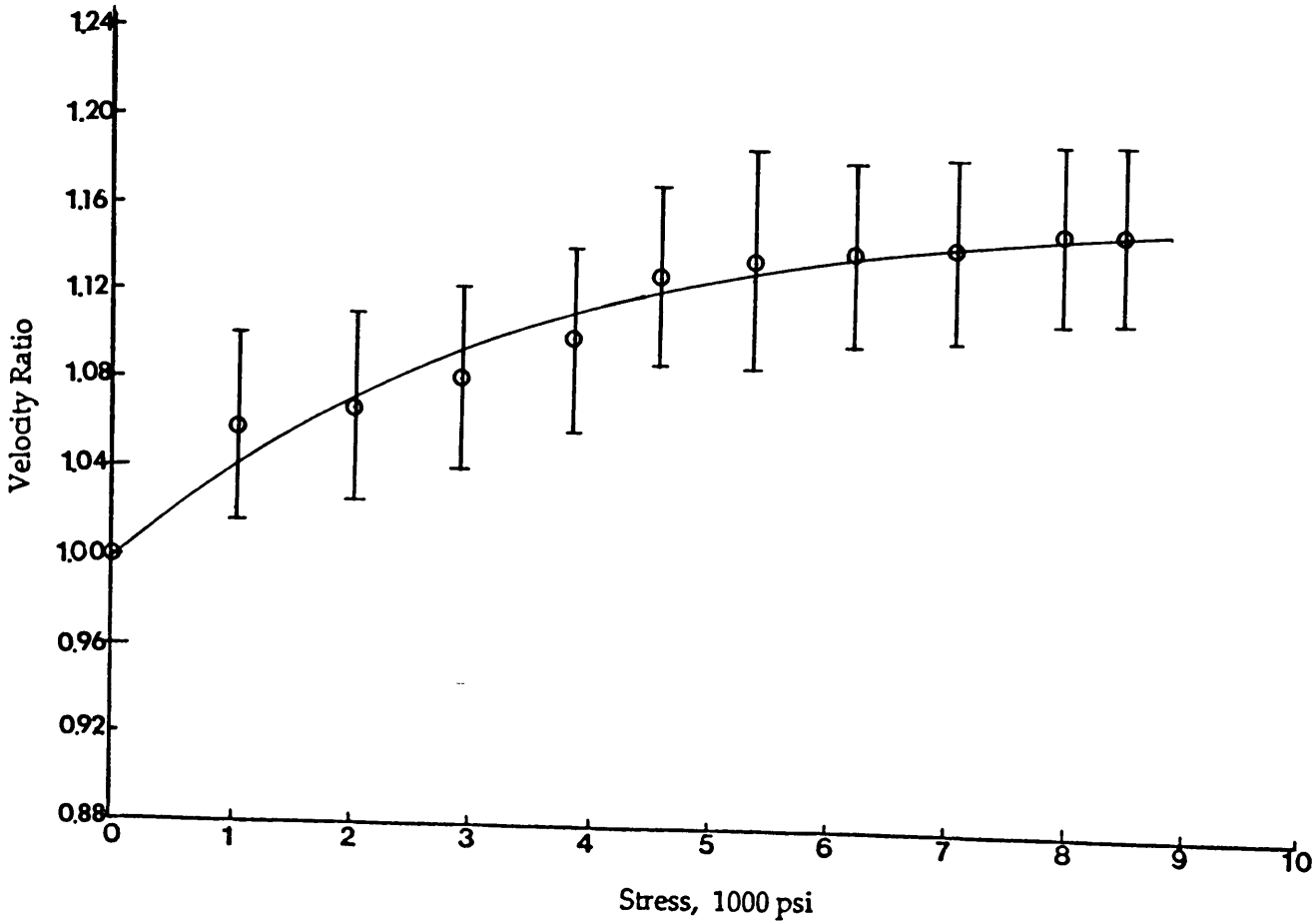

Figure 5.7 Velocity ratio versus uniaxial compressive stress for granite samples. (The applied stress is perpendicular to the mica foliation.)

(applied stress perpendicular to the foliation).

Figure 5.8 is the SAS obtained curve for marble. The equation for the curve is:

$$V/V_o = 1.00 + 1.847 \times 10^{-5}\ \sigma - 3.414 \times 10^{-9}\ \sigma^2. \qquad (5.5)$$

Figure 5.9 and Figure 5.10 are the curves obtained for the two different types of limestone. Only slight changes are observed. The equation obtained for argillaceous limestone is:

$$V/V_o = 1.00 - 1.432 \times 10^{-6}\ \sigma - 1.642 \times 10^{-11}\ \sigma^2. \qquad (5.6)$$

The equation obtained for Five Oaks limestone is:

$$V/V_o = 1.00 + 8.052 \times 10^{-7}\ \sigma - 8.730 \times 10^{-11}\ \sigma^2. \qquad (5.7)$$

The velocity ratios plotted against the applied uniaxial stress for shale are shown in Figures 5.11 and 5.12. The velocity change under stress was very small in directions along the bedding plane and perpendicular to the bedding plane. The calibration curve for shale can be expressed as:

$$V/V_o = 1.00 + 0.235 \times 10^{-5}\ \sigma - 0.197 \times 10^{-9}\ \sigma^2 \qquad (5.8)$$

(applied stress parallel to the bedding plane),

$$V/V_o = 1.00 + 0.007 \times 10^{-5}\ \sigma - 0.004 \times 10^{-9}\ \sigma^2 \qquad (5.9)$$

(applied stress perpendicular to the bedding plane).

The testing results, demonstrate that using wave velocity to predict stress is applicable for sandstone, granite, marble and some limestones but it is not suitable for shale and some other limestones. The relationship between the applied stress and the wave velocity ratio can be expressed by a second order polynomial equation as:

$$V/V_o = a + b\,\sigma + c\,\sigma^2$$

where: V is the wave velocity at a specific stress level,

V_o is the wave velocity at zero stress,

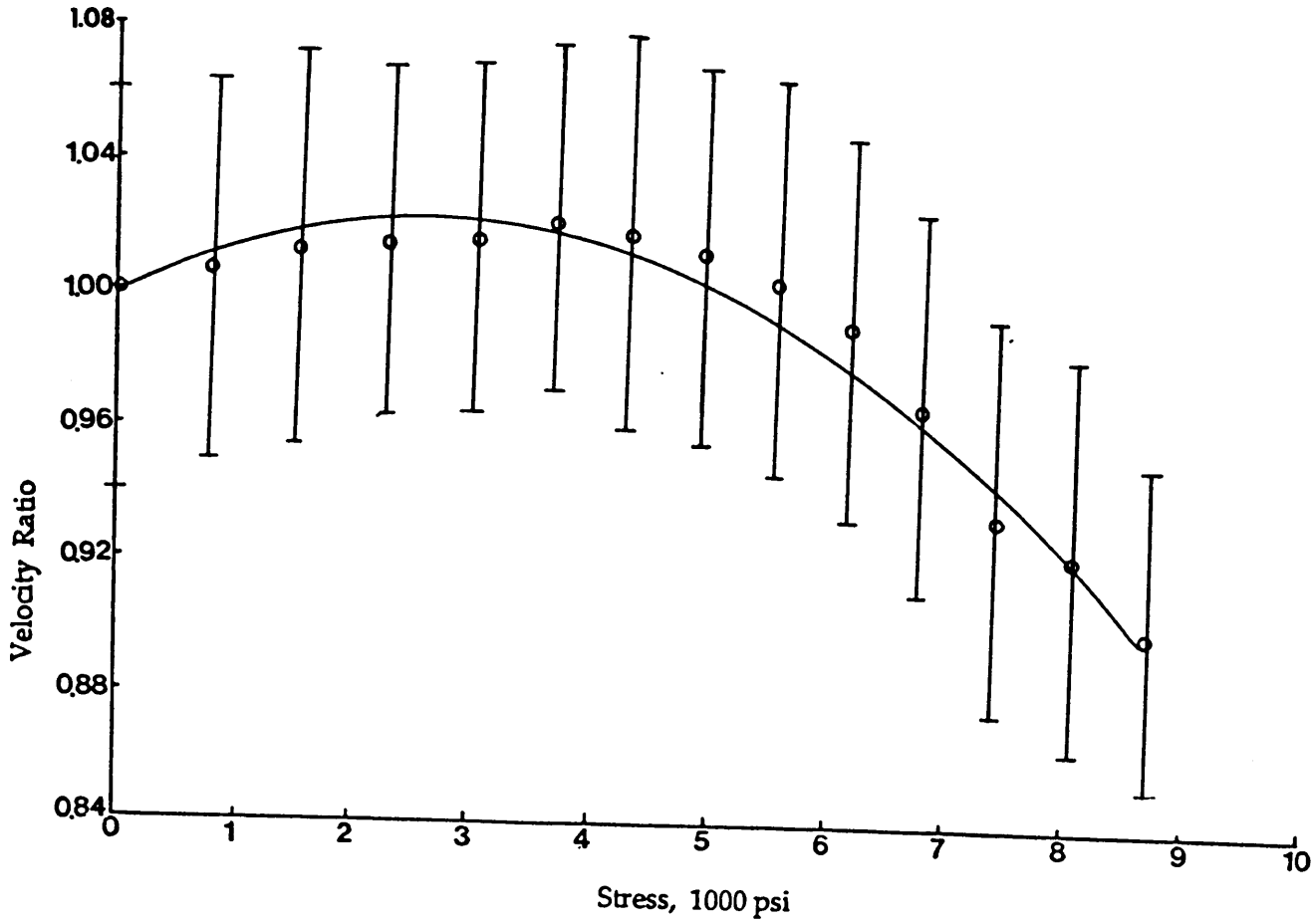

Figure 5.8 Velocity ratio versus uniaxial compressive stress for marble samples.

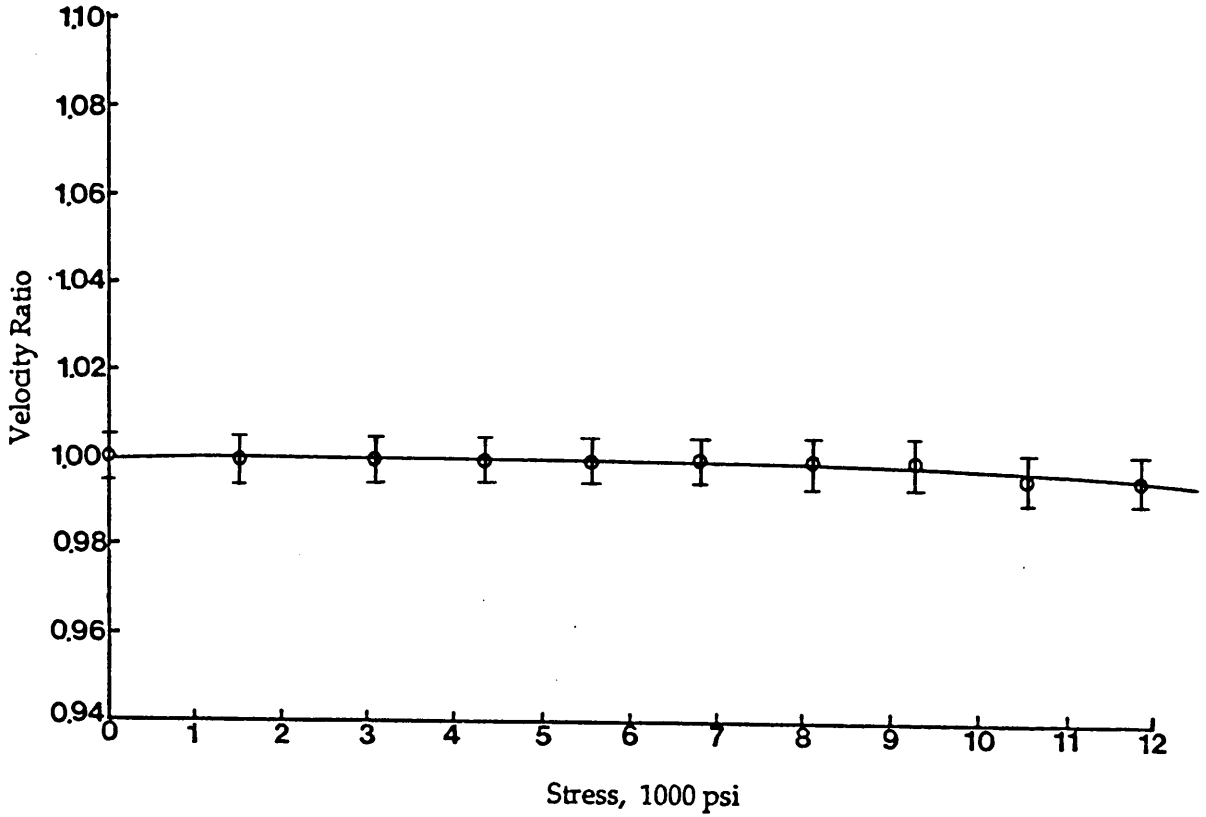

Figure 5.9 Velocity ratio versus uniaxial compressive stress for Five Oaks limestone samples.

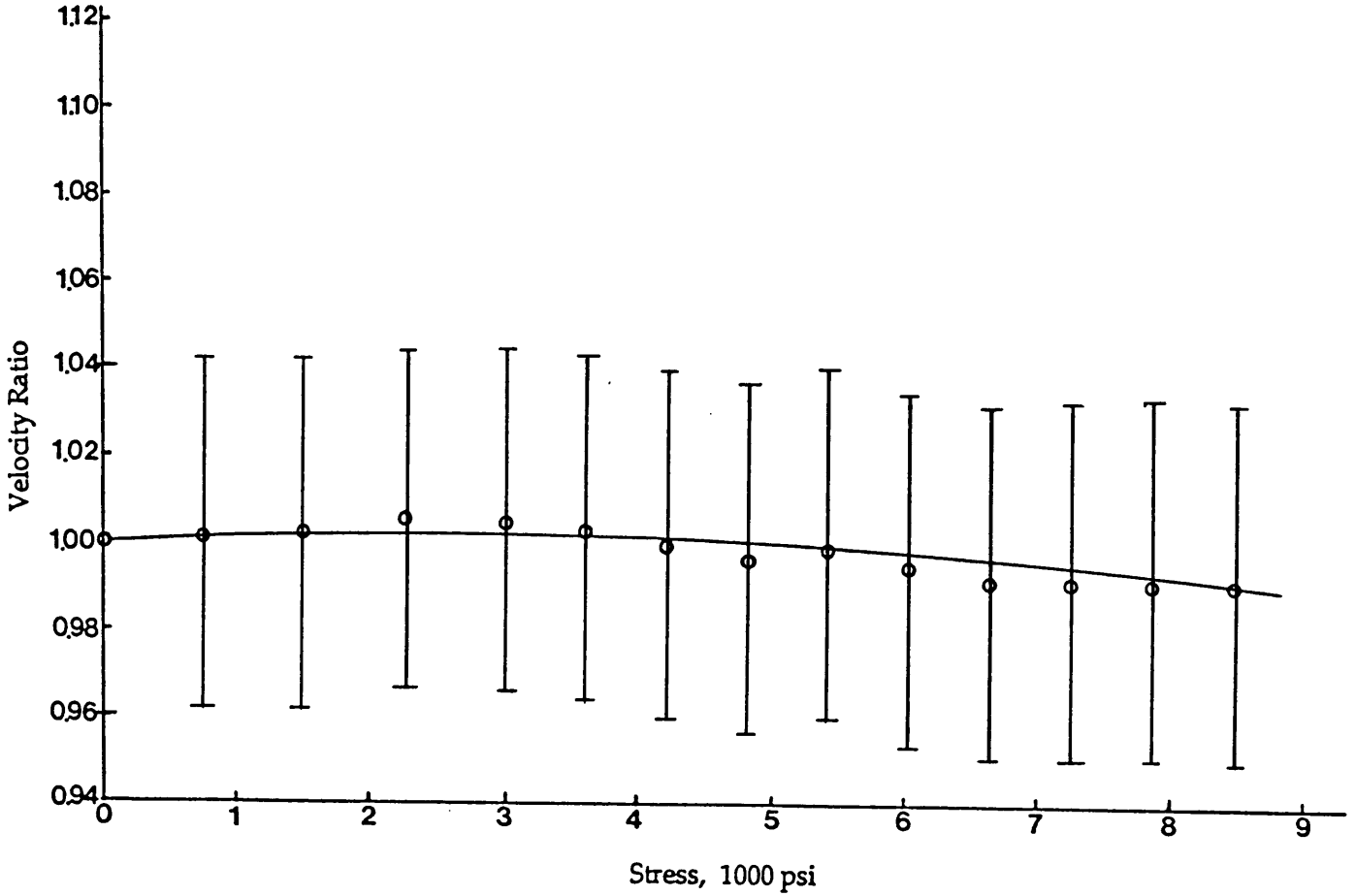

Figure 5.10 Velocity ratio versus uniaxial compressive stress for argillaceous limestone samples.

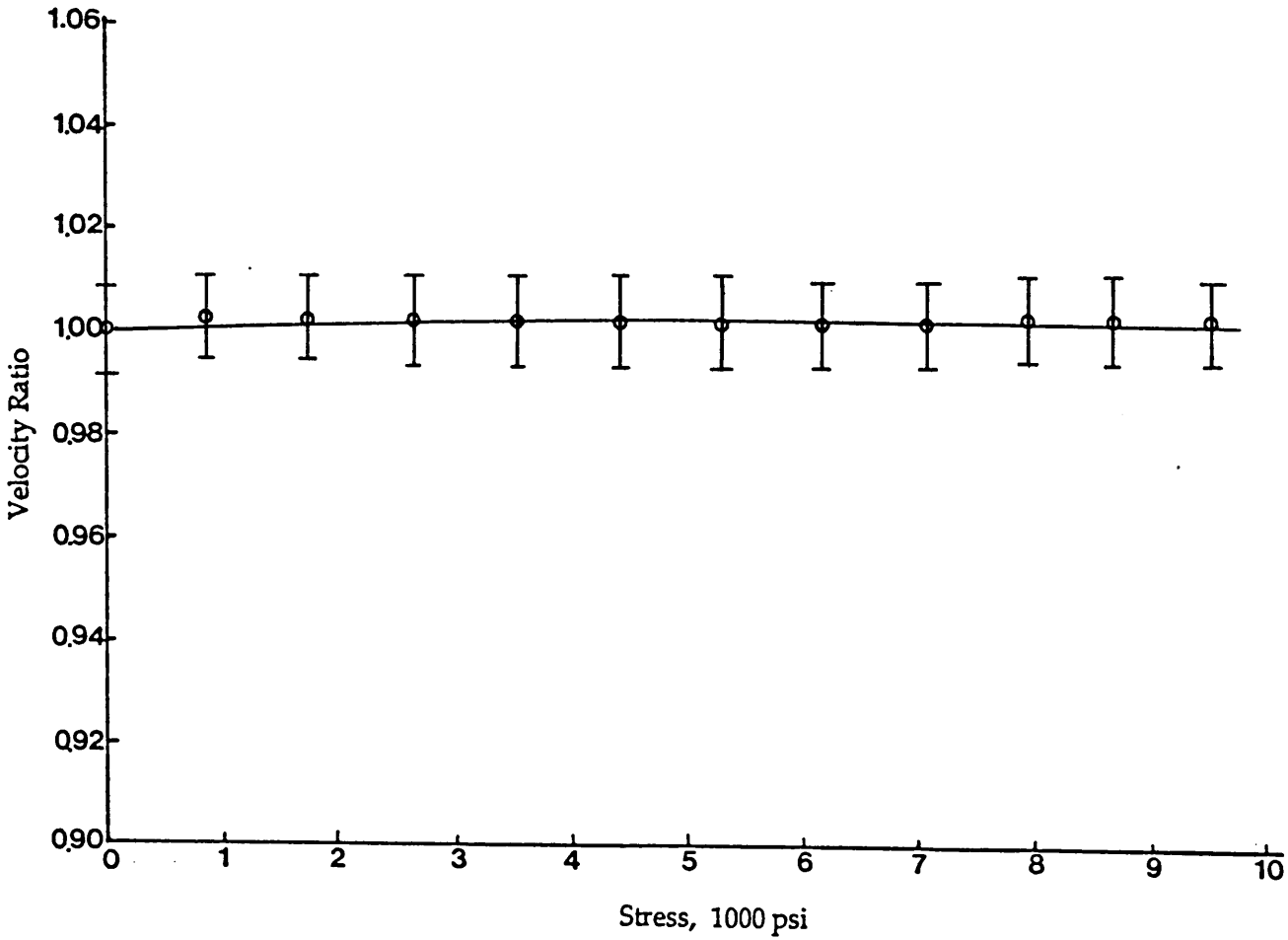

Figure 5.11 Velocity ratio versus uniaxial compressive stress for shale samples. (The applied stress is perpendicular to the bedding plane.)

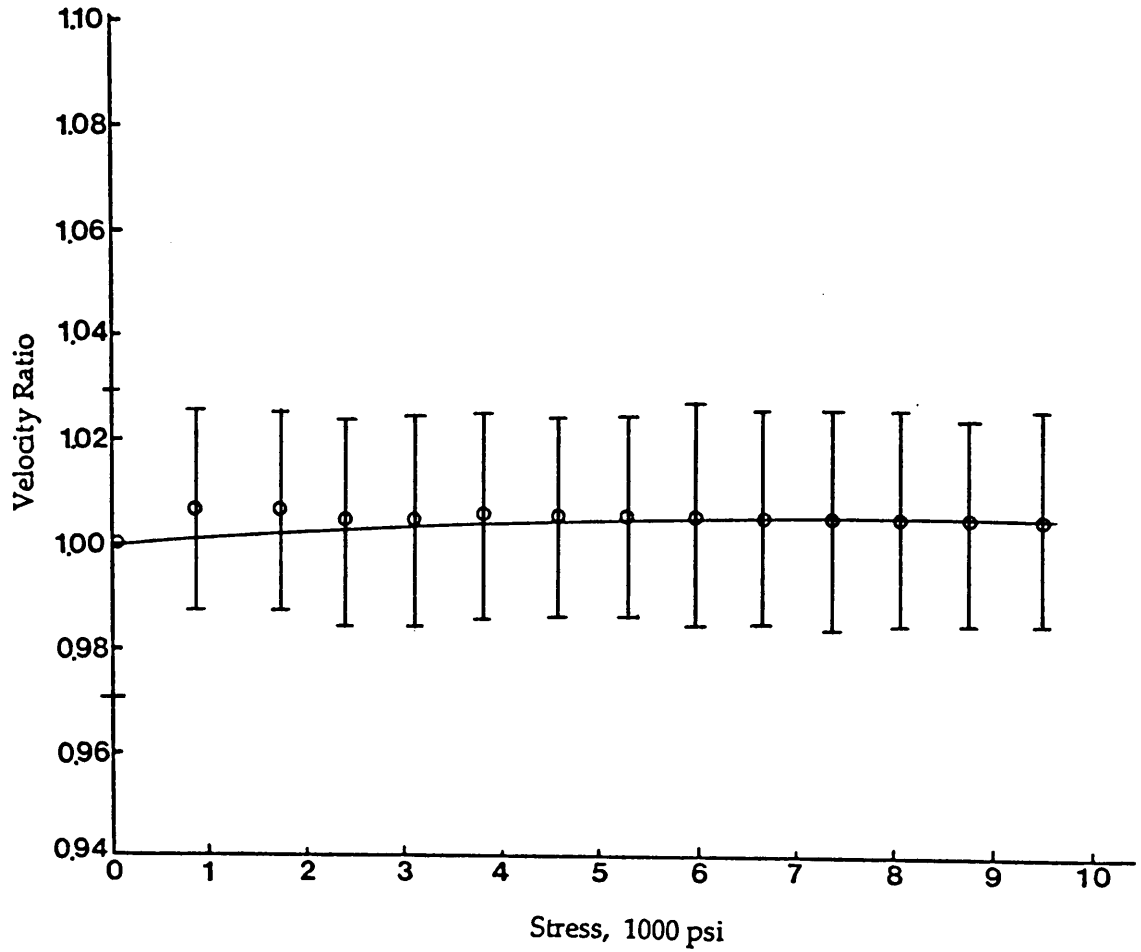

Figure 5.12 Velocity ratio versus uniaxial compressive stress for shale samples. (applied stress is parallel to the bedding plane)

a, b, c are the constants.

The correlation coefficients are 0.90 or higher except for Five Oaks limestone with R^2=0.80.

5. 2. 2 Attenuation Coefficient

Lockner *et al.* (1977) pointed out that attenuation is a measure of the nonelastic components of deformation and may therefore be more sensitive than wave velocity to defects in the medium through which the wave propagates. The attenuation coefficients for different rocks under different stresses are shown in Figures 5.13, 5.14, 5.15, 5.16, 5.17, 5.18, and 5.19. At same stress level, the attenuation coefficient changes dramatically but the wave velocity does not. The results are comparable with that reported by Lockner *et al.* (1977) and Molina and Wack (1982).

As shown in Figures 5.11 and 5.12, the velocities in shale in the directions parallel and perpendicular to the bedding plane were similar. However, the attenuation coefficient show significant change with stress and stress direction (Figures 5.18 and 5.19). This clearly demonstrates that the attenuation is more sensitive than wave velocity to stress change. The relationships between attenuation coefficient ratio and the applied stress are:

$$A/A_0 = 1.00 + 3.883 \times 10^{-6} \sigma + 2.161 \times 10^{-9} \sigma^2 \qquad (5.10)$$

(applied stress parallel to the bedding plane),

$$A/A_0 = 1.00 - 2.769 \times 10^{-5} \sigma + 1.618 \times 10^{-9} \sigma^2 \qquad (5.11)$$

(applied stress perpendicular to the bedding plane).

The attenuation coefficient ratio plotted against the applied uniaxial stress for granite is shown in Figures 5.20 and 5.21 with stress perpendicular and parallel to the mica foliation respectively. The wave velocities in these

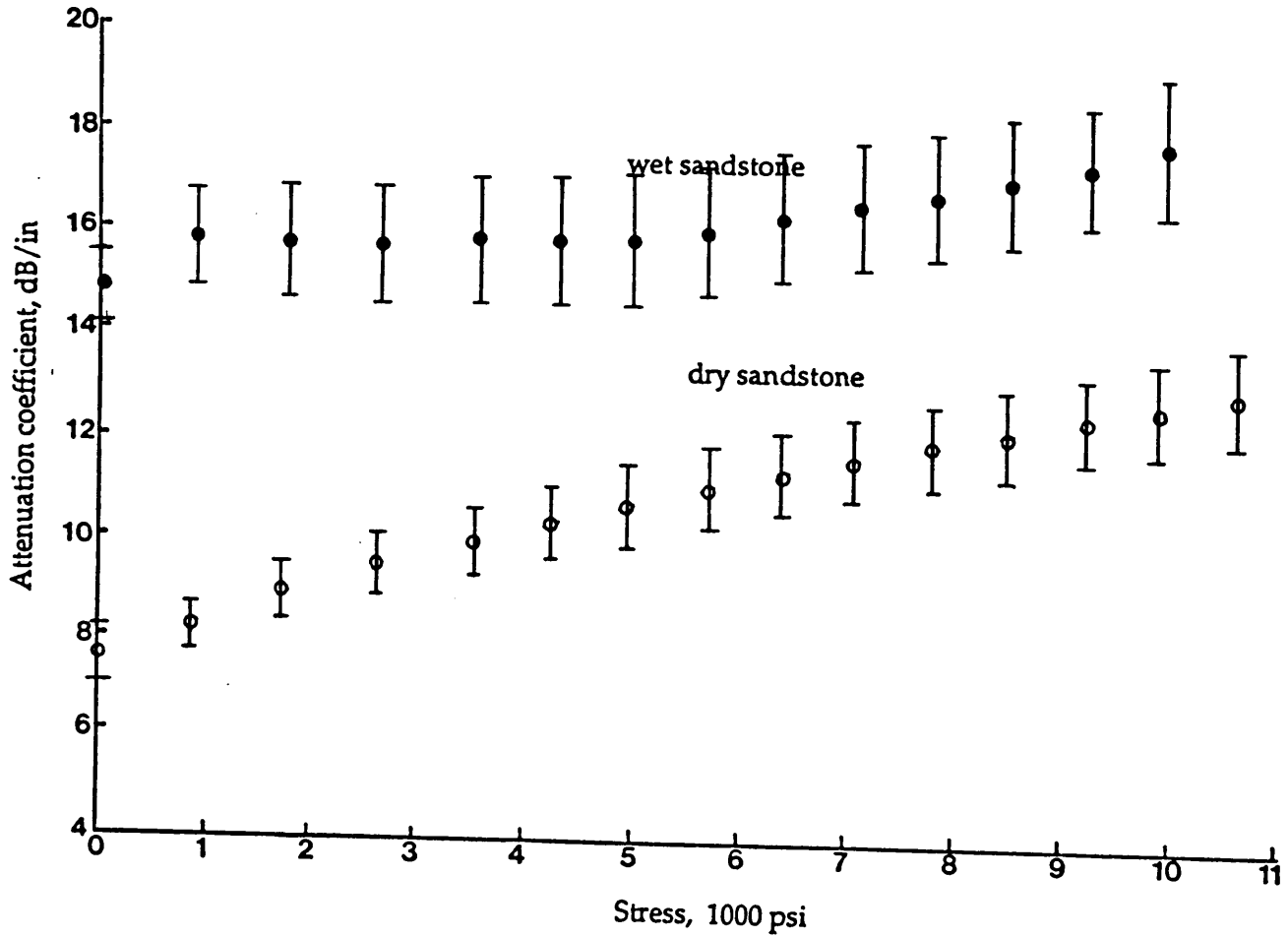

Figure 5.13 Attenuation coefficient versus uniaxial compressive stress for sandstone samples.

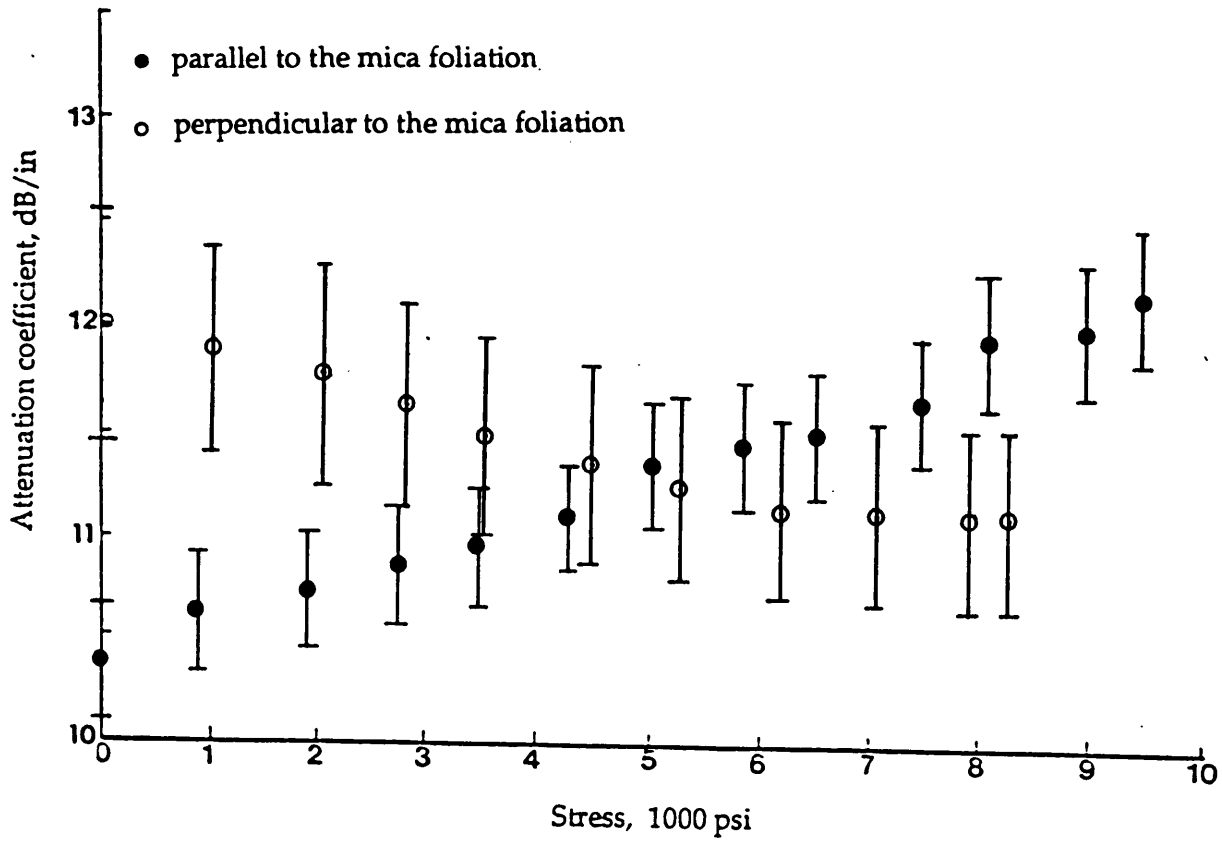

Figure 5.14 Attenuation coefficient versus uniaxial compressive stress for granite samples.

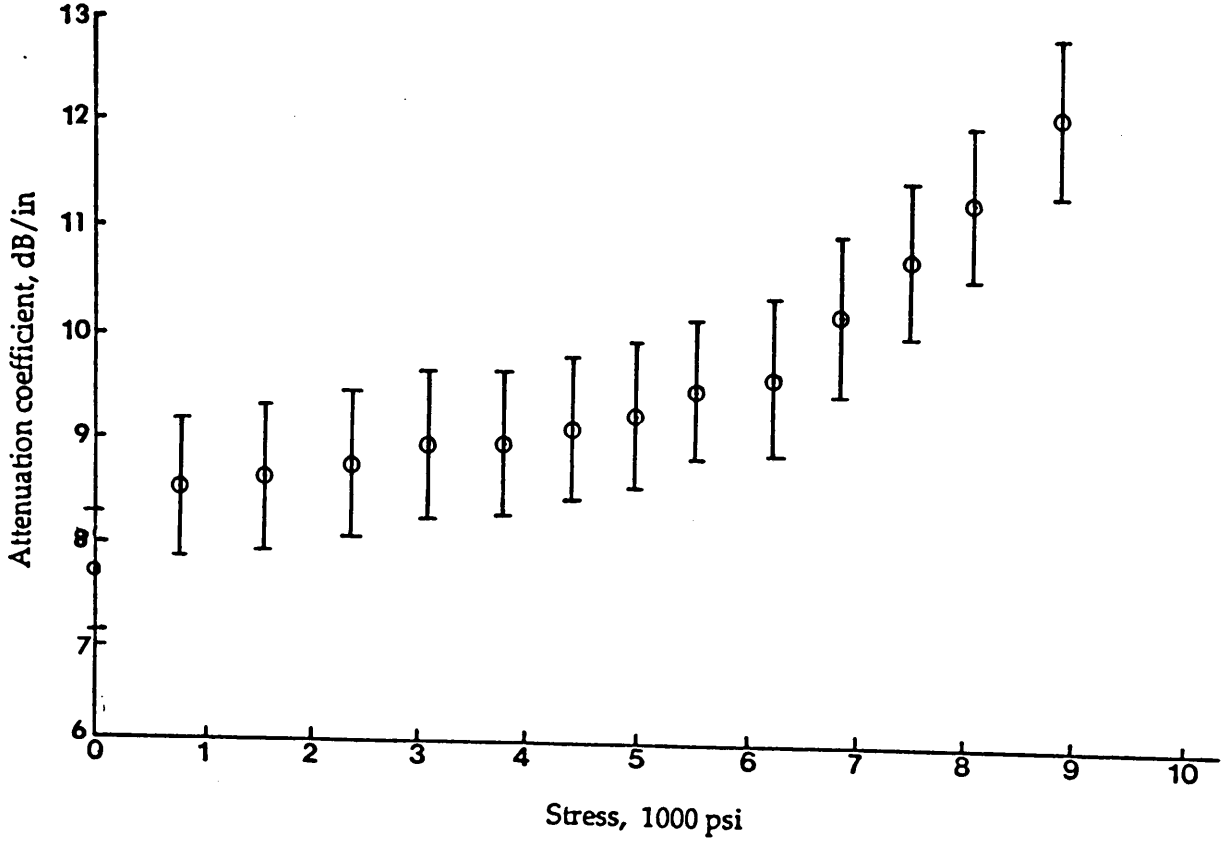

Figure 5.15 Attenuation coefficient versus uniaxial compressive stress for marble samples.

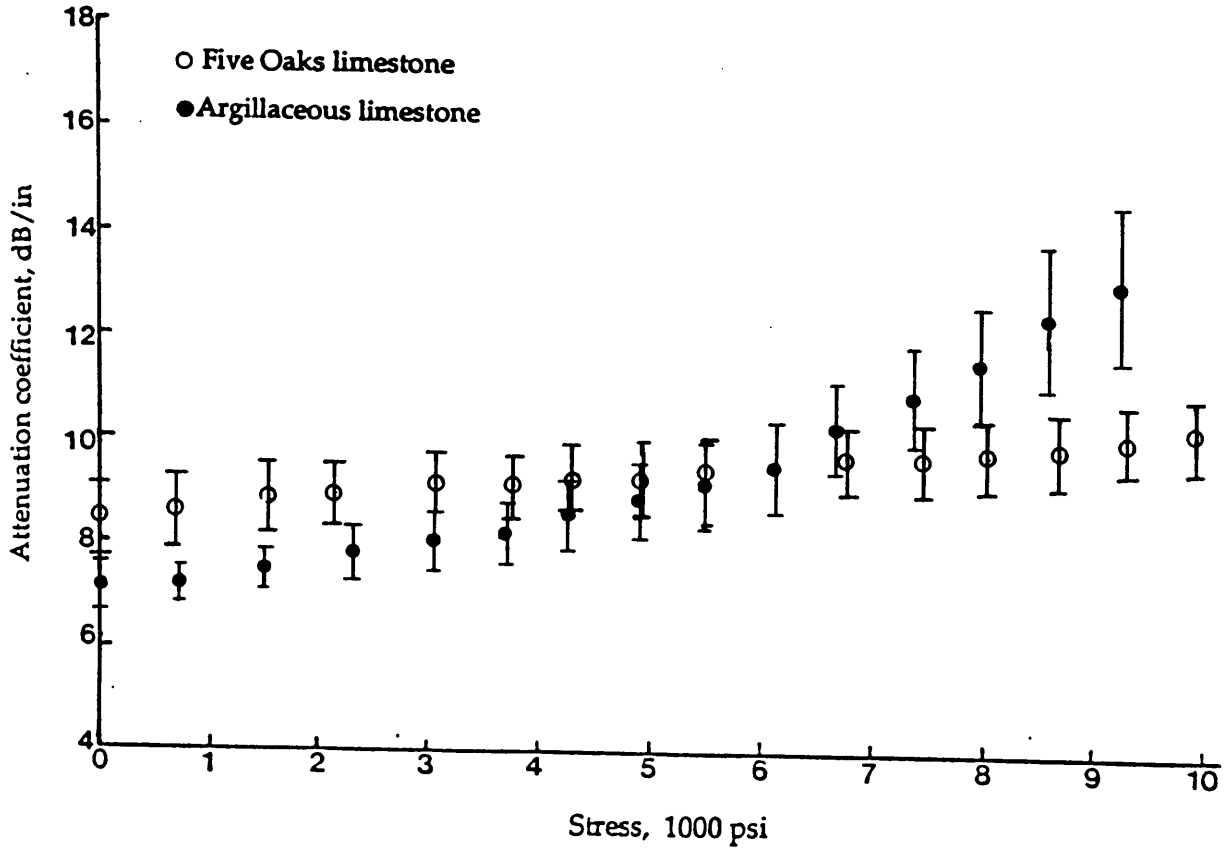

Figure 5.16 Attenuation coefficient versus uniaxial compressive stress for limestone samples.

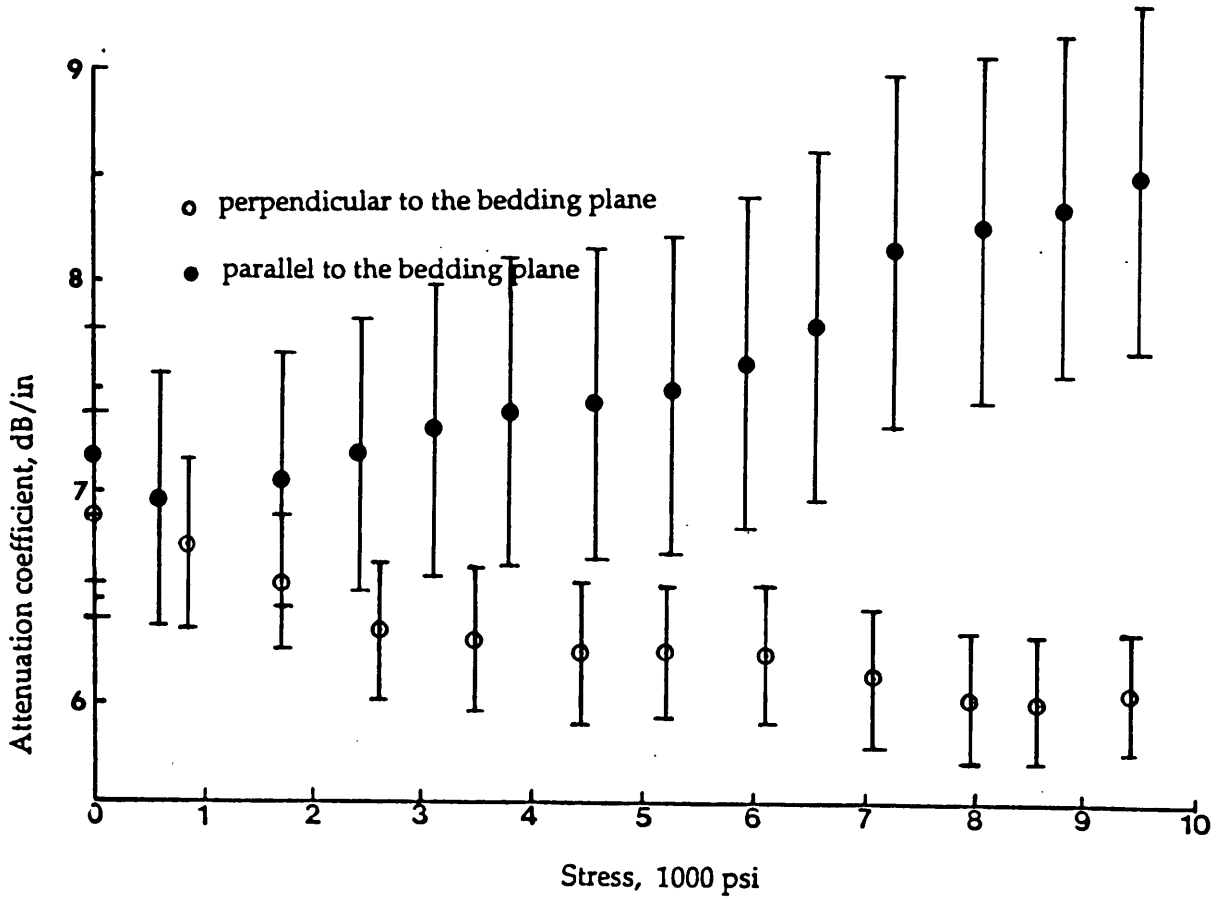

Figure 5.17 Attenuation coefficient versus uniaxial compressive stress for shale samples.

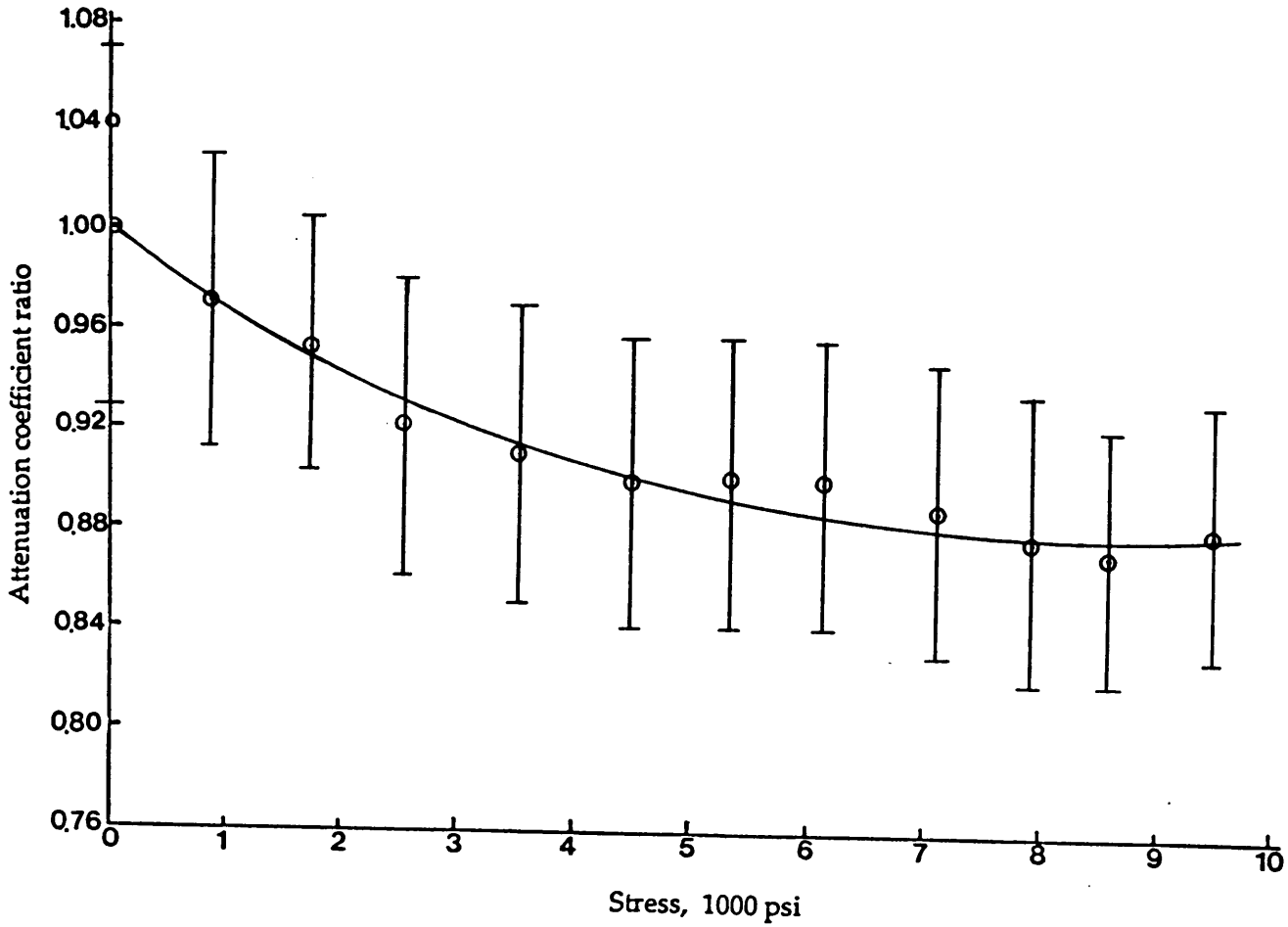

Figure 5.18 Attenuation coefficient ratio versus uniaxial compressive stress for shale samples (applied stress is perpendicular to the bedding plane).

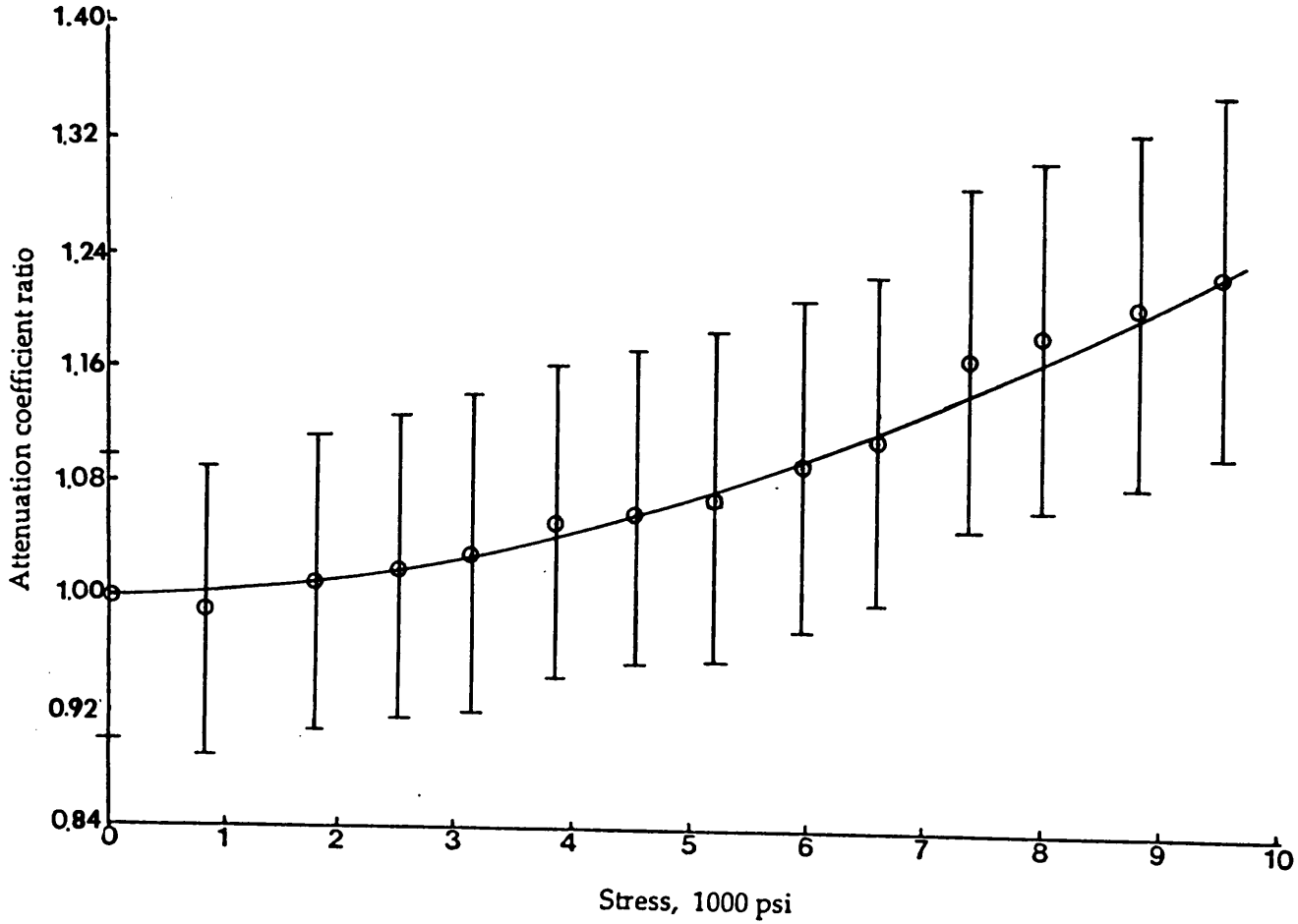

Figure 5.19 Attenuation coefficient ratio versus uniaxial compressive stress for shale samples (applied stress is parallel to the bedding plane).

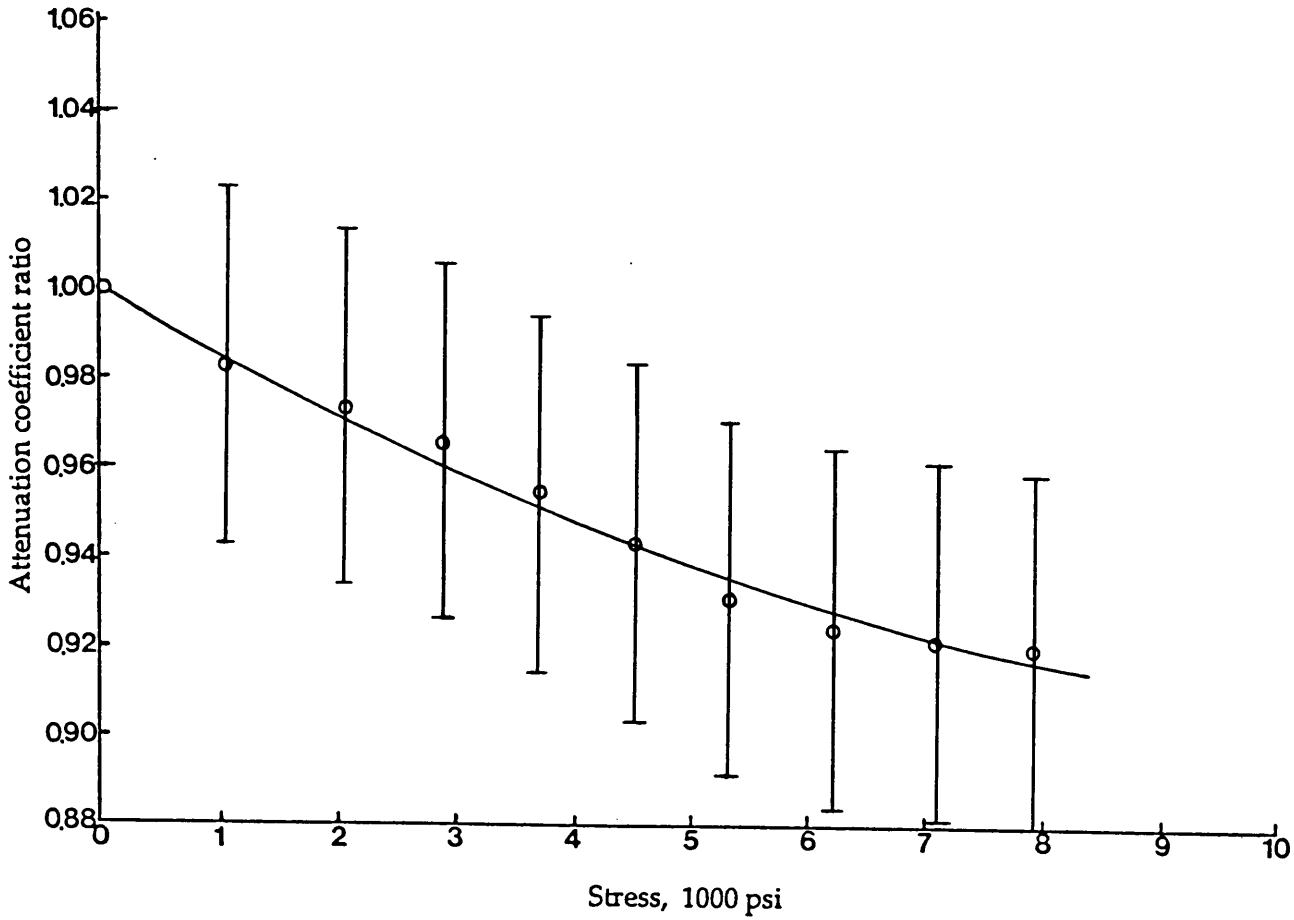

Figure 5.20 Attenuation coefficient ratio versus uniaxial compressive stress for granite samples (applied stress is perpendicular to the mica foliation).

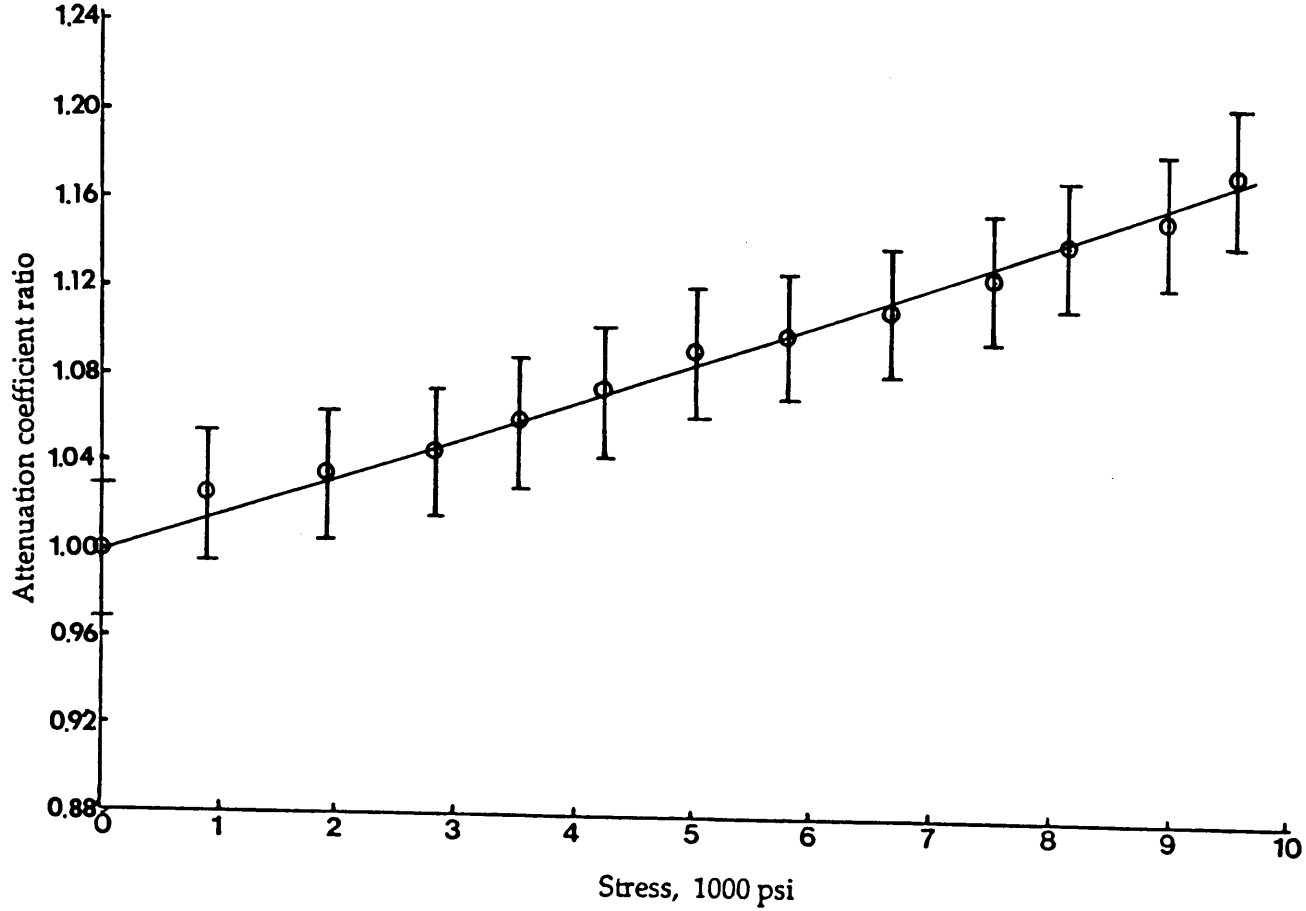

Figure 5.21 Attenuation coefficient ratio versus uniaxial compressive stress for granite samples (applied stress is parallel to the mica foliation).

two directions did not differ much (See figures 5.6 and 5.7). However, the attenuation coefficient differs by about 10% between these two directions. The relationship between the attenuation coefficient ratio and applied stress can be expressed as:

$$A/A_0 = 1.00 - 1.551 \times 10^{-5} \sigma + 6.677 \times 10^{-10} \sigma^2 \qquad (5.12)$$

(applied stress perpendicular to the mica foliation),

$$A/A_0 = 1.00 + 1.766 \times 10^{-5} \sigma - 1.113 \times 10^{-11} \sigma^2 \qquad (5.13)$$

(applied stress parallel to the mica foliation).

Figures 5.22 and 5.23 show attenuation coefficient ratio versus uniaxial stress for water saturated and dry sandstone respectively. Water content affects not only wave velocity but also attenuation. At zero stress the attenuation coefficient of dry sandstone is 7.7 dB/in and that of water saturated samples is 14.8 dB/in. The relationship between attenuation coefficient ratio and stress for both conditions in sandstone can be expressed as:

$$A/A_0 = 1.00 + 1.779 \times 10^{-5} \sigma + 2.095 \times 10^{-10} \sigma^2 \qquad (5.14)$$

(for water saturated sandstone),

$$A/A_0 = 1.00 + 8.584 \times 10^{-5} \sigma - 1.923 \times 10^{-9} \sigma^2 \qquad (5.15)$$

(for air-dried sandstone).

Figures 5.24 and 5.25 show the attenuation coefficient ratio of limestone plotted against the applied uniaxial stress. They also show a greater change as compared to that shown by the wave velocity. The equations are:

$$A/A_0 = 1.00 + 2.823 \times 10^{-5} \sigma + 7.904 \times 10^{-9} \sigma^2 \qquad (5.16)$$

(for argillaceous limestone),

$$A/A_0 = 1.00 + 1.647 \times 10^{-5} \sigma + 2.774 \times 10^{-10} \sigma^2 \qquad (5.17)$$

(for Five Oaks limestone).

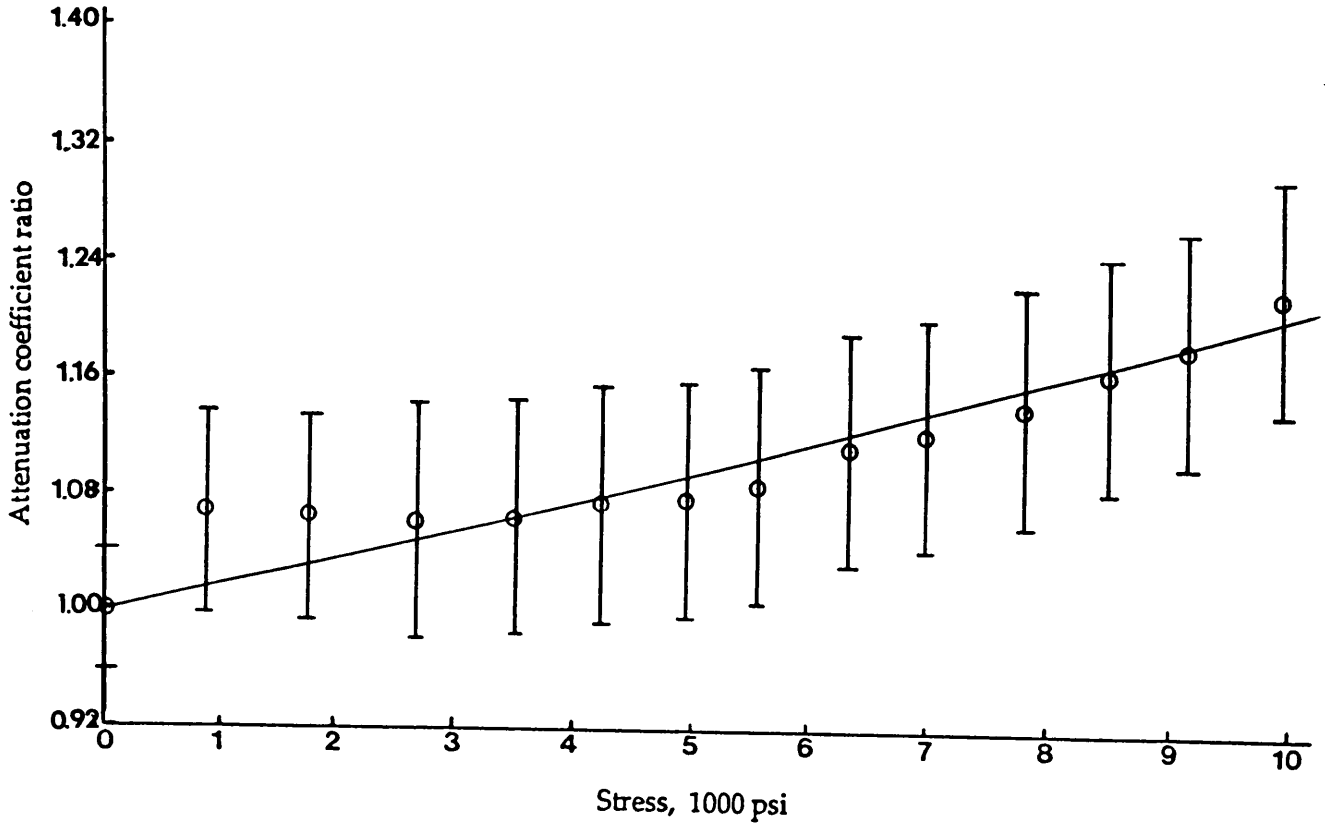

Figure 5.22 Attenuation coefficient ratio versus uniaxial compressive stress for water saturated sandstone samples.

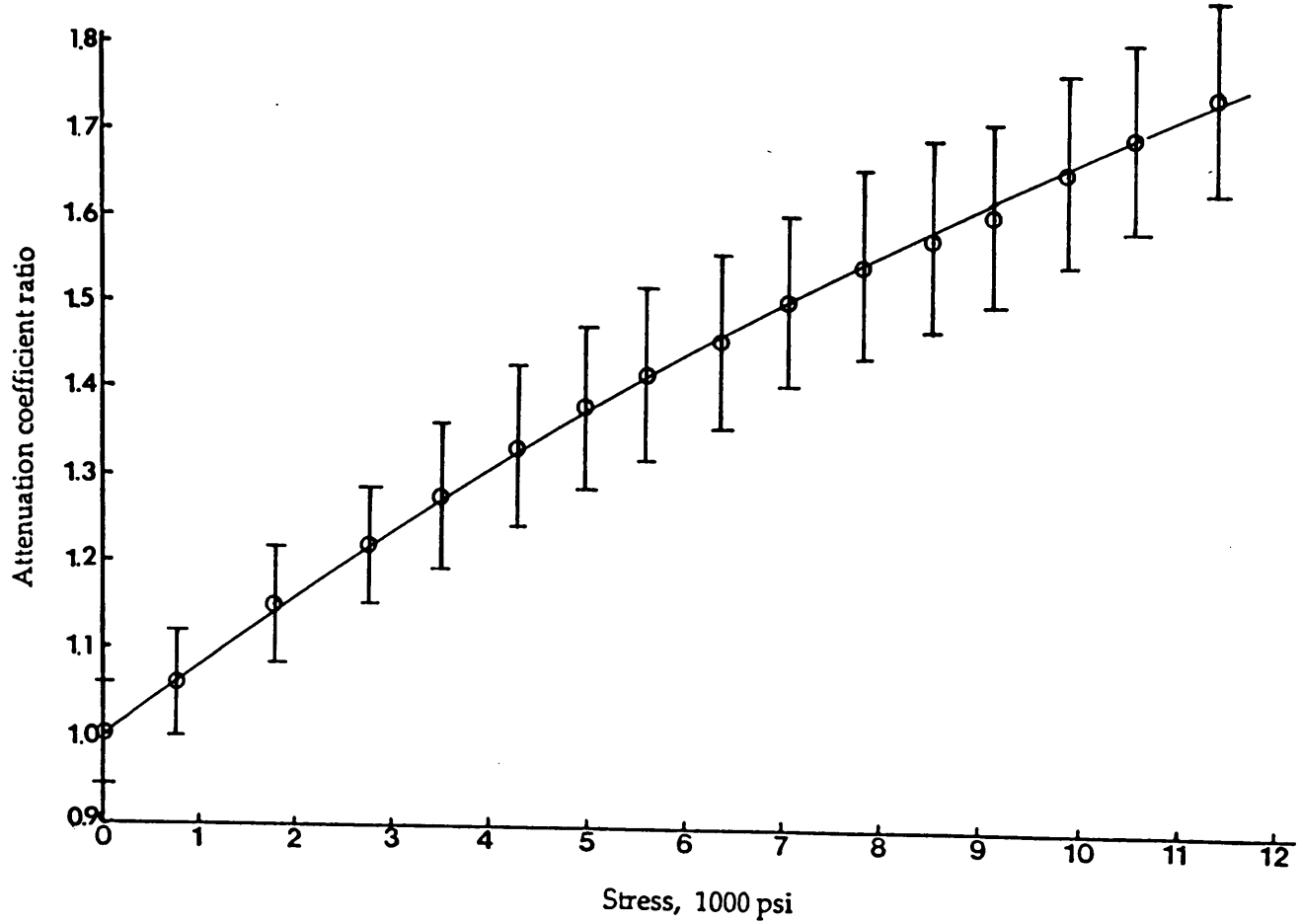

Figure 5.23 Attenuation coefficient ratio versus uniaxial compressive stress for dry sandstone samples.

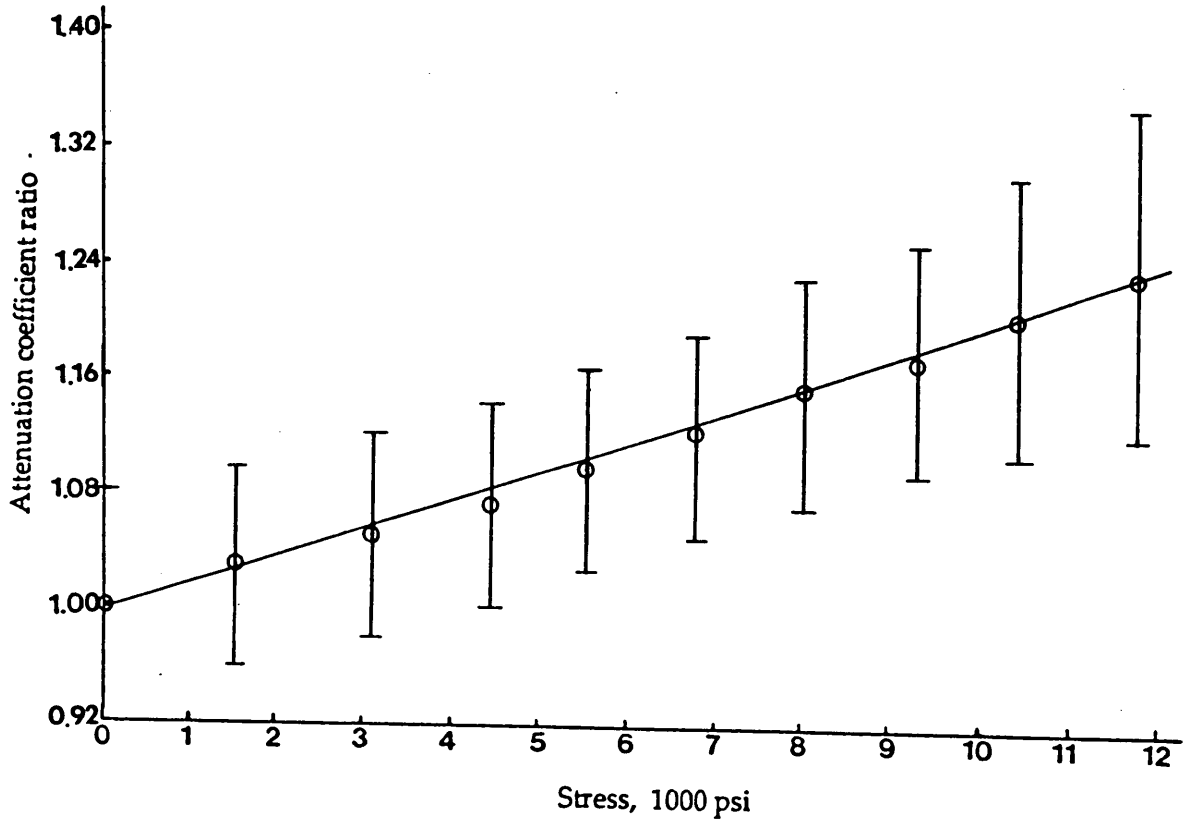

Figure 5.24 Attenuation coefficient ratio versus uniaxial compressive stress for Five Oaks limestone samples.

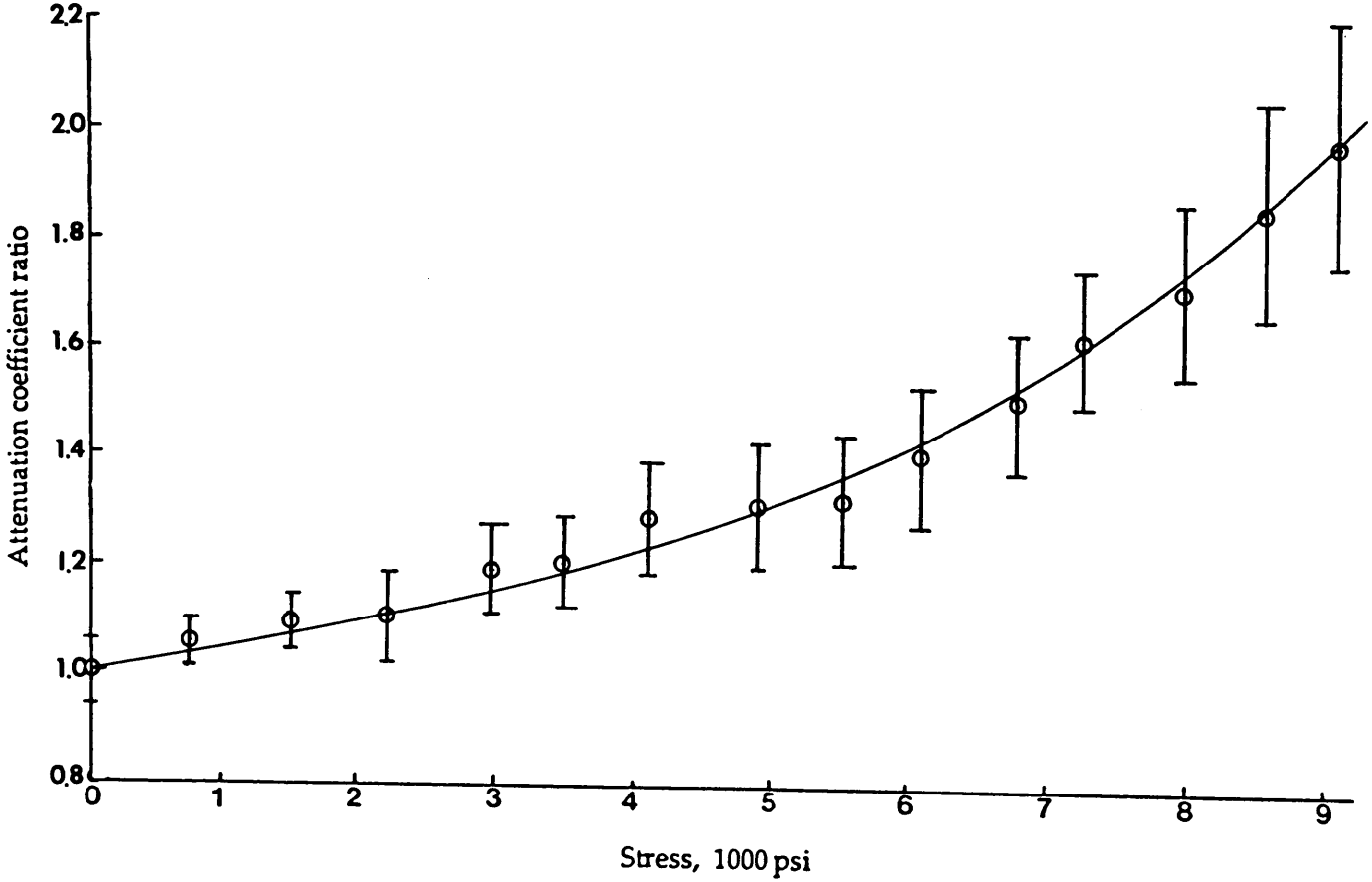

Figure 5.25 Attenuation coefficient ratio versus uniaxial compressive stress for argillaceous limestone samples.

The attenuation coefficient ratio of marble plotted versus applied stress is shown in Figure 5.26. The equation obtained is:

$$A/A_0 = 1.00 + 3.069 \times 10^{-5} \sigma + 3.101 \times 10^{-9} \sigma^2. \qquad (5.18)$$

The relationship between the applied stress and attenuation coefficient ratio can be expressed by a second order polynomial equation as:

$$A/A_0 = a + b\,\sigma + c\,\sigma^2$$

where: A is attenuation coefficient at a specific stress level,

A_0 is attenuation coefficient at zero stress,

a, b, c are the constants.

Based on the results obtained, the correlation coefficient of attenuation and stress is much higher than that of velocity and stress. As expected, attenuation of foliated or stratified rocks is more senstive to stress direction than velocity is. For both shale and granite, the velocity coefficients are similar regardless of direction of applied stress. However, as expected, the attenuation behaves in a complete different manner with different stress directions. Attenuation decreases with stress applied perpendicular to bedding plane or foliation due to crack closing. Attenuation increases with stress applied parallel to bedding plane or foliation due to cracks opening. In summary, the attenuation coefficient has been proven to be more sensitive to stress change and is a more feasible means for stress monitoring.

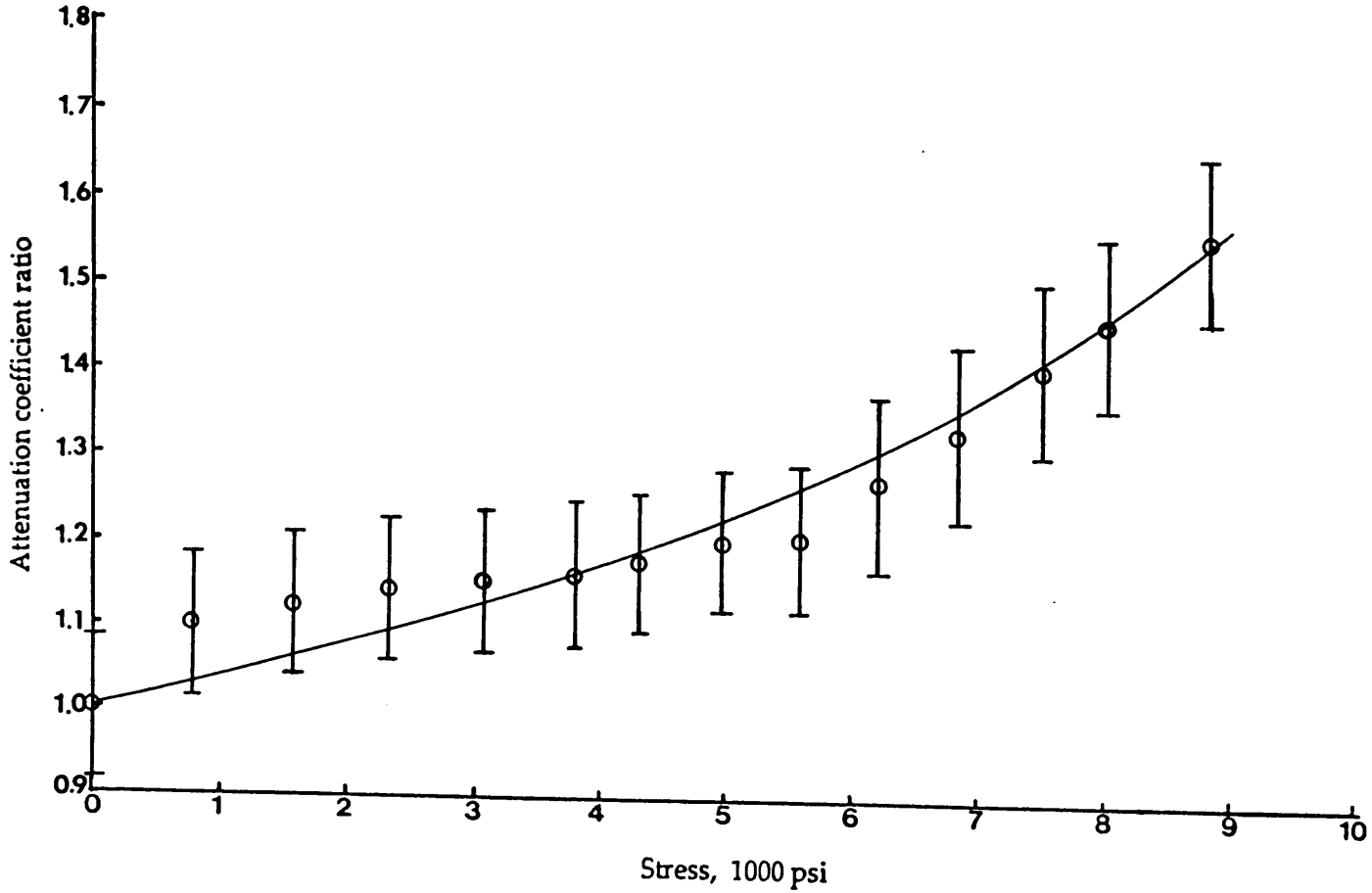

Figure 5.26 Attenuation coefficient ratio versus uniaxial compressive stress for marble samples.

CHAPTER VI

CONCLUSIONS AND RECOMMENDATIONS

In this research wave velocity and wave attenuation methods using sonic frequencies were applied to the monitoring of stress changes in rocks in the laboratory. Several types of rock sample were collected from different areas and studied in the laboratory. Wave velocity and wave attenuation were measured using acoustic methods within the sonic frequency range. Due to the limitations of the ultrasonic equipment, reliable measurements in the ultrasonic range could not be obtained.

In the laboratory, rocks were tested for both velocity change and attenuation change as the load was increased. The wave velocity and attenuation were measured along the direction perpendicular to the stress. All the laboratory testing results showed that the wave attenuation was more sensitive than wave velocity to a stress change. The sensitivity varied with rock type, texture, water content, and stress direction.

Using wave velocity and wave attenuation methods to study rock in the laboratory have some limitations. For instance, both the wave velocity and attenuation may vary because of wave frequency or because of fracturing of the media through which the wave propagated. However, results of this study also show that wave velocity did not vary with increasing stress on some types of rocks such as shale and limestone. These results suggest that wave velocity is not a reliable parameter, nor is it applicable to some types of rock. These rocks may have a special composition or texture which makes wave velocity unable to respond to stress change.

The relationship between the velocity ratio and the applied stress can

be expressed by a second order polynomial equation such as $V/V_0 = a + b\sigma + c\sigma^2$. As mentioned previously, this equation may not be applied to some types of rocks in which wave velocity did not vary with applied stress.

The relationship between the attenuation coefficient ratio and the applied stress can also be expressed by a second order polynomial equation as $A/A_0 = a + b\sigma + c\sigma^2$. According to the testing results, this equation can be applied to a greater variety of rocks. Moreover, the correlation between attenuation and stress is much higher than the correlation between wave velocity and stress.

Attenuation is directly related to energy. Thus, the attenuation coefficient is more sensitive to the stress change. Attenuation is also more sensitive to the coupling condition. Therefore, during the test, the coupling between the transducers and the sample should be under constant pressure. In order to get a more accurate result from the attenuation measurement, one needs to take more precaution than when measuring velocity.

To obtain a clearer reading in future work, a control circuit should be installed on the trigger of the oscilloscope to prevent multiple triggering. However, multiple receivers and multiple channels in the oscilloscope are recommended. More information will be received from these multiple devices simultaneously which will allow more detailed and advanced study of the stress and microcrack distribution in the rock.

REFERENCES

Aggarwal, Y.P., Sykes, L.R., Armbruster, J. and Sbar, M.L. (1973) Premonitory changes in seismic velocities and prediction of earthquakes. Nature, Vol. 241, p. 101-104.

Anstey, N.A. (1977) Seismic Interpretation The Physical Aspects. International Human Resources Development Corporation, Boston, 625p.

Attewell, P.B. (1970) Triaxial anisotropy of wave velocity and elastic moduli in slate and their axial concordance with fabric and tectonic symmetry. Int. J. Rock Mech. Min. Sci. & Geomech. Abstr., Vol. 7, p. 193-207.

_____ and Ramana, Y.V. (1966) Wave attenuation and internal friction as functions of frequency in rocks. Geophysics, Vol. 31, p. 1049-1056.

Auberger, M. and Rinehart, J.S. (1960) Attenuation of longitudinal waves in rocks. J. Geophys. Res., Vol. 66, p. 191-199.

Bates, R.L. (1969) Geology of the Industrial Rocks and Minerals. Dover Publication Inc., New York, 459p.

Bieniawski, Z.T. (1967) Mechanism of brittle fracture of rock, Parts 1, 2 and 3. Int. J. Rock Mech. Min. Sci., Vol. 4, p. 395-430.

Biot, M.A. (1956) Theory of propagation of elastic waves in fluid-saturated porous solid: I. low frequency range. J. Acoust. Soc. Am., Vol. 28, p. 168-178.

Birch, F. (1960) The velocity of compressional waves in rocks to 10 kilobars, Part I. J. Geophys. Res., Vol. 65, p. 1083-1102.

_____ (1961) The velocity of compressional waves in rocks to 10 kilobars, Part II. J. Geophys. Res., Vol. 66, p. 2199-2224.

Born, W.T. (1941) Attenuation constant of earth materials. Geophysics, Vol. 6, p. 132-148.

Brady, B.T. (1974) Seismic precursors before failures in mines. Nature, Vol. 252, p. 549-552.

_____ (1977) Anomalous seismicity prior to rock bursts: implications for earthquake prediction. Pure Appl. Geophys., Vol. 115, p. 357-374.

_____ (1978) Prediction of Failures in Mines - An Overview. U.S. Bureau of Mines, R.I. 8285, 16p.

Bradley, J.J. and Fort, A.N., Jr. (1966) Internal friction in rocks, in Handbook of Geophysics Constants, S.P. Clark, Jr., Ed., GSA publ., p. 175-193.

Broadbent, C.D. (1974) Predictable blasting with in situ seismic surveys. Mining Engineering, Vol 26, p. 37-41.

Brown, E.T. (1981) Rock Characterization Testing and Monitoring. E.T. Brown, Ed., Published for the Commission on Testing Methods, International Society of Rock Mechanics, 211p.

Coon, R.F. and Merritt, A.H. (1970) Predicting in situ modulus of deformation using rock quality indexes. ASTM STP 477, p. 154-173.

Cooper, B. (1944) Industrial limestone and dolomites in Virginia: New River-Roanoke River District. Virginia Geological Survey, Bull. 62, 98p.

Dobrin, M.B. (1976) Introduction to Geophysical Prospecting. McGraw-Hill Inc, 446p.

Ensminger, D. (1973) Ultrasonics: The Low- and High-Intensity Applications. Marcel Dekker Inc.,New York, 570p.

Farmer, I.W. (1968) Engineering Properties of Rocks, E & F.N. Spon Limited, London, 208p.

Fairhurst, C. (1965) Measurement of in situ stresses with particular reference to hydraulic fracturing. Rock Mechanics and Engineering Geology, Vol. II, p. 129-147.

Frederick, J.R. (1965) Ultrasonic Engineering. John Wiley and Son Inc., New York, 379p.

Frisillo, A.L. and Stewart, T.J. (1980) Effect of partial gas/ brine saturation on ultrasonic absorption in sandstone. J. Geophys. Res., Vol. 85, p. 5209-5211.

Gardner, G.H.F., Gardner, L.W., and Gregory, A.R. (1974) Formation velocity and density: the diagnostic basis for stratigraphic traps. Geophysics, Vol. 39, p. 770-780.

Gladwin, M.T. (1982) Ultrasonic stress monitoring in underground mining. Int. J. Rock Mech. Sci. & Geomech. Abstr., Vol. 19, p.221-228.

_____ and Stacey, F.D. (1974a) Ultrasonic pulse velocity as a rock stress sensor. Tectonphysics, Vol. 21, p. 39-45.

_____ and _____ (1974b) Anelastic degradation of acoustic pulse in rock. Physics of Earth and Planetary Interiors, Vol. 8, p.332-336.

Gooberman, G.L. (1968) Ultrasonics: Theory and Application. Hart Publishing Co., New York, 210p.

Greenwald, H.P., Maize, E.R., Hartmann, I. and Rice, G.S. (1937) Study of Roof Movement in Coal Mines. U.S. Bureau of Mines, R.I. 3355, 41p.

Gregory, A.R. (1967) Mode conversion technique employed in shear wave velocity studies of rock samples under axial and uniform compression. Trans. AIME, Vol. 240, p.136-148.

Grujic, N. (1974) Ultrasonic testing of foundation rock. Proc. 3rd Congr. ISRM, Denver, Vol. 2A, p. 404-409.

Haimson, B.C. (1973) Field Testing and Instrumentation. ASTM, STP554, p. 156-182.

_____ (1978) The hydrofracturing stress measuring method and recent field results. Int. J. Rock Mech. Sci. & Geomech. Abstr., Vol. 15, p.167-178.

Hazen, G. and Artler, L. (1976) Practical coal pillar design problems. Mining Congress J., Vol. 21, p. 739-754.

Hewitt, P.C. (1961) The geology of the equinox quadrangle and vicinity, Vermont. Vermont Development Department, Bull. No. 18.

Hooker, V. and Duvall, W.I. (1966) Stress in Outcrops Near Georgia. U.S. Bureau of Mines, R.I. 6860, 18p.

Hughes, D.S. and Jones, H.J. (1950) Variation of elastic moduli of igneous rocks with pressure and temperatures. Geol. Soc. Am. Bull., Vol. 61, p. 843-856.

_____ and _____ (1951) Elastic wave velocities of sedimentary rocks. Trans. Am. Geophys. Union, Vol. 32,

_____ and Maurette, C. (1956) Elastic wave velocities in granite. Geophysics, Vol. 21, p. 277-284.

Jacobi, O. and Braddle, E. (1956) Electric remote measuring instruments. Gluckauf, Vol., 92, No. 1314.

Johnston, D.H. (1981) Attenuation: A state-of-the-art summary. Seismic Wave Attenuation, Toksoz, M.N. & Johnston, D.H., Eds., Society of Exploration Geophysics, 459p.

_____ and Tokson, M.N. (1980) Ultrasonic P and S wave attenuation in dry and saturated rocks under pressure. J. Geophys. Res., Vol. 85, p. 925-936.

_____, _____ and Timur, B. (1979) Attenuation of seismic waves in dry and saturated rocks: II. mechanisms. Geophysics, Vol. 44, p. 691-711.

Kennedy, H. (1984) Personal communication.

King, M.S. (1966) Wave velocities in rocks as a function of changes in overburden pressure and pore-fluid saturants. Geophysics, Vol. 31, p. 50-73.

_____ and Paulsson, B.N.P. (1981) Acoustic velocities in heated block of granite subjected to uniaxial stress. Geophys. Res. Letter, Vol. 8, p. 699-702.

Krishnamurthi, M. and Balakrishna, S. (1957) Attenuation of sound in rocks. Geophysics, Vol. 22, p. 268-274.

Lama, R.D. and Vutukuri, V.S. (1978) Handbook on Mechanical Properties of Rocks. Trans. Tech. Publications, Vol. 2, 481p.

Leeman, E.R. (1964a) The measurement of stress in rock: Part I. The principle of rock stress measuring instruments. J. S. Afr. Inst. Min. Met., Sept., 1964, p. 45-81.

_____ (1964b) The measurement of stress in rock: Part II. Borehole rock stress measuring instruments. J. S. Afr. Inst. Min. Met., Sept., 1964, p. 82-114.

_____ (1964c) The measurement of stress in rock: Part III. The results of some rock stress investigations. J. S. Afr. Inst. Min. Met., Nov., 1964, p. 254-284.

Lessley, J.C. (1984) Personal communication.

Lewis, W.E. and Tandanand, S. (1974) Bureau of Mines Test Procedures for Rock. U. S. Bureau of Mines, I.C. 8628, 223p.

Lockner, D.A., Walsh, J.B. and Byerlee, J.D. (1977) Changes in seismic velocity and attenuation during deformation of granite. J. Geophys. Res. Vol. 82, p. 5374-5377.

Mavko, G. and Nur, A. (1979) Wave attenuation in partially saturated rocks. Geophysics, Vol. 44, p. 161-178.

Mckenzie, C.K., Stacey, G.P. and Gladwin, M.T. (1982) Ultrasonic characteristics of a rock mass. Int. J. Rock Mech. Min. Sci., Vol. 19, p. 25-30.

Molina, J.P. and Wack, B. (1982) Crack field characterization by ultrasonic attenuation - preliminary study on rocks. Int. J. Rock Mech. Min. Sci. & Geomech. Abstr. Vol. 19, p. 267-278.

M.T.S. Publication 160.03-01

New, B.M. and West, G. (1980) The transmission of compressional waves in jointed rock. Engineering Geology, Vol. 15, p. 151-161.

Nur, A.M. (1971) Effects of stress on velocity anisotropy in rocks with cracks. J. Geophys. Res., Vol. 76, p. 2022-2034.

Obert, L. (1939) Measurement of Pressure on Rock Pillars in Underground Mines, Part I. U.S. Bureau of Mines R.I. 3444, 15p.

_____ (1940) Measurement of Pressure on Rock Pillars in Underground Mines, Part II. U.S. Bureau of Mines R.I. 3521, 11p.

_____ and Duvall, W.I. (1967) Rock Mechanics and the Design of Structures in Rock, John Wiley & Sons Inc, 650p.

O'Connel, R.J. and Budiansky, B. (1977) Viscoelastic properties of fluid saturated cracked solids. J. Geophys. Res., Vol. 82, P. 5719-5736.

Panek, L.A. and Stock, J.A. (1964) Development of a Rock Stress Monitoring Station Based on the Flat Slot Method of Measuring Existing Rock Stress. U.S. Bureau of Mines, R.I. 6537, 61p.

Peng, S.S. (1978) Coal Mine Ground Control. John Wiley & Sons Inc., 450p.

Phillips, D.W. (1948) Tectonics of mining. Pt. 5, Colliery Engineering, Nov., 1948, 23p.

Poole, R.W. and Farmer, I.W. (1980) Consistency and repeatability of Schmidt hammer rebound data during testing. Int. J. Rock Mech. Min Sci., Vol. 18, p. 229-234.

Potts, E.L.J. and Tomlin, N. (1960) Investigation into the measurement of rock pressures in the mines and in the laboratory. Inter. Conf. on Strata Control, Rept. D-4.

Price, A.M. (1979) The Effect of Confining Pressure on the Post-Yield Deformation Characteristic of Rocks, Ph.D. Thesis, University of Newcastle-upon-Tyne.

Proskuryakov, V. M. (1975) Seismic investigations of the stress of rock. Soviet Mining Science, Vol. 11, p.193-199.

Roxborough, F.F. (1965) Roof control and coal hardness. Colliery Engineering, January, 1965, p. 19-24.

Rzhevsky, V. and Novik, G. (1971) The Physics of Rocks. Moscow MIR publishers.

Schilizzi, P.P.G. (1982) The Potential of Sonic Wave Propagation in Engineering Rock Classification. Master Thesis, V.P.I. & S.U.

Smith, R.L. (1973) Mine Installation of two Bureau of Mines Hydraulic Pressure Cells and a Borehole Deformation Gage. U.S. Bureau of Mines, I.C. 8585, 76p.

Soboley, G., Spetzler, H. and Salov, B. (1978) Precursors to failure in rocks while undergoing anelastic deformations. J. Geophys. Res., Vol. 83, p. 1775-1784.

Spencer, J.W. (1979) Bulk and shear attenuation in Berea sandstone: The effects of pore fluids. J. Geophys. Res., Vol. 84, p. 7521-7523.

Stacy, T.R. (1976) Seismic assessment of rock masses. Proc. Symp. on Exploration for Rock Engineering, Vol. 2, p. 113-117.

Su, W.H. (1982) Development of Ultrasonic Techniques for the Measurement of In-Site Stress, Dissertation, West Virginia University, 142p.

Thill, R.E. (1972) Acoustic methods for monitoring failure in rock. Proc. 14th Symposium on Rock Mechanics. p. 649-687.

_____ , McWilliams, J.R. and Bur, T.R. (1968) An Acoustical Bench for an Ultrasonic Pulse System. U.S. Bureau of Mines, R.I. 7164, 22p.

_____ , and Jessup, J.A. (1982) Engineering properties of coal measure rocks. Proc. AIME Annual Meeting, Dallas, Texas, Preprint 82-146, 26p.

Tocher, D. (1957) Anisotropy in rocks under simple compression. Trans. Am. Geophys. Union, Vol. 38, p. 89-94.

Toksoz, M.N., Johnston, D.H. and Timur, A. (1979) Attenuation of seismic waves in dry and saturated rocks: 1. laboratory measurements. Geophysics, Vol. 44, p. 681-711.

Tomashevskaya, I.S. and Khamidullin, Ya. N. (1972) Precursors of the destruction of rock specimens. Izv., Earth Physics, No. 5, p. 12-20.

Velonex Instruction Manual.

Whitcomb, J.H., Garmny, J.D. and Anderson, D.L. (1973) Earthquakes prediction: variation of seismic velocities before San Fernando earthquake. Science, Vol. 180, p. 632-635.

Willard, R,J. and McWilliams, J.R. (1969) Microstructural techniques in the study of physical properties of rock. Int. J. Rock Mech. Min. Sci. & Geotech. Abstr. Vol. 6, p. 1-12.

Wilson, A.H. (1961) A laboratory investigation of a high modulus borehole plug gage for the measurement of rock stress. Fourth Symp. on Rock Mech.

Winkler, K.W. and Nur, A. (1982) Seismic attenuation effects of pore fluids and frictional sliding. Geophysics, Vol. 47, p. 1-15.

Wyllie, M.R.J., Gregory, A.R. and Gardner, L.W. (1956) Elastic wave velocities in heterogeneous and porous media. Geophysics, Vol. 21, p. 41-70.

_____, _____ and Gregory, G.H.F. (1958) An experimental investigation of factors affecting elastic wave velocities in p[orous media. Geophysics, Vol. 23, p. 459-493.

Youash, Y.Y. (1970) Dynamic physical properties of rock: Part 1, Theory and procedure. Proc. 2nd Cong. Int. Soc. Rock Mech., Vol. 1, p. 171-183.

TABLE A.1

Mean Testing Result of Granite
(Stress perpendicular to mica foliation)

Stress (psi)	Attenu. (dB/in)	Velocity (ft/sec)	Attenu. Ratio	Velocity Ratio	S. D. of Attenu.	S. D. of Velocity
0.0	12.0501	13640.7	1.00000	1.00000	1.36843	1495.50
512.9	11.9036	14157.5	0.98784	1.03789	1.30100	1322.71
1025.7	11.8414	14469.7	0.98268	1.06077	1.31424	1490.60
1538.6	11.7832	14702.0	0.97785	1.07780	1.32697	1467.85
2051.3	11.7320	14702.0	0.97360	1.07780	1.32312	1467.85
2461.9	11.6694	14765.2	0.96841	1.08244	1.29107	1404.79
2872.1	11.6363	14832.3	0.96566	1.08736	1.25117	1344.32
3282.6	11.5725	14997.4	0.96037	1.09946	1.26659	1409.55
3692.9	11.5078	15139.3	0.95500	1.10986	1.21331	1534.66
4102.9	11.4072	15173.0	0.94665	1.11233	1.13343	1499.42
4513.1	11.3689	15434.5	0.94347	1.13150	1.18428	1607.91
4923.7	11.3359	15470.2	0.94073	1.13412	1.19684	1573.13
5334.1	11.2184	15470.2	0.93098	1.13412	1.10053	1573.13
5799.4	11.1923	15352.6	0.92881	1.12550	1.09698	1358.11
6209.0	11.1431	15538.7	0.92473	1.13914	1.12132	1386.86
6677.6	11.1319	15538.7	0.92380	1.13914	1.13945	1386.86
7086.4	11.1164	15576.2	0.92252	1.14189	1.14978	1354.50
7498.1	11.1054	15576.2	0.92160	1.14189	1.16767	1354.50
7908.3	11.1054	15693.8	0.92160	1.15051	1.16767	1550.34
8315.7	11.1054	15693.8	0.92160	1.15051	1.16767	1550.34

TABLE A.2

Mean Testing Result of Granite
(Stress parallel to mica foliation)

Stress (psi)	Attenu. (dB/in)	Velocity (ft/sec)	Attenu. Ratio	Velocity Ratio	S. D. of Attenu.	S. D. of Velocity
0.00	10.3765	13552.1	1.00000	1.00000	0.772003	1027.07
484.00	10.5316	14028.9	1.01495	1.03518	0.771120	1027.68
967.83	10.6389	14135.8	1.02529	1.04307	0.777826	901.25
1452.00	10.6973	14268.9	1.03092	1.05289	0.746919	938.54
1935.67	10.7343	14533.6	1.03448	1.07242	0.743614	932.40
2323.00	10.7888	14569.9	1.03973	1.07510	0.790282	875.91
2710.17	10.8564	14569.9	1.04625	1.07510	0.745566	875.91
3097.33	10.9354	14607.3	1.05386	1.07786	0.747871	823.54
3484.50	10.9818	14649.3	1.05833	1.08096	0.777883	782.70
3871.67	11.0805	14692.8	1.06785	1.08417	0.777303	752.94
4258.83	11.1830	14824.4	1.07772	1.09388	0.713379	694.29
4646.00	11.2408	14824.4	1.08329	1.09388	0.747150	694.29
5033.17	11.3292	14916.8	1.09181	1.10070	0.817067	663.91
5452.00	11.3943	15173.4	1.09809	1.11963	0.755489	894.71
5870.83	11.4624	15273.2	1.10465	1.12700	0.770083	899.71
6258.00	11.4954	15357.6	1.10783	1.13323	0.771594	794.69
6645.17	11.5293	15357.6	1.11110	1.13323	0.776583	794.69
7032.33	11.5866	15357.6	1.11662	1.13323	0.779566	794.69
7419.50	11.6684	15357.6	1.12450	1.13323	0.776878	794.69
7806.67	11.8194	15357.6	1.13905	1.13323	0.846006	794.69
8144.50	11.9051	15357.6	1.14731	1.13323	0.839273	794.69
8532.33	11.9554	15357.6	1.15216	1.13323	0.831446	794.69
8920.17	11.9984	15357.6	1.15631	1.13323	0.789703	794.69
9308.00	12.1008	15357.6	1.16617	1.13323	0.768217	794.69

TABLE A.3

Mean Testing Result of Five Oaks Limestone

Stress (psi)	Attenu. (dB/in)	Velocity (ft/sec)	Attenu. Ratio	Velocity Ratio	S. D. of Attenu.	S. D. of Velocity
0.0	8.4674	18947.9	1.00000	1.00000	1.93147	268.747
776.9	8.6581	18972.2	1.02252	1.00128	1.74576	218.368
1554.3	8.7533	18972.2	1.03377	1.00128	1.74549	218.368
2294.0	8.8570	18972.2	1.04601	1.00128	1.69140	218.368
3108.9	8.9334	18972.2	1.05504	1.00128	1.66965	218.368
3730.6	9.0260	18972.2	1.06598	1.00128	1.66213	218.368
4352.5	9.0700	18972.2	1.07117	1.00128	1.65020	218.368
4974.3	9.1765	18972.2	1.08374	1.00128	1.67345	218.368
5595.6	9.2978	18972.2	1.09807	1.00128	1.72968	218.368
6217.4	9.4369	18972.2	1.11450	1.00128	1.71001	218.368
6839.3	9.5230	18972.2	1.12467	1.00128	1.74759	218.368
7461.0	9.7017	18972.2	1.14577	1.00128	1.88059	218.368
8083.1	9.7723	18972.2	1.15410	1.00128	1.93225	218.368
8704.5	9.8748	18972.2	1.16621	1.00128	1.94264	218.368
9326.3	9.9451	18972.2	1.17451	1.00128	2.02812	218.368
9948.1	10.0339	18972.2	1.18500	1.00128	2.08795	218.368
10570.4	10.1714	18896.8	1.20124	0.99730	2.27967	240.952
11191.6	10.2726	18896.8	1.21320	0.99730	2.40427	240.952
11813.4	10.4560	18896.8	1.23485	0.99730	2.72073	240.952
12435.3	10.6359	18872.0	1.25610	0.99599	2.91164	257.420

TABLE A.4

Mean Testing Result of Argillaceous Limestone

Stress (psi)	Attenu. (dB/in)	Velocity (ft/sec)	Attenu. Ratio	Velocity Ratio	S. D. of Attenu.	S. D. of Velocity
0	6.7258	15895.4	1.00000	1.00000	0.96404	1303.73
766.4	7.1413	15900.9	1.06178	1.00035	0.62088	1301.37
1532.8	7.3738	15900.9	1.09638	1.00035	0.72744	1301.37
2299.2	7.7478	15900.9	1.15195	1.00035	1.11140	1301.37
3065.8	8.0245	15866.8	1.19309	0.99820	1.21835	1260.15
3679.0	8.1673	15814.4	1.21432	0.99490	1.26456	1299.43
4292.4	8.5777	15763.8	1.27534	0.99172	1.54815	1346.02
4905.2	8.8642	15763.8	1.31794	0.99172	1.63484	1346.02
5518.2	9.2013	15730.9	1.36806	0.98965	1.78844	1357.04
6131.4	9.5792	15730.9	1.42425	0.98965	1.98385	1357.04
6744.8	10.1979	15696.7	1.51624	0.98750	1.94295	1309.13
7358.0	10.8976	15696.7	1.62027	0.98750	2.02710	1309.13
7971.8	11.6325	15696.7	1.72953	0.98750	2.37873	1309.13
8583.8	12.5335	15696.7	1.86350	0.98750	3.04261	1309.13
9197.2	13.0784	15696.7	1.94451	0.98750	3.37395	1309.13

TABLE A.5

Mean Testing Result of Shale
(Stress parallel to the bedding plane)

Stress (psi)	Attenu. (dB/in)	Velocity (ft/sec)	Attenu. Ratio	Velocity Ratio	S. D. of Attenu.	S. D. of Velocity
0.0	7.02791	16992.5	1.00000	1.00000	1.73325	1174.55
435.0	6.94800	17096.4	0.98863	1.00611	1.69293	1055.63
869.6	6.98868	17096.4	0.99442	1.00611	1.70790	1055.63
1301.2	7.04611	17096.4	1.00259	1.00611	1.75275	1055.63
1738.6	7.11431	17096.4	1.01229	1.00611	1.83078	1055.63
2087.2	7.12662	17066.1	1.01405	1.00433	1.81118	1017.19
2435.0	7.18718	17066.1	1.02266	1.00433	1.88868	1017.19
2782.8	7.25192	17066.1	1.03187	1.00433	1.94800	1017.19
3130.8	7.28657	17066.1	1.03680	1.00433	2.01824	1017.19
3478.4	7.34764	17083.9	1.04549	1.00538	2.07579	1009.38
3826.8	7.39679	17083.9	1.05249	1.00538	2.11200	1009.38
4249.6	7.42644	17083.9	1.05671	1.00538	2.13202	1009.38
4597.8	7.44081	17083.9	1.05875	1.00538	2.16069	1009.38
4945.4	7.50317	17083.9	1.06762	1.00538	2.20224	1009.38
5293.6	7.53462	17083.9	1.07210	1.00538	2.22315	1009.38
5641.2	7.61520	17083.9	1.08357	1.00538	2.25549	1009.38
5989.0	7.65975	17083.9	1.08990	1.00538	2.28323	1009.38
6337.0	7.77511	17083.9	1.10632	1.00538	2.36624	1009.38
6684.4	7.81158	17083.9	1.11151	1.00538	2.35020	1009.38
7032.4	8.12061	17083.9	1.15548	1.00538	2.34962	1009.38
7380.6	8.20089	17083.9	1.16690	1.00538	2.40843	1009.38
7728.0	8.24144	17083.9	1.17267	1.00538	2.44053	1009.38
8076.2	8.30948	17083.9	1.18235	1.00538	2.44476	1009.38
8423.4	8.31751	17083.9	1.18350	1.00538	2.43282	1009.38
8772.0	8.39145	17083.9	1.19402	1.00538	2.55022	1009.38
9136.4	8.53752	17083.9	1.21480	1.00538	2.57151	1009.38
9501.8	8.55431	17083.9	1.21719	1.00538	2.54667	1009.38

TABLE A.6

Mean Testing Result of Shale
(Stress perpendicular to the bedding plane)

Stress (psi)	Attenu. (dB/in)	Velocity (ft/sec)	Attenu. Ratio	Velocity Ratio	S. D. of Attenu.	S. D. of Velocity
0.00	6.88999	17846.1	1.00000	1.00000	1.26040	271.513
888.14	6.70810	17885.7	0.97360	1.00222	1.0089	268.782
1776.14	6.58678	17885.7	0.95599	1.00222	0.91453	268.782
2664.43	6.34706	17885.7	0.92120	1.00222	0.96479	268.782
3552.29	6.31806	17885.7	0.91669	1.00222	0.99677	268.782
4440.43	6.24335	17885.7	0.90615	1.00222	1.00055	268.782
5328.29	6.24374	17885.7	0.90620	1.00222	0.96649	268.782
6189.43	6.23168	17885.7	0.90445	1.00222	0.96971	268.782
7105.14	6.14150	17885.7	0.89137	1.00222	0.96475	268.782
7967.14	6.05893	17909.1	0.87938	1.00353	0.93565	238.992
8694.43	6.03145	17909.1	0.87539	1.00353	0.89684	238.992
9535.00	6.06886	17909.1	0.88082	1.00353	0.84416	238.992

TABLE A.7

Mean Testing Result of Marble

Stress (psi)	Attenu. (dB/in).	Velocity (ft/sec)	Attenu. Ratio	Velocity Ratio	S. D. of Attenu.	S. D. of Velocity
0.00	7.7096	17542.7	1.00000	1.00000	1.53904	2554.63
777.86	8.5346	17666.9	1.10701	1.00708	1.83742	2574.91
1555.57	8.6804	17768.2	1.12592	1.01285	1.92644	2601.47
2333.29	8.7592	17792.2	1.13614	1.01422	1.94377	2540.68
3111.14	8.9243	17817.8	1.15756	1.01568	1.92815	2538.25
3733.14	8.9761	17911.8	1.16428	1.02104	1.87384	2517.30
4355.43	9.0724	17872.9	1.17677	1.01882	1.88257	2547.86
4977.43	9.2502	17777.4	1.19983	1.01338	1.91866	2559.98
5599.57	9.4369	17639.3	1.22405	1.00551	1.91739	2651.19
6221.86	9.8004	17439.1	1.27119	0.99409	1.98575	2749.28
6844.14	10.2004	17012.5	1.32308	0.96978	2.07520	2864.17
7466.71	10.7508	16412.7	1.39447	0.93559	1.96928	2888.01
8089.43	11.2720	16211.5	1.46207	0.92412	2.02006	2806.27
8708.57	12.0224	15791.6	1.55941	0.90018	2.05845	2423.68

TABLE A.8

Mean Testing Result of Air-dried Sandstone

Stress (psi)	Attenu. (dB/in)	Velocity (ft/sec)	Attenu. Ratio	Velocity Ratio	S. D. of Attenu.	S. D. of Velocity
0.0	7.7160	12497.9	1.00000	1.00000	1.55570	1006.38
882.9	8.1860	12738.3	1.06091	1.01924	1.43631	945.58
1765.7	8.8719	12916.2	1.14981	1.03347	1.58630	938.88
2648.2	9.4539	13080.8	1.22523	1.04664	1.75394	976.78
3530.9	9.8863	13133.3	1.28127	1.05084	1.95307	947.53
4237.0	10.2696	13164.6	1.33095	1.05331	2.13572	885.59
4943.2	10.6464	13232.2	1.37978	1.05875	2.24797	852.10
5649.3	10.9631	13291.6	1.42083	1.06351	2.35766	846.54
6355.6	11.3418	13340.8	1.46991	1.06744	2.46955	850.95
7061.7	11.6614	13347.6	1.51133	1.06799	2.52253	802.12
7767.9	11.9532	13395.9	1.54914	1.07185	2.62258	794.26
8474.0	12.2058	13372.4	1.58188	1.06137	2.64722	803.21
9180.2	12.4878	13348.5	1.61843	1.06806	2.66341	809.09
9886.3	12.7943	13296.8	1.65815	1.06392	2.66961	774.03
10592.6	13.0642	13249.9	1.69313	1.06017	2.72583	786.50
11298.8	13.3839	13175.2	1.73456	1.05419	2.82283	744.60

TABLE A.9

Mean Testing Result of Water Saturated Sandstone

Stress (psi)	Attenu. (dB/in)	Velocity (ft/sec)	Attenu. Ratio	Velocity Ratio	S. D. of Attenu.	S. D. of Velocity
0.0	14.7999	13950.4	1.00000	1.00000	1.52354	391.08
883.0	15.7937	14332.7	1.06715	1.02740	2.74683	341.39
1766.3	15.7669	14419.9	1.06534	1.03365	2.96092	387.32
2649.8	15.8295	14518.6	1.06957	1.04073	3.21283	342.83
3533.2	15.8591	14532.2	1.07157	1.04170	3.39888	320.71
4239.7	15.8975	14563.3	1.07416	1.04393	3.53863	373.38
4946.7	15.9519	14548.8	1.07784	1.04289	3.53235	369.06
5653.0	16.1229	14451.7	1.08939	1.03593	3.48787	450.43
6360.0	16.5192	14359.8	1.11617	1.02935	3.46149	529.43
7066.3	16.6672	14260.4	1.12617	1.02222	3.49824	556.56
7772.7	16.8891	14216.9	1.14116	1.01910	3.42422	531.85
8480.0	17.2374	14146.1	1.16470	1.01403	3.42752	505.66
9196.0	17.4779	14045.5	1.18095	1.00682	3.40065	419.37
9904.0	18.0277	13916.1	1.21810	0.99754	3.86151	488.27

TABLE B.1

Sonic Testing Results of Argillaceous Limestone

Sample	Stress (psi)	Amplitude	Velocity (ft/sec)	Att. Coef. (dB/in)	Att. Coef. Ratio	Velocity Ratio
AL8	0	1.600	17291.7	5.5328	1.00000	1.0000
AL8	768	1.300	17291.7	6.4020	1.15709	1.0000
AL8	1536	1.300	17291.7	6.4020	1.15709	1.0000
AL8	2304	1.275	17291.7	6.4833	1.17179	1.0000
AL8	3073	1.250	17291.7	6.5662	1.18677	1.0000
AL8	3687	1.250	17291.7	6.5662	1.18677	1.0000
AL8	4302	1.225	17291.7	6.6507	1.20205	1.0000
AL8	4916	1.200	17291.7	6.7371	1.21765	1.0000
AL8	5531	1.175	17291.7	6.8252	1.23358	1.0000
AL8	6145	1.175	17291.7	6.9152	1.24986	1.0000
AL8	6760	0.900	17120.5	7.9413	1.43530	0.9901
AL8	7374	0.700	17120.5	8.9933	1.62544	0.9901
AL8	7989	0.600	17120.5	9.6386	1.74207	0.9901
AL8	8603	0.540	17120.5	10.0796	1.82178	0.9901
AL8	9218	0.480	17120.5	10.5726	1.91089	0.9901
AL8	9832	0.400	17120.5	11.3358	2.04883	0.9901

Table B.1 Continued

Sample	Stress (psi)	Amplitude	Velocity (ft/sec)	Att. Coef. (dB/in)	Att. Coef. Ratio	Velocity Ratio
AL9	0	1.04	14333.3	7.3752	1.00000	1.00000
AL9	766	1.00	14333.3	7.5402	1.02238	1.00000
AL9	1532	0.96	14333.3	7.7120	1.04567	1.00000
AL9	2298	0.92	14333.3	7.8911	1.06996	1.00000
AL9	3064	0.88	14333.3	8.0782	1.09532	1.00000
AL9	3677	0.84	14333.3	8.2740	1.12187	1.00000
AL9	4290	0.76	14333.3	8.6951	1.17897	1.00000
AL9	4903	0.72	14333.3	8.9227	1.20982	1.00000
AL9	5515	0.68	14333.3	9.1632	1.24244	1.00000
AL9	6128	0.64	14333.3	9.4183	1.27703	1.00000
AL9	6741	0.60	14333.3	9.6899	1.31386	1.00000
AL9	7354	0.56	14333.3	9.9803	1.35322	1.00000
AL9	7967	0.52	14333.3	10.2921	1.39551	1.00000
AL9	8579	0.48	14333.3	10.6290	1.44118	1.00000
AL9	9192	0.48	14333.3	10.6290	1.44118	1.00000

Table B.1 Continued

Sample	Stress (psi)	Amplitude	Velocity (ft/sec)	Att. Coef. (dB/in)	Att. Coef. Ratio	Velocity Ratio
AL10	0	1.20	15439.0	6.7371	1.00000	1.00000
AL10	766	1.12	15466.6	7.0259	1.04287	1.00179
AL10	1532	1.10	15466.6	7.1013	1.05406	1.00179
AL10	2298	1.08	15466.6	7.1781	1.06546	1.00179
AL10	3064	1.00	15466.6	7.5003	1.11328	1.00179
AL10	3677	0.96	15466.6	7.6711	1.13865	1.00179
AL10	4290	0.90	15466.6	7.9413	1.17875	1.00179
AL10	4903	0.80	15466.6	8.4343	1.25193	1.00179
AL10	5515	0.70	15302.4	8.9933	1.33489	0.99115
AL10	6128	0.60	15302.4	10.2838	1.52645	0.99115
AL10	6741	0.50	15302.4	10.4018	1.54395	0.99115
AL10	7354	0.40	15302.4	11.3358	1.68260	0.99115
AL10	7967	0.30	15302.4	12.5401	1.86134	0.99115
AL10	8579	0.28	15302.4	12.8289	1.90421	0.99115
AL10	9192	0.16	15302.4	15.1714	2.25192	0.99115

Table B.1 Continued

Sample	Stress (psi)	Amplitude	Velocity (ft/sec)	Att. Coef. (dB/in)	Att. Coef. Ratio	Velocity Ratio
AL13	0	0.90	15204.7	7.9222	1.00000	1.00000
AL13	766	0.89	15204.7	7.9689	1.00589	1.00000
AL13	1532	0.81	15204.7	8.3622	1.05554	1.00000
AL13	2298	0.62	15204.7	9.4785	1.19644	1.00000
AL13	3064	0.56	15204.7	9.9035	1.25009	1.00000
AL13	3677	0.54	14942.5	10.0554	1.26926	0.98276
AL13	4290	0.44	14689.3	10.9106	1.37721	0.96610
AL13	4902	0.40	14689.3	11.3086	1.42725	0.96610
AL13	5515	0.35	14689.3	11.8662	1.49784	0.96610
AL13	6128	0.30	14689.3	12.5099	1.57909	0.96610
AL13	6741	0.25	14689.3	13.2713	1.67520	0.96610
AL13	7354	0.20	14689.3	14.2031	1.79282	0.96610
AL13	7969	0.15	14689.3	15.4044	1.94463	0.96610
AL13	8579	0.10	14689.3	17.0976	2.15819	0.96610
AL13	9192	0.08	14689.3	18.0294	2.27581	0.96610

Table B.1 Continued

Sample	Stress (psi)	Amplitude	Velocity (ft/sec)	Att. Coef. (dB/in)	Att. Coef. Ratio	Velocity Ratio
AL15	0	1.42	17208.3	6.0616	1.00000	1.0000
AL15	766	1.20	17208.3	6.7697	1.11681	1.0000
AL15	1532	1.06	17208.3	7.2915	1.20289	1.0000
AL15	2298	0.96	17208.3	7.7083	1.27165	1.0000
AL15	3064	0.88	17038.0	8.0743	1.33203	0.9901
AL15	3677	0.84	17038.0	8.2699	1.36431	0.9901
AL15	4290	0.76	17038.0	8.6909	1.43376	0.9901
AL15	4902	0.72	17038.0	8.9183	1.47128	0.9901
AL15	5515	0.68	17038.0	9.1588	1.51094	0.9901
AL15	6128	0.64	17038.0	9.4138	1.55301	0.9901
AL15	6741	0.60	17038.0	9.6852	1.59779	0.9901
AL15	7354	0.56	17038.0	9.9754	1.64567	0.9901
AL15	7967	0.52	17038.0	10.2871	1.69709	0.9901
AL15	8579	0.48	17038.0	10.6238	1.75264	0.9901
AL15	9192	0.44	17038.0	10.9898	1.81301	0.9901

TABLE B.2

Sonic Testing Results of Five Oaks Limestone

Sample	Stress (psi)	Amplitude	Velocity (ft/sec)	Att. Coef. (dB/in)	Att. Coef. Ratio	Velocity Ratio
V1	0	0.290	18420.1	12.4011	1.00000	1.00000
V1	777	0.290	18614.0	12.4011	1.00000	1.01053
V1	1555	0.280	18614.0	12.5447	1.01158	1.01053
V1	2332	0.280	18614.0	12.5447	1.01158	1.01053
V1	3110	0.280	18614.0	12.5447	1.01158	1.01053
V1	3732	0.280	18614.0	12.5447	1.01158	1.01053
V1	4354	0.280	18614.0	12.5447	1.01158	1.01053
V1	4976	0.280	18614.0	12.5447	1.01158	1.01053
V1	5598	0.265	18614.0	12.7701	1.02975	1.01053
V1	6220	0.265	18614.0	12.7701	1.02975	1.01053
V1	6842	0.260	18614.0	12.8480	1.03604	1.01053
V1	7464	0.245	18614.0	13.0913	1.05566	1.01053
V1	8086	0.240	18614.0	13.1757	1.06246	1.01053
V1	8708	0.240	18614.0	13.1757	1.06246	1.01053
V1	9330	0.235	18614.0	13.2619	1.06941	1.01053
V1	9952	0.225	18614.0	13.4399	1.08376	1.01053
V1	10574	0.200	18420.1	13.9220	1.12264	1.00000
V1	11196	0.180	18420.1	14.3532	1.15742	1.00000
V1	11818	0.140	18420.1	15.3819	1.24037	1.00000
V1	12440	0.120	18420.1	16.0129	1.29125	1.00000

Table B.2 Continued

Sample	Stress (psi)	Amplitude	Velocity (ft/sec)	Att. Coef. (dB/in)	Att. Coef. Ratio	Velocity Ratio
V2	0	0.900	19014.3	7.76540	1.00000	1.00000
V2	777	0.850	19014.3	7.99936	1.03013	1.00000
V2	1555	0.825	19014.3	8.12156	1.04586	1.00000
V2	2332	0.813	19014.3	8.18153	1.05359	1.00000
V2	3110	0.800	19014.3	8.24751	1.06208	1.00000
V2	3732	0.800	19014.3	8.24751	1.06208	1.00000
V2	4354	0.797	19014.3	8.26289	1.06407	1.00000
V2	4976	0.797	19014.3	8.26289	1.06407	1.00000
V2	5598	0.797	19014.3	8.26289	1.06407	1.00000
V2	6220	0.750	19014.3	8.51169	1.09610	1.00000
V2	6842	0.750	19014.3	8.51169	1.09610	1.00000
V2	7464	0.725	19014.3	8.65045	1.11397	1.00000
V2	8086	0.725	19014.3	8.65045	1.11397	1.00000
V2	8708	0.713	19014.3	8.71877	1.12277	1.00000
V2	9330	0.713	19014.3	8.71877	1.12277	1.00000
V2	9952	0.700	19014.3	8.79409	1.13247	1.00000
V2	10574	0.700	19014.3	8.79409	1.13247	1.00000
V2	11196	0.700	19014.3	8.79409	1.13247	1.00000
V2	11818	0.700	19014.3	8.79409	1.13247	1.00000
V2	12440	0.698	19014.3	8.80580	1.13398	1.00000

Table B.2 Continued

Sample	Stress (psi)	Amplitude	Velocity (ft/sec)	Att. Coef. (dB/in)	Att. Coef. Ratio	Velocity Ratio
V3	0	0.80	19221	8.2475	1.00000	1.00000
V3	777	0.80	19221	8.2475	1.00000	1.00000
V3	1555	0.80	19221	8.2475	1.00000	1.00000
V3	2332	0.80	19221	8.2475	1.00000	1.00000
V3	3110	0.80	19221	8.2475	1.00000	1.00000
V3	3732	0.76	19221	8.4575	1.02546	1.00000
V3	4354	0.75	19221	8.5117	1.03203	1.00000
V3	4976	0.72	19221	8.6788	1.05229	1.00000
V3	5598	0.66	19221	9.0349	1.09548	1.00000
V3	6220	0.60	19221	9.4251	1.14278	1.00000
V3	6842	0.60	19221	9.4251	1.14278	1.00000
V3	7464	0.56	19221	9.7075	1.17702	1.00000
V3	8086	0.56	19221	9.7075	1.17702	1.00000
V3	8708	0.53	19221	9.9328	1.20435	1.00000
V3	9330	0.53	19221	9.9328	1.20435	1.00000
V3	9952	0.50	19221	10.1714	1.23326	1.00000
V3	10574	0.50	19221	10.1714	1.23326	1.00000
V3	11196	0.50	19221	10.1714	1.23326	1.00000
V3	11818	0.50	19221	10.1714	1.23326	1.00000
V3	12440	0.50	19221	10.1714	1.23326	1.00000

Table B.2 Continued

Sample	Stress (psi)	Amplitude	Velocity (ft/sec)	Att. Coef. (dB/in)	Att. Coef. Ratio	Velocity Ratio
V6	0	0.950	19041.2	7.53344	1.00000	1.00000
V6	776	0.950	19041.2	7.53344	1.00000	1.00000
V6	1552	0.950	19041.2	7.53344	1.00000	1.00000
V6	2229	0.900	19041.2	7.75444	1.02934	1.00000
V6	3105	0.900	19041.2	7.75444	1.02934	1.00000
V6	3726	0.900	19041.2	7.75444	1.02934	1.00000
V6	4347	0.875	19041.2	7.86958	1.04462	1.00000
V6	4968	0.875	19041.2	7.86958	1.04462	1.00000
V6	5588	0.850	19041.2	7.98807	1.06035	1.00000
V6	6209	0.825	19041.2	8.11009	1.07655	1.00000
V6	6830	0.813	19041.2	8.16998	1.08450	1.00000
V6	7451	0.810	19041.2	8.18509	1.08650	1.00000
V6	8073	0.805	19041.2	8.21040	1.08986	1.00000
V6	8693	0.800	19041.2	8.23587	1.09324	1.00000
V6	9314	0.800	19041.2	8.23587	1.09324	1.00000
V6	9935	0.800	19041.2	8.23587	1.09324	1.00000
V6	10556	0.800	19041.2	8.23587	1.09324	1.00000
V6	11177	0.790	19041.2	8.28729	1.10007	1.00000
V6	11798	0.790	19041.2	8.28729	1.10007	1.00000
V6	12419	0.730	19041.2	8.61015	1.14292	1.00000

Table B.2 Continued

Sample	Stress (psi)	Amplitude	Velocity (ft/sec)	Att. Coef. (dB/in)	Att. Coef. Ratio	Velocity Ratio
V9	0	1.075	19032.3	7.03148	1.00047	1.00000
V9	776	1.075	19032.3	7.03148	1.00047	1.00000
V9	1552	1.075	19032.3	7.03148	1.00047	1.00000
V9	2229	1.075	19032.3	7.03148	1.00047	1.00000
V9	3105	1.075	19032.3	7.03148	1.00047	1.00000
V9	3726	1.075	19032.3	7.03148	1.00047	1.00000
V9	4347	1.075	19032.3	7.03148	1.00047	1.00000
V9	4968	1.075	19032.3	7.03148	1.00047	1.00000
V9	5588	1.075	19032.3	7.03148	1.00047	1.00000
V9	6209	1.075	19032.3	7.03148	1.00047	1.00000
V9	6830	1.050	19032.3	7.12770	1.01416	1.00000
V9	7451	1.050	19032.3	7.12770	1.01416	1.00000
V9	8073	1.050	19032.3	7.12770	1.01416	1.00000
V9	8693	1.025	19032.3	7.22625	1.02818	1.00000
V9	9314	1.025	19032.3	7.22625	1.02818	1.00000
V9	9935	1.025	19032.3	7.22625	1.02818	1.00000
V9	10556	1.025	19032.3	7.22625	1.02818	1.00000
V9	11177	1.025	19032.3	7.22625	1.02818	1.00000
V9	11798	1.025	19032.3	7.22625	1.02818	1.00000
V9	12419	1.025	19032.3	7.22625	1.02818	1.00000

Table B.2 Continued

Sample	Stress (psi)	Amplitude	Velocity (ft/sec)	Att. Coef. (dB/in)	Att. Coef. Ratio	Velocity Ratio
V11	0	0.59	18812.1	9.4939	1.00000	1.00000
V11	777	0.59	18812.1	9.4939	1.00000	1.00000
V11	1555	0.59	18812.1	9.4939	1.00000	1.00000
V11	2332	0.59	18812.1	9.4939	1.00000	1.00000
V11	3110	0.59	18812.1	9.4939	1.00000	1.00000
V11	3732	0.59	18812.1	9.4939	1.00000	1.00000
V11	4354	0.59	18812.1	9.4939	1.00000	1.00000
V11	4976	0.58	18812.1	9.5638	1.00737	1.00000
V11	5598	0.57	18812.1	9.6350	1.01487	1.00000
V11	6220	0.56	18812.1	9.7075	1.02250	1.00000
V11	6842	0.56	18812.1	9.7075	1.02250	1.00000
V11	7464	0.56	18812.1	9.7075	1.02250	1.00000
V11	8086	0.54	18812.1	9.8563	1.03818	1.00000
V11	8708	0.52	18812.1	10.0108	1.05445	1.00000
V11	9330	0.52	18812.1	10.0108	1.05445	1.00000
V11	9952	0.52	18812.1	10.0108	1.05445	1.00000
V11	10574	0.52	18812.1	10.0108	1.05445	1.00000
V11	11196	0.50	18812.1	10.1714	1.07136	1.00000
V11	11818	0.49	18812.1	10.2541	1.08007	1.00000
V11	12440	0.48	18812.1	10.3385	1.08896	1.00000

Table B.2 Continued

Sample	Stress (psi)	Amplitude	Velocity (ft/sec)	Att. Coef. (dB/in)	Att. Coef. Ratio	Velocity Ratio
V12	0	0.64	18794.3	9.1695	1.00000	0.989363
V12	779	0.63	18794.3	9.2341	1.00704	0.989363
V12	1558	0.62	18794.3	9.2996	1.01419	0.989363
V12	2337	0.61	18794.3	9.3662	1.02145	0.989363
V12	3116	0.61	18794.3	9.3662	1.02145	0.989363
V12	3739	0.60	18794.3	9.4340	1.02884	0.989363
V12	4363	0.60	18794.3	9.4340	1.02884	0.989363
V12	4986	0.59	18794.3	9.5028	1.03635	0.989363
V12	5609	0.59	18794.3	9.5028	1.03635	0.989363
V12	6232	0.58	18794.3	9.5729	1.04398	0.989363
V12	6856	0.58	18794.3	9.5729	1.04398	0.989363
V12	7479	0.57	18794.3	9.6441	1.05176	0.989363
V12	8102	0.56	18794.3	9.7166	1.05966	0.989363
V12	8725	0.56	18794.3	9.7166	1.05966	0.989363
V12	9348	0.55	18794.3	9.7905	1.06772	0.989363
V12	9972	0.54	18794.3	9.8656	1.07591	0.989363
V12	10599	0.52	18794.3	10.0203	1.09278	0.989363
V12	11218	0.52	18794.3	10.0203	1.09278	0.989363
V12	11841	0.52	18794.3	10.0203	1.09278	0.989363
V12	12465	0.52	18794.3	10.0203	1.09278	0.989363

Table B.2 Continued

Sample	Stress (psi)	Amplitude	Velocity (ft/sec)	Att. Coef. (dB/in)	Att. Coef. Ratio	Velocity Ratio
V4	0	1.350	19248.2	6.0971	1.00000	1.00000
V4	776	1.000	19248.2	7.3238	1.20119	1.00000
V4	1552	0.900	19248.2	7.7544	1.27182	1.00000
V4	2229	0.800	19248.2	8.2359	1.35078	1.00000
V4	3105	0.700	19248.2	8.7817	1.44030	1.00000
V4	3726	0.625	19248.2	9.2449	1.51628	1.00000
V4	4347	0.600	19248.2	9.4118	1.54364	1.00000
V4	4968	0.525	19248.2	9.9576	1.63316	1.00000
V4	5588	0.500	19248.2	10.1570	1.66587	1.00000
V4	6209	0.475	19248.2	10.3667	1.70026	1.00000
V4	6830	0.425	19248.2	10.8213	1.77482	1.00000
V4	7451	0.360	19248.2	11.4998	1.88610	1.00000
V4	8073	0.340	19248.2	11.7334	1.92442	1.00000
V4	8693	0.320	19248.2	11.9812	1.96506	1.00000
V4	9314	0.290	19248.2	12.3836	2.03105	1.00000
V4	9935	0.280	19248.2	12.5270	2.05458	1.00000
V4	10556	0.250	18838.7	12.9902	2.13055	0.97872
V4	11177	0.240	18838.7	13.1571	2.15792	0.97872
V4	11798	0.220	18838.7	13.5127	2.21625	0.97872
V4	12419	0.200	18640.4	13.9023	2.28015	0.96842

TABLE B.3

Sonic Testing Result of Air-dried Sandstone

Sample	Stress (psi)	Amplitude	Velocity (ft/sec)	Att. Coef. (dB/in)	Att. Coef. Ratio	Velocity Ratio
C1	0	1.56	12500.0	6.0468	1.00000	1.00000
C1	882	1.50	12797.6	6.2228	1.02911	1.02381
C1	1765	1.22	13004.0	7.1503	1.18249	1.04032
C1	2648	1.09	13217.2	7.6561	1.26614	1.05738
C1	3530	0.96	13304.5	8.2262	1.36042	1.06436
C1	4236	0.88	13326.4	8.6167	1.42501	1.06612
C1	4942	0.80	13437.5	9.0446	1.49576	1.07500
C1	5648	0.78	13437.5	9.1582	1.51456	1.07500
C1	6354	0.72	13550.4	9.5175	1.57398	1.08403
C1	7060	0.69	13550.4	9.7085	1.60557	1.08403
C1	7766	0.68	13665.3	9.7741	1.61641	1.09322
C1	8472	0.68	13665.3	9.7741	1.61641	1.09322
C1	9178	0.65	13665.3	9.9766	1.64990	1.09322
C1	9884	0.60	13665.3	10.3359	1.70932	1.09322
C1	10590	0.54	13665.3	10.8089	1.78754	1.09322
C1	11296	0.52	13665.3	10.9783	1.81555	1.09322
C1	12002	0.48	13550.4	11.3376	1.87497	1.08403
C1	12708	0.44	13550.4	11.7282	1.93957	1.08403
C1	13414	0.44	13550.4	11.7282	1.93957	1.08403
C1	14120	0.41	13437.5	12.0451	1.99199	1.07500
C1	14826	0.39	13437.5	12.2696	2.02911	1.07500
C1	15532	0.38	13326.4	12.3862	2.04840	1.06612
C1	16238	0.32	13004.0	13.1576	2.17597	1.04032

Table B.3 Continued

Sample	Stress (psi)	Amplitude	Velocity (ft/sec)	Att. Coef. (dB/in)	Att. Coef. Ratio	Velocity Ratio
C2	0	1.18	11197.9	7.2999	1.00000	1.00000
C2	884	1.22	11684.8	7.1503	0.97950	1.04348
C2	1768	1.24	11856.6	7.0773	0.96950	1.05883
C2	2651	1.22	12124.1	7.1503	0.97950	1.08271
C2	3535	1.20	12215.9	7.2245	0.98967	1.09091
C2	4242	1.18	12215.9	7.2999	1.00000	1.09091
C2	4949	1.14	12403.8	7.4547	1.02121	1.10769
C2	5656	1.12	12403.8	7.5342	1.03209	1.10769
C2	6363	1.09	12403.8	7.6561	1.04879	1.10769
C2	7070	1.04	12597.7	7.8669	1.07766	1.12500
C2	7777	0.98	12597.7	8.1336	1.11420	1.12500
C2	8484	0.92	12500.0	8.4172	1.15305	1.11628
C2	9191	0.85	12500.0	8.7724	1.20171	1.11628
C2	9898	0.78	12500.0	9.1582	1.25456	1.11628
C2	10605	0.74	12403.8	9.3945	1.28693	1.10769
C2	11312	0.68	12215.9	9.7741	1.33893	1.09091
C2	12019	0.62	12215.9	10.1887	1.39573	1.09091
C2	12726	0.52	12033.6	10.9783	1.50389	1.07463

Table B.3 Continued

Sample	Stress (psi)	Amplitude	Velocity (ft/sec)	Att. Coef. (dB/in)	Att. Coef. Ratio	Velocity Ratio
C3	0	1.20	12130.3	7.2208	1.00000	1.00000
C3	884	0.80	12222.2	9.0399	1.25193	1.00758
C3	1768	0.68	12410.3	9.7690	1.35291	1.02308
C3	2651	0.60	12410.3	10.3306	1.43068	1.02308
C3	3535	0.52	12604.2	10.9726	1.51959	1.03906
C3	4242	0.48	12604.2	11.3317	1.56932	1.03906
C3	4949	0.44	12604.2	11.7221	1.62339	1.03906
C3	5656	0.40	12703.4	12.1497	1.68261	1.04725
C3	6363	0.37	12703.4	12.4995	1.73105	1.04725
C3	7070	0.36	12804.2	12.6224	1.74807	1.05556
C3	7777	0.33	12804.2	13.0128	1.80213	1.05556
C3	8484	0.32	12804.2	13.1508	1.82125	1.05556
C3	9191	0.31	12804.2	13.2933	1.84098	1.05556
C3	9898	0.30	12804.2	13.4404	1.86135	1.05556
C3	10605	0.29	12906.7	13.5925	1.88242	1.06400
C3	11312	0.28	12906.7	13.7499	1.90422	1.06400
C3	12019	0.28	12906.7	13.7499	1.90422	1.06400
C3	12726	0.26	12906.7	14.0824	1.95027	1.06400
C3	13433	0.26	12906.7	14.0824	1.95027	1.06400
C3	14140	0.26	12906.7	14.0824	1.95027	1.06400

Table B.3 Continued

Sample	Stress (psi)	Amplitude	Velocity (ft/sec)	Att. Coef. (dB/in)	Att. Coef. Ratio	Velocity Ratio
C4	0	1.900	12279.0	5.1352	1.00000	1.00000
C4	881	1.450	12467.9	6.3422	1.23506	1.01539
C4	1763	1.150	12564.6	7.3774	1.43664	1.02326
C4	2644	1.025	12662.8	7.8913	1.53671	1.03125
C4	3525	1.000	12662.8	8.0016	1.55818	1.03125
C4	4230	0.975	12762.5	8.1146	1.58020	1.03937
C4	4935	0.950	12863.8	8.2306	1.60279	1.04762
C4	5640	0.900	12966.7	8.4721	1.64981	1.05600
C4	6345	0.800	12966.7	8.9981	1.75223	1.05600
C4	7050	0.700	12966.7	9.5944	1.86836	1.05600
C4	7755	0.620	13071.2	10.1363	1.97390	1.06452
C4	8460	0.550	13071.2	10.6713	2.07808	1.06452
C4	9165	0.490	13071.2	11.1872	2.17854	1.06452
C4	9870	0.440	13071.2	11.6679	2.27214	1.06452
C4	10575	0.410	13071.2	11.9832	2.33355	1.06452
C4	11280	0.370	13071.2	12.4416	2.42282	1.06452
C4	11985	0.340	13071.2	12.8193	2.49635	1.06452
C4	12690	0.320	13071.2	13.0900	2.54908	1.06452
C4	13395	0.310	13071.2	13.2318	2.57669	1.06452
C4	14100	0.290	13071.2	13.5296	2.63468	1.06452
C4	14805	0.290	13071.2	13.5296	2.63468	1.06452
C4	15510	0.290	13071.2	13.5296	2.63468	1.06452

Table B.3 Continued

Sample	Stress (psi)	Amplitude	Velocity (ft/sec)	Att. Coef. (dB/in)	Att. Coef. Ratio	Velocity Ratio
C5	0	0.90	12310.6	8.4503	1.00000	1.00000
C5	884	0.90	12310.6	8.4503	1.00000	1.00000
C5	1768	0.76	12695.3	9.2035	1.08912	1.03125
C5	2651	0.66	12695.3	9.8319	1.16349	1.03125
C5	3535	0.60	12795.3	10.2564	1.21373	1.03937
C5	4242	0.53	12896.8	10.8090	1.27912	1.04762
C5	4949	0.49	12896.8	11.1585	1.32048	1.04762
C5	5656	0.44	13000.0	11.6379	1.37721	1.05600
C5	6363	0.40	13000.0	12.0625	1.42745	1.05600
C5	7070	0.37	13000.0	12.4097	1.46855	1.05600
C5	7777	0.35	13000.0	12.6573	1.49784	1.05600
C5	8484	0.32	13000.0	13.0564	1.54507	1.05600
C5	9191	0.30	13000.0	13.3439	1.57909	1.05600
C5	9898	0.28	12896.8	13.6512	1.61546	1.04762
C5	10605	0.26	12896.8	13.9813	1.65452	1.04762
C5	11312	0.23	12795.3	14.5274	1.71915	1.03937

Table B.3 Continued

Sample	Stress (psi)	Amplitude	Velocity (ft/sec)	Att. Coef. (dB/in)	Att. Coef. Ratio	Velocity Ratio
C7	0	0.72	13000.0	9.4443	1.00000	1.00000
C7	884	0.68	13211.4	9.6989	1.02696	1.01626
C7	1768	0.45	13429.8	11.5378	1.22167	1.03306
C7	2651	0.36	13541.7	12.5318	1.32692	1.04167
C7	3535	0.28	13541.7	13.6512	1.44545	1.04167
C7	4242	0.24	13541.7	14.3378	1.51815	1.04167
C7	4949	0.21	13541.7	14.9326	1.58113	1.04167
C7	5656	0.19	13771.2	15.3784	1.62833	1.05932
C7	6363	0.16	13888.9	16.1439	1.70938	1.06838
C7	7070	0.14	13655.5	16.7387	1.77236	1.05042
C7	7777	0.12	13655.5	17.4253	1.84507	1.05042
C7	8484	0.11	13541.7	17.8129	1.88610	1.04167
C7	9191	0.10	13541.7	18.2374	1.93106	1.04167
C7	9898	0.09	13429.8	18.7068	1.98075	1.03306
C7	10605	0.08	13211.4	19.2314	2.03630	1.01626
C7	11912	0.07	13211.4	19.8262	2.09928	1.01626

Table B.3 Continued

Sample	Stress (psi)	Amplitude	Velocity (ft/sec)	Att. Coef. (dB/in)	Att. Coef. Ratio	Velocity Ratio
C8	0	0.84	12092.7	8.8484	1.00000	1.00000
C8	883	0.72	12467.7	9.5422	1.07840	1.03101
C8	1765	0.71	12565.1	9.6051	1.08552	1.03907
C8	2648	0.57	12764.6	10.5935	1.19722	1.05556
C8	3530	0.56	12764.6	10.6732	1.20623	1.05556
C8	4236	0.48	12866.7	11.3669	1.28463	1.06400
C8	4942	0.44	12970.4	11.7585	1.32889	1.07258
C8	5648	0.41	12970.4	12.0763	1.36480	1.07258
C8	6354	0.40	13075.9	12.1875	1.37736	1.08130
C8	7060	0.38	13075.9	12.4183	1.40345	1.08130
C8	7766	0.38	13183.1	12.4183	1.40345	1.09017
C8	8472	0.38	13183.1	12.4183	1.40345	1.09017
C8	9178	0.38	13075.9	12.4183	1.40345	1.08130
C8	9884	0.38	12970.4	12.4183	1.40345	1.07258
C8	10590	0.38	12866.7	12.4183	1.40345	1.06400
C8	11296	0.38	12764.6	12.4183	1.40345	1.05556
C8	12002	0.38	12565.1	12.4183	1.40345	1.03907
C8	12708	0.39	12565.1	12.3014	1.39024	1.03907

Table B.3 Continued

Sample	Stress (psi)	Amplitude	Velocity (ft/sec)	Att. Coef. (dB/in)	Att. Coef. Ratio	Velocity Ratio
C9	0	1.20	12102.0	7.1837	1.00000	1.00000
C9	881	1.14	12474.4	7.4126	1.03187	1.03077
C9	1761	1.04	12571.1	7.8224	1.08891	1.03876
C9	2642	0.88	12870.4	8.5680	1.19271	1.06349
C9	3523	0.75	12870.4	9.2815	1.29203	1.06349
C9	4227	0.71	12973.3	9.5261	1.32608	1.07200
C9	4932	0.62	13078.0	10.1311	1.41030	1.08064
C9	5636	0.56	13078.0	10.5854	1.47354	1.08064
C9	6341	0.52	13184.3	10.9162	1.51959	1.08943
C9	7045	0.48	13184.3	11.2735	1.56932	1.08943
C9	7750	0.46	13292.3	11.4634	1.59577	1.09836
C9	8454	0.42	13292.3	11.8695	1.65229	1.09836
C9	9159	0.40	13184.3	12.0873	1.68261	1.08943
C9	9863	0.36	13184.3	12.5575	1.74807	1.08943
C9	10568	0.34	13078.0	12.8127	1.78358	1.08064
C9	11273	0.32	13078.0	13.0833	1.82124	1.08064

Table B.3 Continued

Sample	Stress (psi)	Amplitude	Velocity (ft/sec)	Att. Coef. (dB/in)	Att. Coef. Ratio	Velocity Ratio
C10	0	0.68	14868.8	9.8147	1.00000	1.00000
C10	883	0.68	15007.8	9.8147	1.00000	1.00935
C10	1765	0.61	15149.4	10.3043	1.04989	1.01887
C10	2648	0.58	15440.7	10.5316	1.07305	1.03846
C10	3530	0.56	15440.7	10.6898	1.08917	1.03846
C10	4236	0.52	15293.7	11.0238	1.12320	1.02857
C10	4942	0.48	15293.7	11.3846	1.15996	1.02857
C10	5648	0.45	15293.7	11.6755	1.18960	1.02857
C10	6354	0.41	15293.7	12.0951	1.23236	1.02857
C10	7060	0.39	15293.7	12.3206	1.25532	1.02857
C10	7766	0.37	15293.7	12.5579	1.27950	1.02857
C10	8472	0.36	15293.7	12.6814	1.29208	1.02857
C10	9178	0.33	15293.7	13.0736	1.33204	1.02857
C10	9884	0.32	15149.4	13.2123	1.34618	1.01887
C10	10590	0.31	15149.4	13.3554	1.36076	1.01887
C10	11296	0.29	14868.8	13.6560	1.39139	1.00000

Table B.3 Continued

Sample	Stress (psi)	Amplitude	Velocity (ft/sec)	Att. Coef. (dB/in)	Att. Coef. Ratio	Velocity Ratio
C17	0	0.32	13829.0	13.2260	1.00000	1.00000
C17	884	0.28	14196.2	13.8285	1.04555	1.02655
C17	1768	0.28	14196.2	13.8285	1.04555	1.02655
C17	2653	0.29	14322.9	13.6702	1.03358	1.03572
C17	3537	0.29	14322.9	13.6702	1.03358	1.03572
C17	4244	0.29	14322.9	13.6702	1.03358	1.03572
C17	4952	0.29	14322.9	13.6702	1.03358	1.03572
C17	5659	0.29	14322.9	13.6702	1.03358	1.03572
C17	6367	0.28	14196.2	13.8285	1.04555	1.02655
C17	7074	0.28	14196.2	13.8285	1.04555	1.02655
C17	7781	0.26	14071.6	14.1629	1.07084	1.01755
C17	8489	0.24	13829.0	14.5241	1.09814	1.00000
C17	9196	0.22	13829.0	14.9167	1.12783	1.00000
C17	9904	0.20	13829.0	15.3467	1.16034	1.00000

TABLE B.4

Sonic Testing Results of Shale Specimens

Sample	Stress (psi)	Amplitude	Velocity (ft/sec)	Att. Coef. (dB/in)	Att. Coef. Ratio	Velocity Ratio
S1	0	1.19	17800	5.26295	1.00000	1.00000
S1	413	1.20	17800	5.23573	0.99483	1.00000
S1	826	1.20	17800	5.23573	0.99483	1.00000
S1	1238	1.22	17800	5.18196	0.98461	1.00000
S1	1651	1.22	17800	5.18196	0.98461	1.00000
S1	1981	1.24	17800	5.12906	0.97456	1.00000
S1	2312	1.25	17800	5.10293	0.96960	1.00000
S1	2642	1.26	17800	5.07701	0.96467	1.00000
S1	2972	1.26	17800	5.07701	0.96467	1.00000
S1	3302	1.28	17800	5.02578	0.95494	1.00000
S1	3633	1.28	17800	5.02578	0.95494	1.00000
S1	3963	1.28	17800	5.02578	0.95494	1.00000
S1	4293	1.28	17800	5.02578	0.95494	1.00000
S1	4623	1.28	17800	5.02578	0.95494	1.00000
S1	4953	1.30	17800	4.97534	0.94535	1.00000
S1	5284	1.30	17800	4.97534	0.94535	1.00000
S1	5614	1.30	17800	4.97534	0.94535	1.00000
S1	5944	1.30	17800	4.97534	0.94535	1.00000
S1	6274	1.32	17800	4.92567	0.93591	1.00000
S1	6605	1.32	17800	4.92567	0.93591	1.00000
S1	6935	1.32	17800	4.92567	0.93591	1.00000
S1	7265	1.32	17800	4.92567	0.93591	1.00000
S1	7595	1.34	17800	4.87675	0.92662	1.00000
S1	7926	1.34	17800	4.87675	0.92662	1.00000
S1	8256	1.36	17800	4.82856	0.91746	1.00000
S1	9082	1.36	17800	4.82856	0.91746	1.00000

Table B.4 Continued

Sample	Stress (psi)	Amplitude	Velocity (ft/sec)	Att. Coef. (dB/in)	Att. Coef. Ratio	Velocity Ratio
S421K	0	0.700	17538.6	8.20988	1.00000	1.00000
S421K	984	0.725	17538.6	8.07579	0.98367	1.00000
S421K	1968	0.800	17538.6	7.69962	0.93785	1.00000
S421K	2952	0.800	17538.6	7.69962	0.93785	1.00000
S421K	3936	0.800	17538.6	7.69962	0.93785	1.00000
S421K	4920	0.800	17538.6	7.69962	0.93785	1.00000
S421K	5904	0.800	17538.6	7.69962	0.93785	1.00000
S421K	6889	0.800	17538.6	7.69962	0.93785	1.00000
S421K	7873	0.800	17538.6	7.69962	0.93785	1.00000
S421K	8857	0.825	17702.5	7.58203	0.92352	1.00934
S421K	9841	0.850	17702.5	7.46795	0.90963	1.00934
S421K	10825	0.850	17702.5	7.46795	0.90963	1.00934

Table B.4 Continued

Sample	Stress (psi)	Amplitude	Velocity (ft/sec)	Att. Coef. (dB/in)	Att. Coef. Ratio	Velocity Ratio
S4	0	0.92	15821.0	6.35477	1.00000	1.00000
S4	472	0.94	16429.5	6.28188	0.98853	1.03846
S4	944	0.94	16429.5	6.28188	0.98853	1.03846
S4	1416	0.93	16429.5	6.31813	0.99423	1.03846
S4	1888	0.93	16429.5	6.31813	0.99423	1.03846
S4	2266	0.93	16429.5	6.31813	0.99423	1.03846
S4	2643	0.92	16429.5	6.35477	1.00000	1.03846
S4	3021	0.90	16429.5	6.42925	1.01172	1.03846
S4	3399	0.90	16429.5	6.42925	1.01172	1.03846
S4	3776	0.90	16429.5	6.42925	1.01172	1.03846
S4	4154	0.88	16429.5	6.50541	1.02371	1.03846
S4	4909	0.86	16429.5	6.58332	1.03597	1.03846
S4	5287	0.86	16429.5	6.58332	1.03597	1.03846
S4	5664	0.84	16429.5	6.66307	1.04851	1.03846
S4	6042	0.84	16429.5	6.66307	1.04851	1.03846
S4	6419	0.81	16429.5	6.78631	1.06791	1.03846
S4	6797	0.80	16429.5	6.82841	1.07453	1.03846
S4	7175	0.74	16429.5	7.09262	1.11611	1.03846
S4	7552	0.73	16429.5	7.13873	1.12337	1.03846
S4	7930	0.48	16429.5	8.55958	1.34695	1.03846
S4	8308	0.47	16429.5	8.63093	1.35818	1.03846
S4	8685	0.47	16429.5	8.63093	1.35818	1.03846
S4	9063	0.46	16429.5	8.70381	1.36965	1.03846
S4	9440	0.46	16429.5	8.70381	1.36965	1.03846
S4	9818	0.46	16429.5	8.70381	1.36965	1.03846
S4	10196	0.46	16429.5	8.70381	1.36965	1.03846
S4	10573	0.46	16429.5	8.70381	1.36965	1.03846

Table B.4 Continued

Sample	Stress (psi)	Amplitude	Velocity (ft/sec)	Att. Coef. (dB/in)	Att. Coef. Ratio	Velocity Ratio
S313K	0	0.900	18090.3	6.32559	1.00000	1.00000
S313K	831	0.900	18090.3	6.32559	1.00000	1.00000
S313K	1661	0.950	18090.3	6.14532	0.97150	1.00000
S313K	2492	1.100	18090.3	5.65650	0.89422	1.00000
S313K	3323	1.050	18090.3	5.81161	0.91875	1.00000
S313K	4153	1.000	18090.3	5.97429	0.94446	1.00000
S313K	4983	0.975	18090.3	6.05871	0.95781	1.00000
S313K	5814	1.000	18090.3	5.97429	0.94446	1.00000
S313K	6645	1.025	18090.3	5.89196	0.93145	1.00000
S313K	7475	1.050	18090.3	5.81161	0.91875	1.00000
S313K	8306	1.050	18090.3	5.81161	0.91875	1.00000
S313K	9136	1.000	18090.3	5.97429	0.94446	1.00000
S313K	9635	1.000	18090.3	5.97429	0.94446	1.00000

Table B.4 Continued

Sample	Stress (psi)	Amplitude	Velocity (ft/sec)	Att. Coef. (dB/in)	Att. Coef. Ratio	Velocity Ratio
S813K	0	0.475	17711.5	7.97291	1.00000	1.00000
S813K	775	0.750	17988.3	6.53702	0.81990	1.01563
S813K	1550	0.750	17988.3	6.53702	0.81990	1.01563
S813K	2326	0.800	17988.3	6.33414	0.79446	1.01563
S813K	3101	0.800	17988.3	6.33414	0.79446	1.01563
S813K	3876	0.850	17988.3	6.14356	0.77055	1.01563
S813K	4651	0.850	17988.3	6.14356	0.77055	1.01563
S813K	5426	0.850	17988.3	6.14356	0.77055	1.01563
S813K	6202	0.900	17988.3	5.96387	0.74802	1.01563
S813K	6977	0.900	17988.3	5.96387	0.74802	1.01563
S813K	7132	0.900	17988.3	5.96387	0.74802	1.01563
S813K	7752	0.900	17988.3	5.96387	0.74802	1.01563

Table B.4 Continued

Sample	Stress (psi)	Amplitude	Velocity (ft/sec)	Att. Coef. (dB/in)	Att. Coef. Ratio	Velocity Ratio
S3	0	0.61	15944.4	7.68735	1.00000	1.00000
S3	419	0.70	15944.4	7.22457	0.93980	1.00000
S3	838	0.68	15944.4	7.32205	0.95248	1.00000
S3	1240	0.68	15944.4	7.32205	0.95248	1.00000
S3	1675	0.67	15944.4	7.37187	0.95896	1.00000
S3	2010	0.67	15944.4	7.37187	0.95896	1.00000
S3	2345	0.66	15944.4	7.42243	0.96554	1.00000
S3	2680	0.66	15944.4	7.42243	0.96554	1.00000
S3	3016	0.68	15944.4	7.32205	0.95248	1.00000
S3	3350	0.68	15944.4	7.32205	0.95248	1.00000
S3	3686	0.68	15944.4	7.32205	0.95248	1.00000
S3	4021	0.68	15944.4	7.32205	0.95248	1.00000
S3	4356	0.68	15944.4	7.32205	0.95248	1.00000
S3	4691	0.67	15944.4	7.37187	0.95896	1.00000
S3	5026	0.67	15944.4	7.37187	0.95896	1.00000
S3	5361	0.66	15944.4	7.42243	0.96554	1.00000
S3	5695	0.65	15944.4	7.47377	0.97222	1.00000
S3	6030	0.64	15944.4	7.52591	0.97900	1.00000
S3	6365	0.63	15944.4	7.57887	0.98589	1.00000
S3	6700	0.62	15944.4	7.63267	0.99289	1.00000
S3	7035	0.61	15944.4	7.68735	1.00000	1.00000
S3	7370	0.60	15944.4	7.74293	1.00723	1.00000
S3	7706	0.60	15944.4	7.74293	1.00723	1.00000
S3	8041	0.60	15944.4	7.74293	1.00723	1.00000
S3	8376	0.60	15944.4	7.74293	1.00723	1.00000
S3	8710	0.50	15944.4	8.35603	1.08698	1.00000
S3	9050	0.50	15944.4	8.35603	1.08698	1.00000

Table B.4 Continued

Sample	Stress (psi)	Amplitude	Velocity (ft/sec)	Att. Coef. (dB/in)	Att. Coef. Ratio	Velocity Ratio
S13	0	0.76	17608	7.86448	1.00000	1.00000
S13	956	0.76	17608	7.86448	1.00000	1.00000
S13	1913	0.80	17608	7.66925	0.97518	1.00000
S13	2869	0.90	17608	7.22094	0.91817	1.00000
S13	3825	0.90	17608	7.22094	0.91817	1.00000
S13	4782	0.95	17608	7.01514	0.89200	1.00000
S13	5356	0.95	17608	7.01514	0.89200	1.00000
S13	5738	1.00	17608	6.81991	0.86718	1.00000
S13	6121	1.00	17608	6.81991	0.86718	1.00000
S13	6503	1.00	17608	6.81991	0.86718	1.00000
S13	6886	1.10	17608	6.45713	0.82105	1.00000
S13	7268	1.10	17608	6.45713	0.82105	1.00000
S13	7651	1.10	17608	6.45713	0.82105	1.00000
S13	8033	1.15	17608	6.28794	0.79954	1.00000
S13	8416	1.20	17608	6.12594	0.77894	1.00000
S13	8798	1.20	17608	6.12594	0.77894	1.00000
S13	9181	1.25	17608	5.97056	0.75918	1.00000
S13	9564	1.25	17608	5.97056	0.75918	1.00000

Table B.4 Continued

Sample	Stress (psi)	Amplitude	Velocity (ft/sec)	Att. Coef. (dB/in)	Att. Coef. Ratio	Velocity Ratio
S9	0	0.89	18225.3	7.01745	1.00000	1.00000
S9	422	0.83	18225.3	7.27412	1.03658	1.00000
S9	843	0.84	18225.3	7.23008	1.03030	1.00000
S9	1265	0.84	18225.3	7.23008	1.03030	1.00000
S9	1688	0.82	18225.3	7.31869	1.04293	1.00000
S9	2025	0.82	18225.3	7.31869	1.04293	1.00000
S9	2363	0.82	18225.3	7.31869	1.04293	1.00000
S9	2699	0.83	18225.3	7.27412	1.03658	1.00000
S9	3037	0.81	18225.3	7.36381	1.04936	1.00000
S9	3374	0.80	18225.3	7.40949	1.05587	1.00000
S9	3712	0.80	18225.3	7.40949	1.05587	1.00000
S9	4049	0.80	18225.3	7.40949	1.05587	1.00000
S9	4387	0.80	18225.3	7.40949	1.05587	1.00000
S9	4724	0.80	18225.3	7.40949	1.05587	1.00000
S9	5062	0.79	18225.3	7.45575	1.06246	1.00000
S9	5399	0.79	18225.3	7.45575	1.06246	1.00000
S9	5737	0.78	18225.3	7.50260	1.06913	1.00000
S9	6074	0.78	18225.3	7.50260	1.06913	1.00000
S9	6412	0.77	18225.3	7.55005	1.07590	1.00000
S9	6749	0.79	18225.3	7.45575	1.06246	1.00000
S9	7087	0.78	18225.3	7.50260	1.06913	1.00000
S9	7424	0.77	18225.3	7.55005	1.07590	1.00000
S9	7761	0.76	18225.3	7.59812	1.08275	1.00000
S9	8098	0.76	18225.3	7.59812	1.08275	1.00000
S9	8436	0.76	18225.3	7.59812	1.08275	1.00000
S9	8858	0.76	18225.3	7.59812	1.08275	1.00000
S9	9279	0.76	18225.3	7.59812	1.08275	1.00000

Table B.4 Continued

Sample	Stress (psi)	Amplitude	Velocity (ft/sec)	Att. Coef. (dB/in)	Att. Coef. Ratio	Velocity Ratio
S701K	0	0.68	18305.1	7.29662	1.00000	1.00000
S701K	861	0.76	18305.1	6.92390	0.94892	1.00000
S701K	1722	0.77	18305.1	6.88010	0.94292	1.00000
S701K	2583	0.77	18305.1	6.88010	0.94292	1.00000
S701K	3443	0.78	18305.1	6.83686	0.93699	1.00000
S701K	4304	0.79	18305.1	6.79417	0.93114	1.00000
S701K	5165	0.78	18305.1	6.83686	0.93699	1.00000
S701K	6026	0.78	18305.1	6.83686	0.93699	1.00000
S701K	6887	0.77	18305.1	6.88010	0.94292	1.00000
S701K	7758	0.77	18305.1	6.88010	0.94292	1.00000
S701K	7921	0.77	18305.1	6.88010	0.94292	1.00000
S701K	8610	0.77	18305.1	6.88010	0.94292	1.00000

Table B.4 Continued

Sample	Stress (psi)	Amplitude	Velocity (ft/sec)	Att. Coef. (dB/in)	Att. Coef. Ratio	Velocity Ratio
S413K	0	1.50	17869.5	5.29749	1.00001	1.00000
S413K	984	1.25	17869.5	5.99420	1.13152	1.00000
S413K	1968	1.25	17869.5	5.99420	1.13152	1.00000
S413K	2952	1.40	17869.5	5.56114	1.04977	1.00000
S413K	3936	1.50	17869.5	5.29749	1.00001	1.00000
S413K	4920	1.60	17869.5	5.05087	0.95345	1.00000
S413K	5904	1.55	17869.5	5.17219	0.97635	1.00000
S413K	6889	1.55	17869.5	5.17219	0.97635	1.00000
S413K	7873	1.55	17869.5	5.17219	0.97635	1.00000
S413K	8857	1.55	17869.5	5.17219	0.97635	1.00000
S413K	9841	1.50	17869.5	5.29749	1.00001	1.00000
S413K	10825	1.50	17869.5	5.29749	1.00001	1.00000

Table B.4 Continued

Sample	Stress (psi)	Amplitude	Velocity (ft/sec)	Att. Coef. (dB/in)	Att. Coef. Ratio	Velocity Ratio
S5	0	0.360	18207.3	9.3988	1.00000	1.00000
S5	427	0.370	18207.3	9.3073	0.99026	1.00000
S5	854	0.360	18207.3	9.3988	1.00000	1.00000
S5	1281	0.340	18207.3	9.5898	1.02032	1.00000
S5	1708	0.320	18207.3	9.7923	1.04186	1.00000
S5	2050	0.320	18055.6	9.7923	1.04186	0.99167
S5	2391	0.300	18055.6	10.0079	1.06480	0.99167
S5	2733	0.280	18055.6	10.2384	1.08933	0.99167
S5	3074	0.265	18055.6	10.4223	1.10890	0.99167
S5	3416	0.250	18055.6	10.6170	1.12961	0.99167
S5	3758	0.240	18055.6	10.7534	1.14412	0.99167
S5	4099	0.235	18055.6	10.8237	1.15160	0.99167
S5	4441	0.230	18055.6	10.8956	1.15925	0.99167
S5	4782	0.220	18055.6	11.0441	1.17505	0.99167
S5	5124	0.215	18055.6	11.1209	1.18322	0.99167
S5	5466	0.205	18055.6	11.2800	1.20015	0.99167
S5	5807	0.200	18055.6	11.3625	1.20892	0.99167
S5	6149	0.185	18055.6	11.6229	1.23663	0.99167
S5	6490	0.185	18055.6	11.6229	1.23663	0.99167
S5	6832	0.180	18055.6	11.7145	1.24637	0.99167
S5	7174	0.170	18055.6	11.9054	1.26669	0.99167
S5	7515	0.165	18055.6	12.0051	1.27730	0.99167
S5	7857	0.160	18055.6	12.1079	1.28824	0.99167
S5	8198	0.160	18055.6	12.1079	1.28824	0.99167
S5	8540	0.145	18055.6	12.4368	1.32323	0.99167
S5	8882	0.140	18055.6	12.5540	1.33570	0.99167
S5	9223	0.140	18055.6	12.5540	1.33570	0.99167
S5	9565	0.140	18055.6	12.5540	1.33570	0.99167

Table B.4 Continued

Sample	Stress (psi)	Amplitude	Velocity (ft/sec)	Att. Coef. (dB/in)	Att. Coef. Ratio	Velocity Ratio
S6	0	0.79	16764.7	4.68115	1.00000	1.00000
S6	435	0.80	16675.5	4.65211	0.99380	0.99468
S6	869	0.78	16675.5	4.71056	1.00628	0.99468
S6	1304	0.76	16675.5	4.77054	1.01909	0.99468
S6	1734	0.76	16675.5	4.77054	1.01909	0.99468
S6	2085	0.74	16675.5	4.83211	1.03225	0.99468
S6	2433	0.74	16675.5	4.83211	1.03225	0.99468
S6	2781	0.72	16675.5	4.89537	1.04576	0.99468
S6	3128	0.72	16675.5	4.89537	1.04576	0.99468
S6	3476	0.70	16764.7	4.96041	1.05966	1.00000
S6	3824	0.69	16764.7	4.99363	1.06675	1.00000
S6	4170	0.69	16764.7	4.99363	1.06675	1.00000
S6	4518	0.69	16764.7	4.99363	1.06675	1.00000
S6	4866	0.68	16764.7	5.02734	1.07395	1.00000
S6	5214	0.67	16764.7	5.06154	1.08126	1.00000
S6	5561	0.65	16764.7	5.13151	1.09621	1.00000
S6	5909	0.65	16764.7	5.13151	1.09621	1.00000
S6	6257	0.65	16764.7	5.13151	1.09621	1.00000
S6	6603	0.64	16764.7	5.16731	1.10386	1.00000
S6	6951	0.62	16764.7	5.24061	1.11951	1.00000
S6	7299	0.61	16764.7	5.27816	1.12753	1.00000
S6	7646	0.61	16764.7	5.27816	1.12753	1.00000
S6	7994	0.58	16764.7	5.39459	1.15241	1.00000
S6	8340	0.57	16764.7	5.43475	1.16099	1.00000
S6	8690	0.56	16764.7	5.47562	1.16972	1.00000
S6	9036	0.56	16764.7	5.47562	1.16972	1.00000
S6	9384	0.54	16764.7	5.55958	1.18765	1.00000

TABLE B.5

Sonic Testing Result of Water Saturated Sandstone

Sample	Stress (psi)	Amplitude	Velocity (ft/sec)	Att. Coef. (dB/in)	Att. Coef. Ratio	Velocity Ratio
C18	0	0.2400	14181.3	14.4118	1.00000	1.00000
C18	881	0.2000	14434.5	15.2281	1.05664	1.01786
C18	1763	0.1850	14697.0	15.5771	1.08086	1.03636
C18	2644	0.1700	14697.0	15.9557	1.10713	1.03636
C18	3526	0.1650	14697.0	16.0894	1.11640	1.03636
C18	4231	0.1700	14831.8	15.9557	1.10713	1.04587
C18	4936	0.1675	14831.8	16.0220	1.11173	1.04587
C18	5641	0.1600	14697.0	16.2271	1.12596	1.03636
C18	6346	0.1500	14460.3	16.5161	1.14601	1.01968
C18	7051	0.1400	14306.8	16.8250	1.16744	1.00885
C18	7756	0.1300	14306.8	17.1568	1.19047	1.00885
C18	8462	0.1150	14181.3	17.7057	1.22856	1.00000
C18	9196	0.1100	14181.3	17.9047	1.24237	1.00000
C18	9904	0.1000	14181.3	18.3315	1.27198	1.00000

Table B.5 Continued

Sample	Stress (psi)	Amplitude	Velocity (ft/sec)	Att. Coef. (dB/in)	Att. Coef. Ratio	Velocity Ratio
C19	0	0.290	14367.6	13.6277	1.00000	1.00000
C19	884	0.160	14628.8	16.3028	1.19630	1.01818
C19	1768	0.145	14899.7	16.7456	1.22879	1.03703
C19	2651	0.135	14899.7	17.0670	1.25237	1.03703
C19	3536	0.130	14899.7	17.2367	1.26483	1.03703
C19	4244	0.120	14899.7	17.5968	1.29125	1.03703
C19	4952	0.115	14899.7	17.7882	1.30530	1.03703
C19	5659	0.113	14899.7	17.8671	1.31109	1.03703
C19	6367	0.110	14899.7	17.9882	1.31997	1.03703
C19	7074	0.103	14763.0	18.2839	1.34167	1.02752
C19	7781	0.095	14628.8	18.6476	1.36836	1.01818
C19	8489	0.090	14628.8	18.8908	1.38621	1.01818
C19	9196	0.083	14240.4	19.2550	1.41293	0.99115
C19	9904	0.080	14240.4	19.4206	1.42508	0.99115

Table B.5 Continued

Sample	Stress (psi)	Amplitude	Velocity (ft/sec)	Att. Coef. (dB/in)	Att. Coef. Ratio	Velocity Ratio
C20	0	0.325	14621.2	13.1219	1.00000	1.00000
C20	884	0.200	14892.0	15.3070	1.16652	1.01852
C20	1768	0.220	15031.2	14.8780	1.13383	1.02804
C20	2653	0.230	15031.2	14.6780	1.11859	1.02804
C20	3537	0.245	15031.2	14.3936	1.09692	1.02804
C20	4244	0.260	15031.2	14.1262	1.07654	1.02804
C20	4952	0.260	15173.0	14.1262	1.07654	1.03774
C20	5659	0.260	15173.0	14.1262	1.07654	1.03774
C20	6367	0.250	15173.0	14.3027	1.08999	1.03774
C20	7074	0.240	15031.2	14.4864	1.10399	1.02804
C20	7781	0.225	15031.2	14.7769	1.12612	1.02804
C20	8489	0.210	14892.0	15.0874	1.14979	1.01852
C20	9196	0.190	14621.2	15.5378	1.18411	1.00000
C20	9904	0.175	14360.1	15.9079	1.21232	0.98214

Table B.5 Continued

Sample	Stress (psi)	Amplitude	Velocity (ft/sec)	Att. Coef. (dB/in)	Att. Coef. Ratio	Velocity Ratio
C21	0	0.180	13402.8	15.7811	1.00000	1.00000
C21	881	0.223	13746.4	14.8171	0.93891	1.02564
C21	1763	0.235	13864.9	14.5812	0.92396	1.03448
C21	2644	0.240	13985.5	14.4864	0.91796	1.04348
C21	3526	0.233	14108.2	14.6196	0.92640	1.05263
C21	4231	0.230	14108.2	14.6780	0.93010	1.05263
C21	4936	0.225	14108.2	14.7769	0.93637	1.05263
C21	5641	0.213	13864.9	15.0235	0.95200	1.03448
C21	6346	0.200	13864.9	15.3070	0.96995	1.03448
C21	7051	0.195	13402.8	15.4209	0.97718	1.00000
C21	7756	0.180	13402.8	15.7811	1.00000	1.00000
C21	8462	0.170	13402.8	16.0384	1.01630	1.00000
C21	9196	0.165	13402.8	16.1727	1.02482	1.00000
C21	9904	0.140	13402.8	16.9122	1.07167	1.00000

Table B.5 Continued

Sample	Stress (psi)	Amplitude	Velocity (ft/sec)	Att. Coef. (dB/in)	Att. Coef. Ratio	Velocity Ratio
C22	0	0.116	13541.7	17.5763	1.00000	1.00000
C22	884	0.036	14008.6	22.7882	1.29653	1.03448
C22	1768	0.033	14130.4	23.1758	1.31858	1.04348
C22	2653	0.029	14254.4	23.7513	1.35133	1.05263
C22	3537	0.026	14254.4	24.2377	1.37900	1.05263
C22	4244	0.024	14254.4	24.5943	1.39929	1.05263
C22	4952	0.024	14254.4	24.5943	1.39929	1.05263
C22	5659	0.024	14254.4	24.5943	1.39929	1.05263
C22	6367	0.023	14254.4	24.7838	1.41007	1.05263
C22	7074	0.022	14254.4	24.9818	1.42134	1.05263
C22	7781	0.022	14254.4	24.9818	1.42134	1.05263
C22	8489	0.021	14254.4	25.1890	1.43313	1.05263
C22	9196	0.020	14008.6	25.4064	1.44549	1.03448
C22	9904	0.013	13104.8	27.3252	1.55466	0.96774

Table B.5 Continued

Sample	Stress (psi)	Amplitude	Velocity (ft/sec)	Att. Coef. (dB/in)	Att. Coef. Ratio	Velocity Ratio
C23	0	0.265	13922.4	13.9825	1.00000	1.00000
C23	881	0.200	14419.6	15.2438	1.09020	1.03572
C23	1763	0.200	14292.0	15.2438	1.09020	1.02655
C23	2644	0.195	14419.6	15.3572	1.09832	1.03572
C23	3526	0.200	14419.6	15.2438	1.09020	1.03572
C23	4231	0.200	14292.0	15.2438	1.09020	1.02655
C23	4936	0.200	14292.0	15.2438	1.09020	1.02655
C23	5641	0.170	13922.4	15.9722	1.14230	1.00000
C23	6346	0.120	13458.3	17.5332	1.25394	0.96667
C23	7051	0.120	13458.3	17.5332	1.25394	0.96667
C23	7756	0.120	13458.3	17.5332	1.25394	0.96667
C23	8462	0.100	13458.3	18.3504	1.31238	0.96667
C23	9196	0.100	13458.3	18.3504	1.31238	0.96667
C23	9904	0.090	13458.3	18.8226	1.34615	0.96667

Table B.5 Continued

Sample	Stress (psi)	Amplitude	Velocity (ft/sec)	Att. Coef. (dB/in)	Att. Coef. Ratio	Velocity Ratio
C29	0	0.155	13987.1	16.3104	1.00000	1.00000
C29	884	0.205	14486.6	15.0631	0.92353	1.03571
C29	1768	0.220	14486.6	14.7481	0.90422	1.03571
C29	2653	0.225	14750.0	14.6479	0.89807	1.05454
C29	3537	0.235	14750.0	14.4539	0.88617	1.05454
C29	4244	0.240	15023.1	14.3599	0.88042	1.07407
C29	4952	0.240	14750.0	14.3599	0.88042	1.05454
C29	5659	0.240	14750.0	14.3599	0.88042	1.05454
C29	6367	0.240	14750.0	14.3599	0.88042	1.05454
C29	7074	0.237	14750.0	14.4161	0.88386	1.05454
C29	7781	0.230	14617.1	14.5498	0.89206	1.04504
C29	8489	0.220	14486.6	14.7481	0.90422	1.03571
C29	9196	0.210	14486.6	14.9556	0.91694	1.03571
C29	9904	0.200	14486.6	15.1733	0.93028	1.03571

Table B.5 Continued

Sample	Stress (psi)	Amplitude	Velocity (ft/sec)	Att. Coef. (dB/in)	Att. Coef. Ratio	Velocity Ratio
C32	0	0.203	13700.6	15.1614	1.00000	1.00000
C32	884	0.290	14181.3	13.5645	0.89467	1.03509
C32	1768	0.320	14181.3	13.1237	0.86560	1.03509
C32	2653	0.340	14306.8	12.8523	0.84770	1.04425
C32	3537	0.345	14306.8	12.7869	0.84339	1.04425
C32	4244	0.340	14306.8	12.8523	0.84770	1.04425
C32	4952	0.330	14306.8	12.9860	0.85651	1.04425
C32	5659	0.310	14181.3	13.2659	0.87498	1.03509
C32	6367	0.260	14181.3	14.0534	0.92692	1.03509
C32	7074	0.250	14181.3	14.2290	0.93850	1.03509
C32	7781	0.240	14181.3	14.4118	0.95056	1.03509
C32	8489	0.230	14181.3	14.6023	0.96312	1.03509
C32	9196	0.220	14181.3	14.8013	0.97625	1.03509
C32	9904	0.210	14181.3	15.0096	0.98999	1.03509

TABLE B.6

Sonic Testing Results of Granite Specimens

Sample	Stress (psi)	Amplitude	Velocity (ft/sec)	Att. Coef. (dB/in)	Att. Coef. Ratio	Velocity Ratio
G1	0	0.280	13413.8	11.4053	1.00000	1.00000
G1	486	0.270	13892.9	11.5406	1.01186	1.03571
G1	972	0.260	13892.9	11.6810	1.02418	1.03571
G1	1458	0.260	13892.9	11.6810	1.02418	1.03571
G1	1944	0.260	14407.4	11.6810	1.02418	1.07407
G1	2334	0.250	14407.4	11.8270	1.03697	1.07407
G1	2723	0.250	14407.4	11.8270	1.03697	1.07407
G1	3112	0.250	14407.4	11.8270	1.03697	1.07407
G1	3501	0.250	14407.4	11.8270	1.03697	1.07407
G1	3890	0.240	14407.4	11.9789	1.05029	1.07407
G1	4279	0.240	14407.4	11.9789	1.05029	1.07407
G1	4668	0.230	14407.4	12.1373	1.06418	1.07407
G1	5057	0.220	14961.5	12.3027	1.07869	1.11538
G1	5446	0.220	14961.5	12.3027	1.07869	1.11538
G1	5835	0.210	15560.0	12.4759	1.09386	1.16000
G1	6224	0.205	15560.0	12.5655	1.10173	1.16000
G1	6613	0.200	15560.0	12.6574	1.10978	1.16000
G1	7002	0.195	15560.0	12.7516	1.11805	1.16000
G1	7391	0.190	15560.0	12.8483	1.12652	1.16000
G1	7780	0.185	15560.0	12.9476	1.13522	1.16000
G1	8169	0.180	15560.0	13.0495	1.14416	1.16000
G1	8558	0.180	15560.0	13.0495	1.14416	1.16000
G1	8947	0.180	15560.0	13.0495	1.14416	1.16000
G1	9336	0.180	15560.0	13.0495	1.14416	1.16000
G1	9725	0.180	15560.0	13.0495	1.14416	1.16000

Table B.6 Continued

Sample	Stress (psi)	Amplitude	Velocity (ft/sec)	Att. Coef. (dB/in)	Att. Coef. Ratio	Velocity Ratio
G2	0	0.42	13488.5	9.8415	1.00000	1.00004
G2	478	0.38	13970.2	10.2119	1.03764	1.03575
G2	955	0.36	13970.2	10.4120	1.05797	1.03575
G2	1434	0.35	14487.7	10.5163	1.06856	1.07411
G2	1910	0.34	14487.7	10.6235	1.07946	1.07411
G2	2292	0.34	14487.7	10.6235	1.07946	1.07411
G2	2674	0.33	14487.7	10.7340	1.09069	1.07411
G2	3056	0.32	14487.7	10.8479	1.10226	1.07411
G2	3438	0.32	14487.7	10.8479	1.10226	1.07411
G2	3820	0.32	14487.7	10.8479	1.10226	1.07411
G2	4202	0.30	15044.9	11.0867	1.12653	1.11543
G2	4584	0.30	15044.9	11.0867	1.12653	1.11543
G2	4966	0.29	15044.9	11.2122	1.13928	1.11543
G2	5348	0.29	15044.9	11.2122	1.13928	1.11543
G2	5730	0.28	15044.9	11.3421	1.15247	1.11543
G2	6112	0.28	15044.9	11.3421	1.15247	1.11543
G2	6494	0.28	15044.9	11.3421	1.15247	1.11543
G2	6876	0.27	15044.9	11.4767	1.16615	1.11543
G2	7258	0.26	15044.9	11.6163	1.18034	1.11543
G2	7640	0.26	15044.9	11.6163	1.18034	1.11543
G2	8022	0.25	15044.9	11.7615	1.19509	1.11543
G2	8404	0.24	15044.9	11.9126	1.21044	1.11543
G2	8786	0.24	15044.9	11.9126	1.21044	1.11543
G2	9168	0.23	15044.9	12.0701	1.22644	1.11543
G2	9550	0.23	15044.9	12.0701	1.22644	1.11543

Table B.6 Continued

Sample	Stress (psi)	Amplitude	Velocity (ft/sec)	Att. Coef. (dB/in)	Att. Coef. Ratio	Velocity Ratio
G3	0	0.440	12510.8	9.7525	1.00000	1.00000
G3	480	0.430	13146.9	9.8383	1.00880	1.05084
G3	960	0.400	13373.6	10.1082	1.03648	1.06896
G3	1440	0.380	13373.6	10.2997	1.05611	1.06896
G3	1920	0.370	13851.2	10.3992	1.06632	1.10714
G3	2304	0.360	13851.2	10.5015	1.07680	1.10714
G3	2688	0.350	13851.2	10.6066	1.08759	1.10714
G3	3072	0.340	13851.2	10.7148	1.09868	1.10714
G3	3456	0.340	14103.0	10.7148	1.09868	1.12727
G3	3840	0.325	14364.2	10.8833	1.11595	1.14814
G3	4224	0.320	14364.2	10.9411	1.12188	1.14814
G3	4608	0.320	14364.2	10.9411	1.12188	1.14814
G3	4992	0.320	14364.2	10.9411	1.12188	1.14814
G3	5376	0.320	14364.2	10.9411	1.12188	1.14814
G3	5760	0.320	14364.2	10.9411	1.12188	1.14814
G3	6144	0.320	14364.2	10.9411	1.12188	1.14814
G3	6528	0.320	14364.2	10.9411	1.12188	1.14814
G3	6912	0.320	14364.2	10.9411	1.12188	1.14814
G3	7296	0.320	14364.2	10.9411	1.12188	1.14814
G3	7680	0.320	14364.2	10.9411	1.12188	1.14814
G3	8064	0.320	14364.2	10.9411	1.12188	1.14814
G3	8448	0.320	14364.2	10.9411	1.12188	1.14814
G3	8832	0.320	14364.2	10.9411	1.12188	1.14814
G3	9216	0.320	14364.2	10.9411	1.12188	1.14814

Table B.6 Continued

Sample	Stress (psi)	Amplitude	Velocity (ft/sec)	Att. Coef. (dB/in)	Att. Coef. Ratio	Velocity Ratio
G4	0	0.40	15083.3	9.9965	1.00000	1.00000
G4	485	0.38	15686.7	10.1859	1.01894	1.04000
G4	970	0.38	15686.7	10.1859	1.01894	1.04000
G4	1455	0.37	15686.7	10.2843	1.02879	1.04000
G4	1940	0.36	15686.7	10.3855	1.03891	1.04000
G4	2328	0.36	15686.7	10.3855	1.03891	1.04000
G4	2716	0.35	15686.7	10.4895	1.04931	1.04000
G4	3104	0.35	15686.7	10.4895	1.04931	1.04000
G4	3492	0.34	15686.7	10.5964	1.06001	1.04000
G4	3880	0.34	15686.7	10.5964	1.06001	1.04000
G4	4268	0.32	15686.7	10.8202	1.08240	1.04000
G4	4656	0.32	15686.7	10.8202	1.08240	1.04000
G4	5044	0.32	15686.7	10.8202	1.08240	1.04000
G4	5044	0.30	16340.3	11.0585	1.10623	1.08334
G4	5820	0.30	16340.3	11.0585	1.10623	1.08334
G4	6208	0.30	16340.3	11.0585	1.10623	1.08334
G4	6596	0.30	16340.3	11.0585	1.10623	1.08334
G4	6984	0.30	16340.3	11.0585	1.10623	1.08334
G4	7372	0.28	16340.3	11.3132	1.13171	1.08334
G4	7760	0.26	16340.3	11.5867	1.15907	1.08334
G4	8148	0.25	16340.3	11.7315	1.17356	1.08334
G4	8536	0.24	16340.3	11.8822	1.18863	1.08334
G4	8924	0.24	16340.3	11.8822	1.18863	1.08334
G4	9312	0.22	16340.3	12.2034	1.22077	1.08334
G4	9700	0.22	16340.3	12.2034	1.22077	1.08334

Table B.6 Continued

Sample	Stress (psi)	Amplitude	Velocity (ft/sec)	Att. Coef. (dB/in)	Att. Coef. Ratio	Velocity Ratio
G5	0	0.340	15854.2	10.9214	1.00000	1.00000
G5	500	0.370	16191.5	10.5996	0.97054	1.02127
G5	1000	0.380	16543.5	10.4982	0.96125	1.04348
G5	1500	0.390	16543.5	10.3994	0.95220	1.04348
G5	2000	0.400	16543.5	10.3030	0.94338	1.04348
G5	2400	0.405	16543.5	10.2558	0.93905	1.04348
G5	2800	0.400	16543.5	10.3030	0.94338	1.04348
G5	3200	0.415	16543.5	10.1630	0.93056	1.04348
G5	3600	0.420	17295.5	10.1174	0.92638	1.09091
G5	4000	0.425	17295.5	10.0724	0.92226	1.09091
G5	4400	0.440	18119.0	9.9404	0.91018	1.14285
G5	4800	0.450	18119.0	9.8549	0.90235	1.14285
G5	5200	0.460	18119.0	9.7713	0.89469	1.14285
G5	5600	0.470	17295.5	9.6895	0.88720	1.09091
G5	6000	0.480	17295.5	9.6094	0.87987	1.09091
G5	6400	0.490	17295.5	9.5309	0.87268	1.09091
G5	6800	0.490	17295.5	9.5309	0.87268	1.09091
G5	7200	0.500	17295.5	9.4541	0.86565	1.09091
G5	7600	0.500	18119.0	9.4541	0.86565	1.14285
G5	8000	0.500	18119.0	9.4541	0.86565	1.14285
G5	8400	0.520	18119.0	9.3048	0.85198	1.14285
G5	8800	0.520	18119.0	9.3048	0.85198	1.14285
G5	9200	0.520	17295.5	9.3048	0.85198	1.09091
G5	9600	0.520	17295.5	9.3048	0.85198	1.09091
G5	10000	0.520	17295.5	9.3048	0.85198	1.09091

Table B.6 Continued

Sample	Stress (psi)	Amplitude	Velocity (ft/sec)	Att. Coef. (dB/in)	Att. Coef. Ratio	Velocity Ratio
G6	0	0.310	12090.9	10.7501	1.00000	1.00000
G6	506	0.320	12871.0	10.6349	0.98929	1.06452
G6	1012	0.310	12871.0	10.7501	1.00000	1.06452
G6	1518	0.320	13300.0	10.6349	0.98929	1.10000
G6	2024	0.320	13300.0	10.6349	0.98929	1.10000
G6	2430	0.320	13300.0	10.6349	0.98929	1.10000
G6	2835	0.320	13525.4	10.6349	0.98929	1.11864
G6	3240	0.320	13758.6	10.6349	0.98929	1.13793
G6	3645	0.320	14000.0	10.6349	0.98929	1.15790
G6	4050	0.320	14000.0	10.6349	0.98929	1.15790
G6	4455	0.320	14000.0	10.6349	0.98929	1.15790
G6	4860	0.325	14250.0	10.5787	0.98405	1.17857
G6	5265	0.325	14250.0	10.5787	0.98405	1.17857
G6	5670	0.325	14250.0	10.5787	0.98405	1.17857
G6	6070	0.330	14250.0	10.5233	0.97890	1.17857
G6	6480	0.330	14250.0	10.5233	0.97890	1.17857
G6	6885	0.340	14250.0	10.4150	0.96883	1.17857
G6	7290	0.340	14250.0	10.4150	0.96883	1.17857
G6	7695	0.340	14250.0	10.4150	0.96883	1.17857
G6	8100	0.340	14250.0	10.4150	0.96883	1.17857

Table B.6 Continued

Sample	Stress (psi)	Amplitude	Velocity (ft/sec)	Att. Coef. (dB/in)	Att. Coef. Ratio	Velocity Ratio
G7	0	0.420	14351.9	9.9346	1.00000	1.00000
G7	500	0.420	14622.6	9.9346	1.00000	1.01886
G7	1000	0.425	14622.6	9.8904	0.99555	1.01886
G7	1500	0.430	14903.8	9.8467	0.99115	1.03846
G7	2000	0.440	15500.0	9.7608	0.98251	1.08000
G7	2400	0.440	15500.0	9.7608	0.98251	1.08000
G7	2800	0.430	15500.0	9.8467	0.99115	1.08000
G7	3200	0.420	15500.0	9.9346	1.00000	1.08000
G7	3600	0.420	15500.0	9.9346	1.00000	1.08000
G7	4000	0.400	15500.0	10.1169	1.01835	1.08000
G7	4400	0.390	15500.0	10.2115	1.02787	1.08000
G7	4800	0.380	15500.0	10.3085	1.03764	1.08000
G7	5200	0.375	15500.0	10.3580	1.04262	1.08000
G7	5600	0.360	16145.8	10.5105	1.05797	1.12500
G7	6000	0.350	16145.8	10.6158	1.06856	1.12500
G7	6400	0.340	16145.8	10.7241	1.07946	1.12500
G7	6800	0.330	16145.8	10.8356	1.09069	1.12500
G7	7200	0.320	16145.8	10.9505	1.10226	1.12500
G7	7600	0.320	16145.8	10.9505	1.10226	1.12500
G7	8000	0.310	16145.8	11.0692	1.11420	1.12500
G7	8400	0.300	16145.8	11.1917	1.12653	1.12500
G7	8800	0.300	16145.8	11.1917	1.12653	1.12500
G7	9200	0.280	16145.8	11.4494	1.15247	1.12500
G7	9600	0.270	16145.8	11.5853	1.16615	1.12500
G7	10000	0.260	16145.8	11.7263	1.18034	1.12500

Table B.6 Continued

Sample	Stress (psi)	Amplitude	Velocity (ft/sec)	Att. Coef. (dB/in)	Att. Coef. Ratio	Velocity Ratio
G8	0	0.240	12464.6	11.3285	1.00000	1.00000
G8	475	0.230	12854.2	11.4783	1.01322	1.03125
G8	950	0.225	13268.8	11.5557	1.02005	1.06452
G8	1425	0.225	13268.8	11.5557	1.02005	1.06452
G8	1900	0.225	13268.8	11.5557	1.02005	1.06452
G8	2280	0.220	13486.3	11.6348	1.02703	1.08197
G8	2660	0.220	13486.3	11.6348	1.02703	1.08197
G8	3040	0.210	13711.1	11.7985	1.04149	1.10000
G8	3420	0.200	13711.1	11.9702	1.05664	1.10000
G8	3800	0.195	13711.1	12.0593	1.06451	1.10000
G8	4180	0.195	13943.5	12.0593	1.06451	1.11865
G8	4560	0.190	13943.5	12.1507	1.07258	1.11865
G8	4940	0.180	13943.5	12.3410	1.08938	1.11865
G8	5510	0.180	14183.9	12.3410	1.08938	1.13794
G8	6080	0.180	14183.9	12.3410	1.08938	1.13794
G8	6460	0.180	14690.5	12.3410	1.08938	1.17858
G8	6840	0.180	14690.5	12.3410	1.08938	1.17858
G8	7220	0.180	14690.5	12.3410	1.08938	1.17858
G8	7600	0.180	14690.5	12.3410	1.08938	1.17858
G8	7980	0.160	14183.9	12.7555	1.12597	1.13794
G8	8360	0.160	14183.9	12.7555	1.12597	1.13794
G8	8740	0.160	14690.5	12.7555	1.12597	1.17858
G8	9120	0.160	14690.5	12.7555	1.12597	1.17858
G8	9500	0.160	14690.5	12.7555	1.12597	1.17858
G8	9880	0.160	14690.5	12.7555	1.12597	1.17858

Table B.6 Continued

Sample	Stress (psi)	Amplitude	Velocity (ft/sec)	Att. Coef. (dB/in)	Att. Coef. Ratio	Velocity Ratio
G9	0	0.190	12112.7	12.1360	1.00000	1.00000
G9	544	0.200	12869.8	11.9557	0.98514	1.06250
G9	1088	0.210	13284.9	11.7842	0.97101	1.09678
G9	1632	0.210	13284.9	11.7842	0.97101	1.09678
G9	2175	0.215	13284.9	11.7014	0.96419	1.09678
G9	2611	0.220	13727.8	11.6206	0.95753	1.13334
G9	3046	0.220	13727.8	11.6206	0.95753	1.13334
G9	3482	0.225	13727.8	11.5416	0.95102	1.13334
G9	3917	0.230	13727.8	11.5416	0.94466	1.13334
G9	4350	0.230	13727.8	11.4644	0.94466	1.13334
G9	4785	0.240	14201.1	11.3148	0.93233	1.17242
G9	5222	0.240	14201.1	11.3148	0.93233	1.17242
G9	5658	0.245	14201.1	11.2423	0.92636	1.17242
G9	6090	0.245	14201.1	11.2423	0.92636	1.17242
G9	6525	0.260	14201.1	11.0334	0.90915	1.17242
G9	6963	0.260	14201.1	11.0334	0.90915	1.17242
G9	7388	0.260	14201.1	11.0334	0.90915	1.17242
G9	7833	0.260	14201.1	11.0334	0.90915	1.17242
G9	8269	0.260	14201.1	11.0334	0.90915	1.17242
G9	8682	0.260	14201.1	11.0334	0.90915	1.17242

Table B.6 Continued

Sample	Stress (psi)	Amplitude	Velocity (ft/sec)	Att. Coef. (dB/in)	Att. Coef. Ratio	Velocity Ratio
G10	0	0.520	14724.6	10.4542	1.00000	1.00000
G10	570	0.500	15393.9	10.6219	1.01604	1.04546
G10	1140	0.520	15393.9	10.4542	1.00000	1.04546
G10	1710	0.524	16127.0	10.4215	0.99687	1.09524
G10	2280	0.530	16127.0	10.3728	0.99221	1.09524
G10	2736	0.530	16127.0	10.3728	0.99221	1.09524
G10	3192	0.540	16127.0	10.2929	0.98457	1.09524
G10	3648	0.550	16127.0	10.2145	0.97707	1.09524
G10	4104	0.550	16127.0	10.2145	0.97707	1.09524
G10	4560	0.550	16127.0	10.2145	0.97707	1.09524
G10	5016	0.560	16127.0	10.1374	0.96970	1.09524
G10	5472	0.560	16127.0	10.1374	0.96970	1.09524
G10	5928	0.560	16127.0	10.1374	0.96970	1.09524
G10	6384	0.560	16127.0	10.1374	0.96970	1.09524
G10	6840	0.560	16933.3	10.1374	0.96970	1.15000
G10	7296	0.560	16933.3	10.1374	0.96970	1.15000
G10	7752	0.560	16933.3	10.1374	0.96970	1.15000
G10	8208	0.560	16933.3	10.1374	0.96970	1.15000
G10	8664	0.560	16933.3	10.1374	0.96970	1.15000
G10	9120	0.560	16933.3	10.1374	0.96970	1.15000

Table B.6 Continued

Sample	Stress (psi)	Amplitude	Velocity (ft/sec)	Att. Coef. (dB/in)	Att. Coef. Ratio	Velocity Ratio
G14	0	0.125	12809.5	13.8888	1.00000	1.00000
G14	485	0.133	13450.0	13.6663	0.98398	1.05000
G14	970	0.133	13678.0	13.6663	0.98398	1.06780
G14	1455	0.135	13913.8	13.6127	0.98012	1.08621
G14	1940	0.140	13913.8	13.4822	0.97073	1.08621
G14	2328	0.140	13913.8	13.4822	0.97073	1.08621
G14	2716	0.148	14157.9	13.2829	0.95637	1.10527
G14	3104	0.150	14410.7	13.2347	0.95290	1.12500
G14	3492	0.160	14410.7	13.0031	0.93623	1.12500
G14	3880	0.160	14410.7	13.0031	0.93623	1.12500
G14	4268	0.160	14944.4	13.0031	0.93623	1.16667
G14	4656	0.160	14944.4	13.0031	0.93623	1.16667
G14	5044	0.175	14944.4	12.6816	0.91308	1.16667
G14	5820	0.180	14944.4	12.5806	0.90581	1.16667
G14	6208	0.180	14944.4	12.5806	0.90581	1.16667
G14	6596	0.180	14944.4	12.5806	0.90581	1.16667
G14	6984	0.180	14944.4	12.5806	0.90581	1.16667
G14	7372	0.180	14944.4	12.5806	0.90581	1.16667
G14	7760	0.180	14944.4	12.5806	0.90581	1.16667
G14	8148	0.180	14944.4	12.5806	0.90581	1.16667

Table B.6 Continued

Sample	Stress (psi)	Amplitude	Velocity (ft/sec)	Att. Coef. (dB/in)	Att. Coef. Ratio	Velocity Ratio
G16	0	0.170	14876.5	12.8440	1.00000	1.000
G16	500	0.170	14876.5	12.8440	1.00000	1.000
G16	1000	0.170	16066.7	12.8440	1.00000	1.080
G16	1500	0.170	16066.7	12.8440	1.00000	1.080
G16	2000	0.170	16066.7	12.8440	1.00000	1.080
G16	2400	0.180	16066.7	12.6380	0.98396	1.080
G16	2800	0.180	16066.7	12.6380	0.98396	1.080
G16	3200	0.180	16736.1	12.6380	0.98396	1.125
G16	3600	0.180	16736.1	12.6380	0.98396	1.125
G16	4000	0.200	16736.1	12.2583	0.95440	1.125
G16	4400	0.200	16736.1	12.2583	0.95440	1.125
G16	4800	0.205	16736.1	12.1693	0.94747	1.125
G16	5200	0.220	16736.1	11.9148	0.92765	1.125
G16	5600	0.220	16736.1	11.9148	0.92765	1.125
G16	6000	0.220	16736.1	11.9148	0.92765	1.125
G16	6800	0.220	16736.1	11.9148	0.92765	1.125
G16	7200	0.220	16736.1	11.9148	0.92765	1.125
G16	7600	0.220	16736.1	11.9148	0.92765	1.125
G16	8000	0.220	16736.1	11.9148	0.92765	1.125
G16	8400	0.220	16736.1	11.9148	0.92765	1.125

Table B.6 Continued

Sample	Stress (psi)	Amplitude	Velocity (ft/sec)	Att. Coef. (dB/in)	Att. Coef. Ratio	Velocity Ratio
G13	0	0.145	13016.1	13.3563	1.00000	1.00000
G13	485	0.160	13450.0	13.0031	0.97356	1.03334
G13	970	0.165	13450.0	12.8927	0.96529	1.03334
G13	1455	0.170	13678.0	12.7856	0.95727	1.05085
G13	1940	0.170	13678.0	12.7856	0.95727	1.05085
G13	2328	0.175	13678.0	12.6816	0.94949	1.05085
G13	2716	0.175	13678.0	12.6816	0.94949	1.05085
G13	3104	0.180	13678.0	12.5806	0.94192	1.05085
G13	3492	0.185	13678.0	12.4823	0.93456	1.05085
G13	3880	0.200	13913.8	12.2026	0.91362	1.06897
G13	4268	0.195	13913.8	12.2934	0.92042	1.06897
G13	4656	0.195	13913.8	12.2934	0.92042	1.06897
G13	5044	0.200	13913.8	12.2026	0.91362	1.06897
G13	5432	0.200	13913.8	12.2026	0.91362	1.06897
G13	5820	0.200	14410.7	12.2026	0.91362	1.10715
G13	6208	0.200	14410.7	12.2026	0.91362	1.10715
G13	6596	0.200	14672.7	12.2026	0.91362	1.12728
G13	6984	0.200	14410.7	12.2026	0.91362	1.10715
G13	7372	0.200	14410.7	12.2026	0.91362	1.10715
G13	7760	0.200	14672.7	12.2026	0.91362	1.12728

TABLE B.7

Sonic Testing Results of Marble Specimens

Sample	Stress (psi)	Amplitude	Velocity (ft/sec)	Att. Coef. (dB/in)	Att. Coef. Ratio	Velocity Ratio
M1	0	1.34	18201.8	6.27515	1.00000	1.00000
M1	782	1.00	18395.4	7.50025	1.19523	1.01064
M1	1564	0.96	18593.2	7.67113	1.22246	1.02150
M1	2346	0.92	18593.2	7.84929	1.25085	1.02150
M1	3128	0.88	18593.2	8.03536	1.28050	1.02150
M1	3753	0.85	18593.2	8.18055	1.30364	1.02150
M1	4379	0.81	18593.2	8.38233	1.33580	1.02150
M1	5004	0.81	18395.4	8.38233	1.33580	1.01064
M1	5630	0.81	18201.8	8.38233	1.33580	1.00000
M1	6255	0.81	18012.2	8.38233	1.33580	0.98958
M1	6881	0.81	17291.7	8.38233	1.33580	0.95000
M1	7506	0.81	16626.6	8.38233	1.33580	0.91346
M1	8132	0.81	16010.8	8.38233	1.33580	0.87963
M1	8758	0.81	16010.8	8.38233	1.33580	0.87963

Table B.7 Continued

Sample	Stress (psi)	Amplitude	Velocity (ft/sec)	Att. Coef. (dB/in)	Att. Coef. Ratio	Velocity Ratio
M2	0	1.32	17333.3	6.3229	1.00000	1.00000
M2	777	1.11	17508.4	7.0464	1.11444	1.01010
M2	1554	1.08	17508.4	7.1608	1.13253	1.01010
M2	2331	1.04	17508.4	7.3184	1.15746	1.01010
M2	3108	0.94	17687.1	7.7406	1.22423	1.02041
M2	3729	0.90	18055.6	7.9222	1.25295	1.04167
M2	4351	0.84	17869.4	8.2103	1.29851	1.03093
M2	4972	0.73	17687.1	8.7964	1.39121	1.02041
M2	5594	0.63	17161.7	9.4116	1.48851	0.99010
M2	6215	0.46	16666.7	10.7249	1.69622	0.96154
M2	6837	0.36	15476.2	11.7485	1.85811	0.89286
M2	7458	0.30	13978.5	12.5099	1.97852	0.80645
M2	8079	0.25	13978.5	13.2713	2.09892	0.80645
M2	8701	0.20	13978.5	14.2031	2.24629	0.80645

Table B.7 Continued

Sample	Stress (psi)	Amplitude	Velocity (ft/sec)	Att. Coef. (dB/in)	Att. Coef. Ratio	Velocity Ratio
M3	0	0.78	18668.5	8.5983	1.00000	1.00000
M3	778	0.44	18668.5	11.0111	1.28062	1.00000
M3	1555	0.40	18668.5	11.4128	1.32733	1.00000
M3	2333	0.38	18668.5	11.6290	1.35247	1.00000
M3	3110	0.36	18668.5	11.8569	1.37897	1.00000
M3	3732	0.36	18668.5	11.8569	1.37897	1.00000
M3	4354	0.34	18668.5	12.0977	1.40699	1.00000
M3	4976	0.32	18668.5	12.3532	1.43670	1.00000
M3	5598	0.32	18668.5	12.3532	1.43670	1.00000
M3	6220	0.30	18668.5	12.6252	1.46834	1.00000
M3	6842	0.29	18668.5	12.7681	1.48495	1.00000
M3	7464	0.28	18668.5	12.9160	1.50215	1.00000
M3	8086	0.26	18668.5	13.2283	1.53848	1.00000
M3	8708	0.24	18271.3	13.5656	1.57771	0.97872

Table B.7 Continued

Sample	Stress (psi)	Amplitude	Velocity (ft/sec)	Att. Coef. (dB/in)	Att. Coef. Ratio	Velocity Ratio
M4	0	0.88	18523.6	8.1532	1.00000	1.00000
M4	779	0.60	18523.6	9.7800	1.19952	1.00000
M4	1558	0.56	18523.6	10.0730	1.23546	1.00000
M4	2336	0.56	18523.6	10.0730	1.23546	1.00000
M4	3115	0.56	18523.6	10.0730	1.23546	1.00000
M4	3738	0.57	18727.1	9.9978	1.22624	1.01099
M4	4361	0.58	18727.1	9.9239	1.21718	1.01099
M4	4984	0.54	18523.6	10.2275	1.25440	1.00000
M4	5607	0.50	18523.6	10.5543	1.29450	1.00000
M4	6230	0.48	18324.4	10.7277	1.31576	0.98924
M4	6853	0.44	18129.4	11.0973	1.36109	0.97872
M4	7476	0.42	17041.7	11.2949	1.38532	0.92000
M4	8099	0.40	17041.7	11.5021	1.41096	0.92000
M4	8723	0.38	17041.7	11.7200	1.43747	0.92000

Table B.7 Continued

Sample	Stress (psi)	Amplitude	Velocity (ft/sec)	Att. Coef. (dB/in)	Att. Coef. Ratio	Velocity Ratio
M5	0	0.495	11965.1	10.1981	1.00000	1.00000
M5	775	0.480	12046.5	10.3239	1.01233	1.00680
M5	1550	0.475	12129.0	10.3667	1.01653	1.01370
M5	2325	0.475	12297.5	10.3667	1.01653	1.02778
M5	3100	0.460	12297.5	10.4978	1.02939	1.02778
M5	3720	0.460	12383.4	10.4978	1.02939	1.03496
M5	4340	0.460	12297.5	10.4978	1.02939	1.02778
M5	4960	0.460	12212.6	10.4978	1.02939	1.02069
M5	5580	0.440	11965.1	10.6795	1.04721	1.00000
M5	6200	0.405	11650.2	11.0183	1.08043	0.97368
M5	6820	0.350	11351.5	11.6149	1.13893	0.94872
M5	7443	0.300	11351.5	12.2450	1.20071	0.94872
M5	8066	0.240	11207.8	12.9902	1.27379	0.93671
M5	8689	0.200	11207.8	13.9023	1.36323	0.93671

Table B.7 Continued

Sample	Stress (psi)	Amplitude	Velocity (ft/sec)	Att. Coef. (dB/in)	Att. Coef. Ratio	Velocity Ratio
M6	0	0.78	19675.9	8.3394	1.00000	1.00000
M6	775	0.86	19897.0	7.9403	0.95214	1.01124
M6	1550	0.88	20123.1	7.8463	0.94087	1.02273
M6	2325	0.88	20123.1	7.8463	0.94087	1.02273
M6	3100	0.86	20123.1	7.9403	0.95214	1.02273
M6	3720	0.85	20123.1	7.9881	0.95788	1.02273
M6	4340	0.86	20123.1	7.9403	0.95214	1.02273
M6	4960	0.86	20123.1	7.9403	0.95214	1.02273
M6	5580	0.85	20123.1	7.9881	0.95788	1.02273
M6	6200	0.84	20123.1	8.0364	0.96368	1.02273
M6	6820	0.82	20123.1	8.1349	0.97549	1.02273
M6	7440	0.79	19897.0	8.2873	0.99376	1.01124
M6	8060	0.64	19248.2	9.1480	1.09696	0.97826
M6	8680	0.40	16706.0	11.0691	1.32733	0.84906

Table B.7 Continued

Sample	Stress (psi)	Amplitude	Velocity (ft/sec)	Att. Coef. (dB/in)	Att. Coef. Ratio	Velocity Ratio
M7	0	1.40	18430.9	6.08007	1.00000	1.00000
M7	779	1.38	18629.0	6.14018	1.00989	1.01075
M7	1558	1.35	18831.5	6.23201	1.02499	1.02174
M7	2337	1.35	18831.5	6.23201	1.02499	1.02174
M7	3117	1.32	18831.5	6.32590	1.04043	1.02174
M7	3740	1.30	18831.5	6.38969	1.05092	1.02174
M7	4363	1.28	18831.5	6.45446	1.06158	1.02174
M7	4986	1.25	18831.5	6.55355	1.07787	1.02174
M7	5608	1.21	18831.5	6.68943	1.10022	1.02174
M7	6233	1.10	18629.0	7.08762	1.16571	1.01075
M7	6856	0.96	18046.9	7.65637	1.25926	0.97916
M7	7480	0.60	17325.0	9.62001	1.58222	0.94000
M7	8104	0.50	17325.0	10.38173	1.70750	0.94000
M7	8728	0.40	17325.0	11.31401	1.86084	0.94000

The vita has been removed from the scanned document